Autre référence / Other reference :
ESTEC/Contract N° 4000102571/10/NL/AF
Type :
Rapport d'essai final/qualification/validation.
Description :
Radiation Characterization of LAPLACE/TANDEM RH Optocouplers, Sensors and Detectors
Titre du document / Title of document :
HAS2 proton SET test report

	Noms Names	Dates
Etabli par Prepared by	BEAUMEL Matthieu (SODERN) HERVE Dominique (SODERN) POIZAT Marc (ESA) VAN AKEN Dirk (ON Semiconductor)	02/08/2012
Vérifié par Checked by	BEAUMEL Matthieu HERVE Dominique	02/08/2012
Approuvé par Approved by	HERVE Dominique ; LEDOUX Thierry	22/10/2012
Approbation client Customer approval	-	-

REPERTOIRE DES MISES A JOUR / *CHANGE RECORD*	
Révision / Revision	Nature de la mise à jour / Description of change
A	Première diffusion / First issue

SOMMAIRE / TABLE OF CONTENTS

1.SCOPE AND APPLICABILITY

1.1.Scope

This test report presents the result of the proton irradiation of the HAS2 CMOS image sensor performed in the frame of ESTEC contract N° 4000102571/10/NL/AF “Radiation Characterization of Laplace/Tandem RH optocouplers, sensors and detectors”.

The irradiations were performed at the proton irradiation facility of Paul Scherrer Institute (PSI – Switzerland) February 10th to 12th 2012 with ESA (Marc Poizat) on site support.

1.2.Purpose

Proton irradiation effect is investigated at high energy levels in order to complete proton data currently available at lower energy. Energy range below 62 MeV is covered by the proton test campaigns reported in [RD 2] and [RD 3].

2.REFERENCES

2.1.Applicable documents

[AD 1] ITT 6429 HAS Irradiation Test Plan, PR__00004584, D

2.2.Reference documents

[RD 1] ON Semiconductor HAS2 Detailed Specification NOIH2SM1000A/D, Rev. 3

[RD 2] HAS2 Proton irradiation test report, HAS2-CY-FVD-07-021, Rev. 2.0, D. Van Aken, ON Semiconductor, December 3rd 2007

[RD 3] HAS2 low temperature proton test report, RP__00000533, Rev. B, D. Hervé, M.Beaumel, Sodern, February 21st 2008

[RD 4] Total Dose, Displacement Damage and Single Event Effects in the Radiation Hardened CMOS APS HAS2, ON Semiconductor & Sodern publication, Proceedings SPIE Remote sensing, D. Van Aken, D. Hervé, M. Beaumel, Berlin September 2009

[RD 5] Evaluation of STR performance in high radiation environments, Final Report, ESA contract 40001011530/10/NL/AF, January 2012

[RD 6] Proton Test Guidelines development – Lessons Learned,” NASA-NEPP report, 2002

[RD 7] HAS2 Heavy Ion Test report, RE__00007891, Rev. D. Hervé, D. Van Aken, M. Beaumel, A., in the frame of ESA study “Radiation Characterization of Laplace/Tandem RH Optocouplers, Sensors and Detectors”.

3.ABBREVIATIONS

AD	Applicable Document
APS	Active Pixel Sensor
CDS	Correlated Double Sampling
CMOS	Complementary Metal-Oxide Semiconductor
DC	DateCode
DDD	Displacement Damage Dose
DR	Destructive Readout
DS	Double Sampling
DSNU	Dark Signal Non Uniformity
ECSS	European Cooperation for Space Standardization
EOL	End Of Life
ESA	European Space Agency
FPN	Fixed Pattern Noise
HAS2	High Accuracy STR 2
LET	Linear Energy Transfer
LSB	Least Significant Bit
N/A	Not Applicable
NDR	Non-Destructive Readout
PCB	Printed Circuit Board
RD	Reference Document
SEE	Single Event Effect
SET	Single Event Transient
SEU	Single Event Upset
SEFI	Single Event Failure interrupt
TID	Total Ionizing Dose

4.DEVICE INFORMATION

4.1.HAS2 presentation

The Accuracy STR 2 sensor (HAS2) is a 1024 x 1024 pixel rolling shutter Active Pixel Sensor (APS), featuring a programmable (gain and offset) output amplifier (PGA) and an internal 12 bits ADC.

The CMOS image was sensor designed and manufactured by ON Semiconductor[1] under ESA contract 17235/03/NL/FM for star tracker applications.

The block diagram of HAS2 is presented in Figure 4-1.

Pixel design is based on a photodiode coupled with a three transistor readout circuit. The HAS2 is the descendant from a lineage radiation-hardened by design sensors from ON Semiconductor: the photodiodes includes a doped surface protection layer to prevent the depleted area from reaching the field oxide interface, while the CMOS readout circuitry is designed using enclosed geometry transistor layouts.

The wafers are produced by Plessey Semiconductors[2] on the standard XC035P311 CMOS process (0.35 µm).

In order to reduce the variation in signal offset from pixel to pixel (known as Fixed Pattern Noise, or FPN) typically seen on APS, the HAS2 implements two different noise reduction techniques: Double Sampling (DS) also called Destructive Readout (DR) and Correlated Double Sampling (CDS) also called Non Destructive Readout (NDR). In DR mode, the pixel is reset at the end of the signal integration time in order to sample the pixel reference level. The reference level is subtracted from the signal level in order to cancel the pixel offset. This internal analog operation is performed before digitization. In NDR mode, two images are sampled and digitized: a reference image at the beginning of the integration time, and a signal image at its end. Offset correction must be performed off-chip by subtracting these two images.

A temperature sensor is also integrated on chip, which can be addressed through an internal multiplexer. This MUX can also address analogue inputs to be digitized by the internal ADC.

[1] Formerly Cypress BVBA and Fillfactory.
[2] Formerly X-FAB.

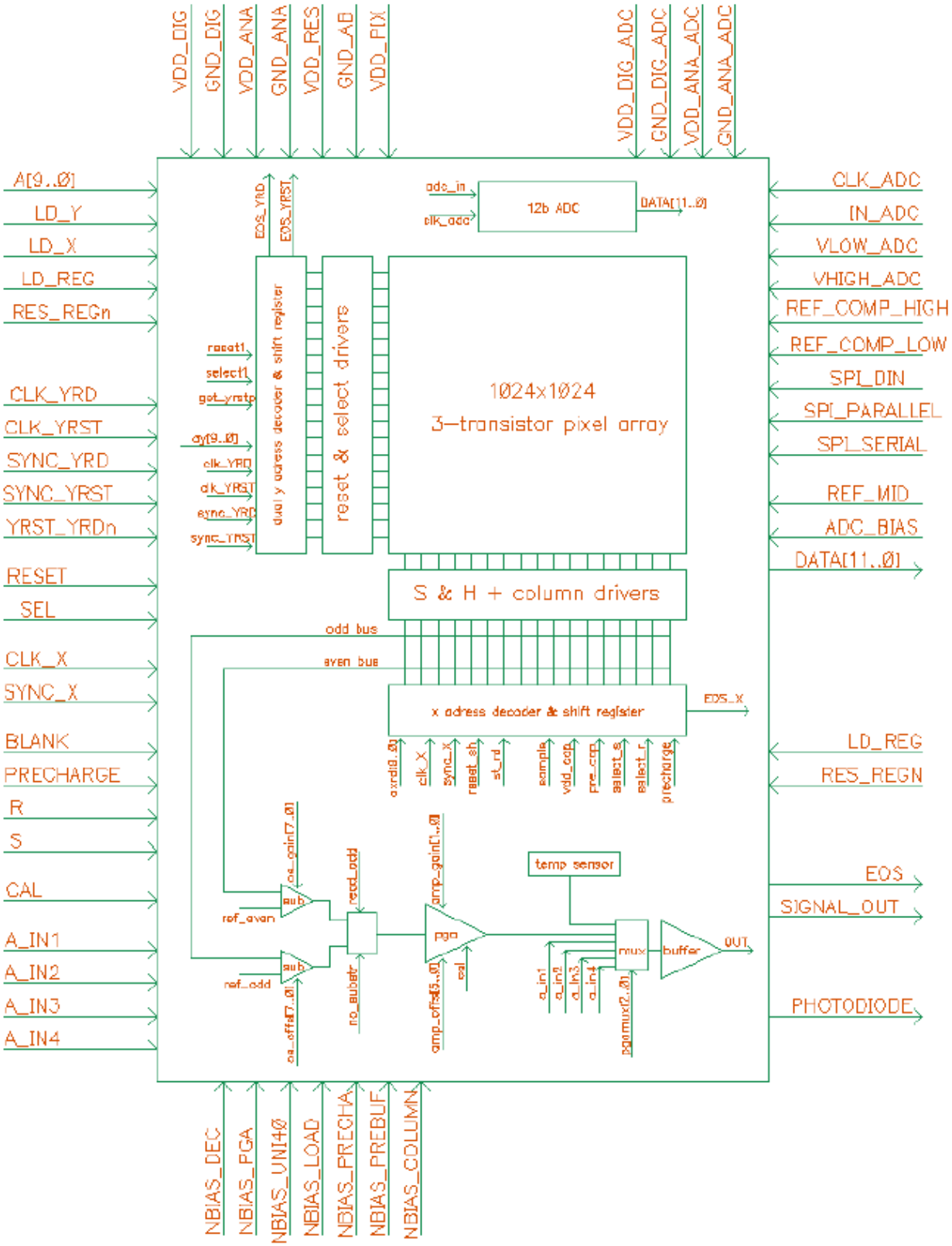

Figure 4-1 : HAS2 block diagram

4.2.Samples identification

Part type:	HAS2
Manufacturer:	ON Semiconductor
Package:	JLCC84
Tested Samples:	s/n692 (Sample A: no radiation test prior to proton SEE test), s/n741 (Sample B: submitted to 55 krad(Si) prior to proton SEE test), s/n700 (Sample C: 1.17E+12 neutrons(1 MeV)/cm² prior to proton SEE test), s/n686 (Sample D: 1.17E+12 neutrons(1 MeV)/cm² prior to proton SEE test),
Backside marking:	NOIH2SM1000A HHC (Engineering Models)
Date code:	110414 (April 14, 2011)

TID campaign had been performed beginning of October 2011, i.e. 4 months before the proton campaign.

Neutron campaign had been performed on December 7th 2011, i.e. 2 months before the proton campaign.

Specifically for these Engineering Model devices, a burn-in 168 hours 125°C has been performed prior to irradiation.

All the devices were irradiated with glass lid.

All the devices are coming from the same silicon wafer lot P29506.1.

All neutron samples have been irradiated for 45’48”.

5.IRRADIATION FACILITY

Irradiation have been performed at Paul Scherrer Institute (PSI – Switzerland), on the Proton Irradiation Facility (PIF) High Energy site. The PIF experimental set-up consists of the local PIF energy degrader, beam collimating and monitoring devices (Figure 5-1 and Figure 5-2).

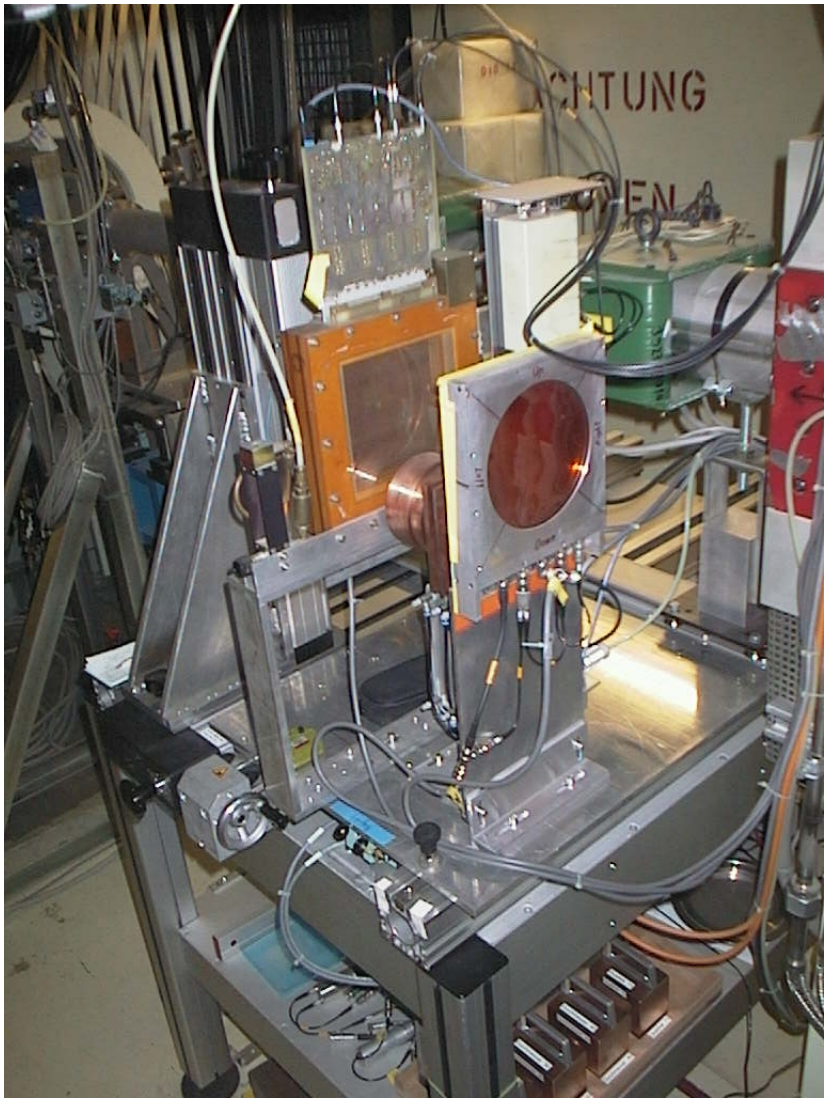

Figure 5-1 : PIF-PROSCAN downstream view with ionization chamber, energy degrader and wire chamber

Maximum beam intensity in the PIF area is around 2 nA for energies above 200 MeV, and 5 nA for energies from 100 MeV to 200 MeV. Delivered from PROSCAN accelerator used for cancer treatment, PIF exposures are mostly conducted during weekends and nightshifts. Irradiations are carried out in air. The maximum energy is 230 MeV. Beam diameter is 60 mm. Dosimetry is performed using the monitor detectors with an accuracy of the flux/dose determination of 5%. A laser pattern calibrated on the beam axis is used to place the DUT in the middle of the beam.

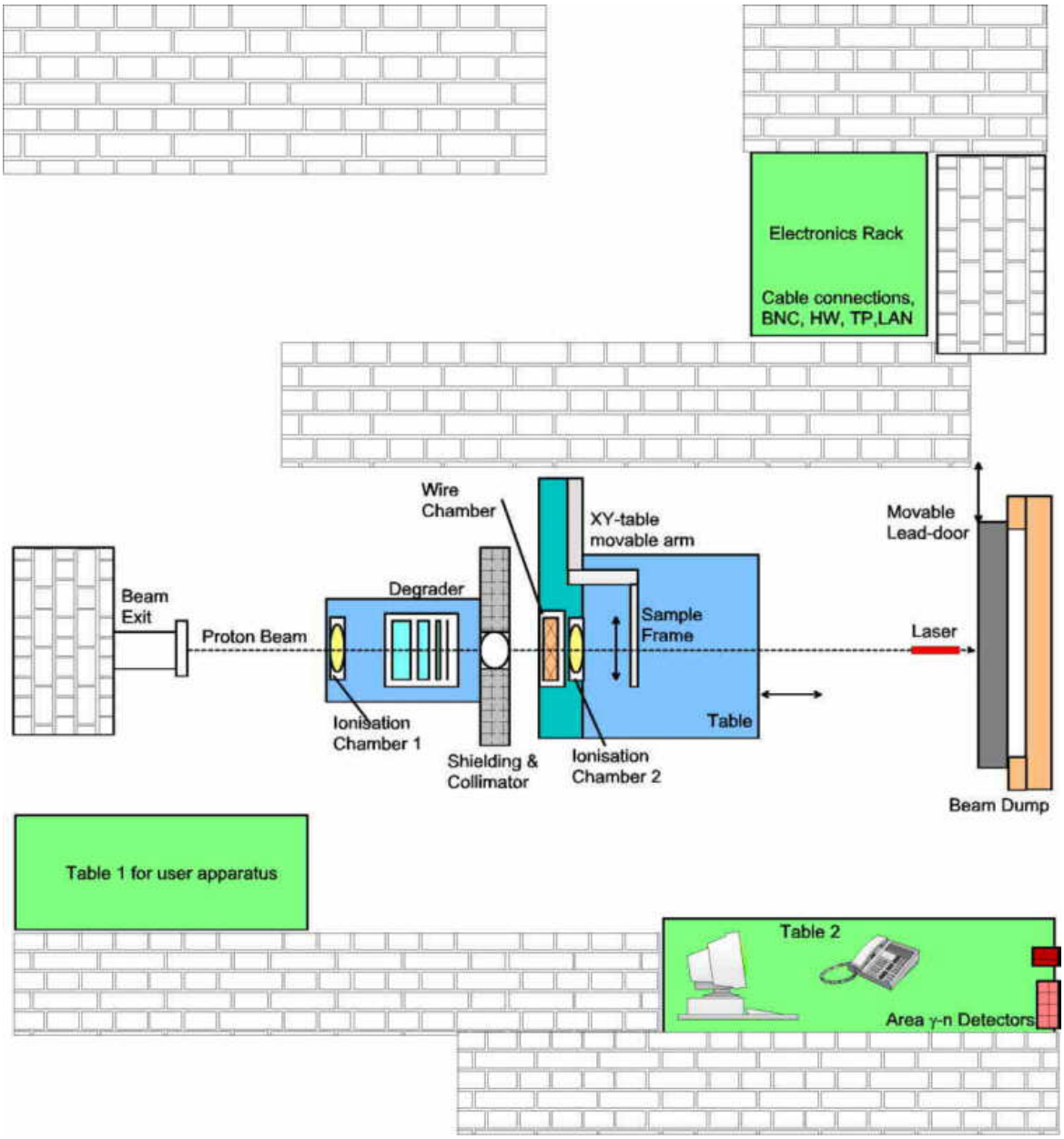

Figure 5-2 : PIF-PROSCAN experimental set-up layout

A proton flux of less than 1.0E+06 protons/cm²/s was applied. The following energies were selected:

Energy [MeV]	*Range [mm Si]*	*LET [e-/µm]*
100	4.18E+01	3.78E+02
175	1.11E+02	2.56E+02
230	1.76E+02	2.15E+02

Table 5-1 : proton range and stopping power in silicon versus energy

6.TEST SETUP

The irradiations and electrical characterizations have been performed at room temperature. Image acquisition was carried out by ON Semiconductor using dedicated driving boards and acquisition system. The whole setup had the capability to operate the device under beam flux at long distance from the control room.

The figure hereafter presents the geometry of the irradiation setup. The dimensions of the radiation board and proximity electronics are compatible with the beam site holders. The device could be tilted manually with respect to proton beam.

Image data processing was not carried out on site, but afterwards on stored images. A few images were checked quickly on site.

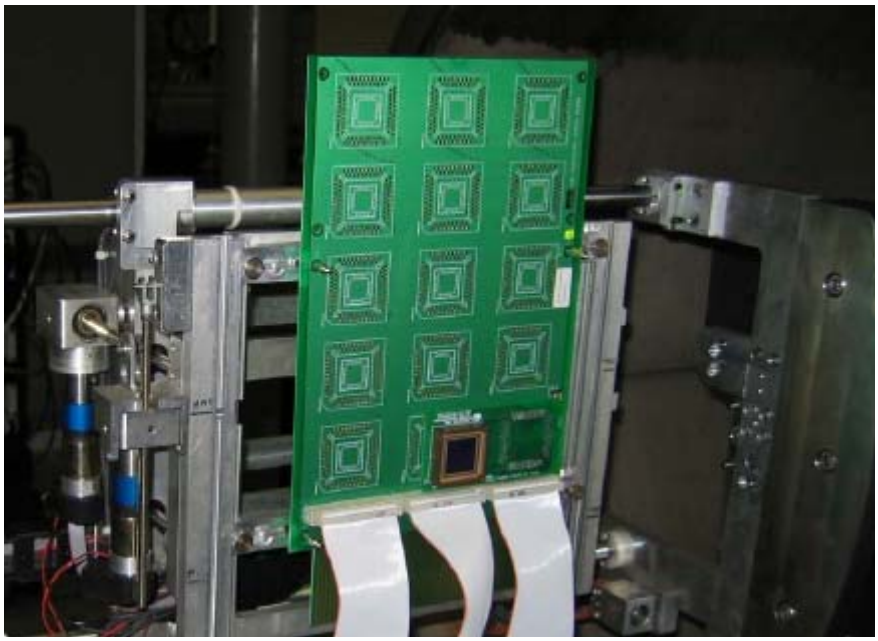

Figure 6-1 : HAS2 PCB

HAS2 is operated under beam in Hard Reset condition to eliminate lag effects.

During image acquisition under beam flux, the test chamber is placed in darkness to avoid light to be captured by the sensor.

Both DR and NDR mode are investigated (for details on readout modes refer to [RD 1]. In DR mode, full frame images are acquired with a frame rate of 5 images/s (around 100 images per movie). In NDR mode, full frames are grabbed with a frame rate of 2.5 images/s (around 3x30 images per movie including reference, video, and final image).

In DR mode, the integration time is 2 ms. In NDR mode, the integration time is 200 ms (shorter integration time is not possible in this mode on the test setup).

In each movie, mode of operation is refreshed at each frame. The rolling shutter scheme is applied according to the following addressing modes:

- addressing per frame.

The operation of the sensor in this mode is detailed here after.

The rolling shutter scheme involves two line address pointers called Y-Readout (YRD) and Y-Reset (YRST) pointers. Integration time is based on the time shift between these two pointers (refer to Figure 6-2). For instance, the integration time of 2 ms used in DR mode implies a shift of 10 lines between Reset and Video rolling pointers.

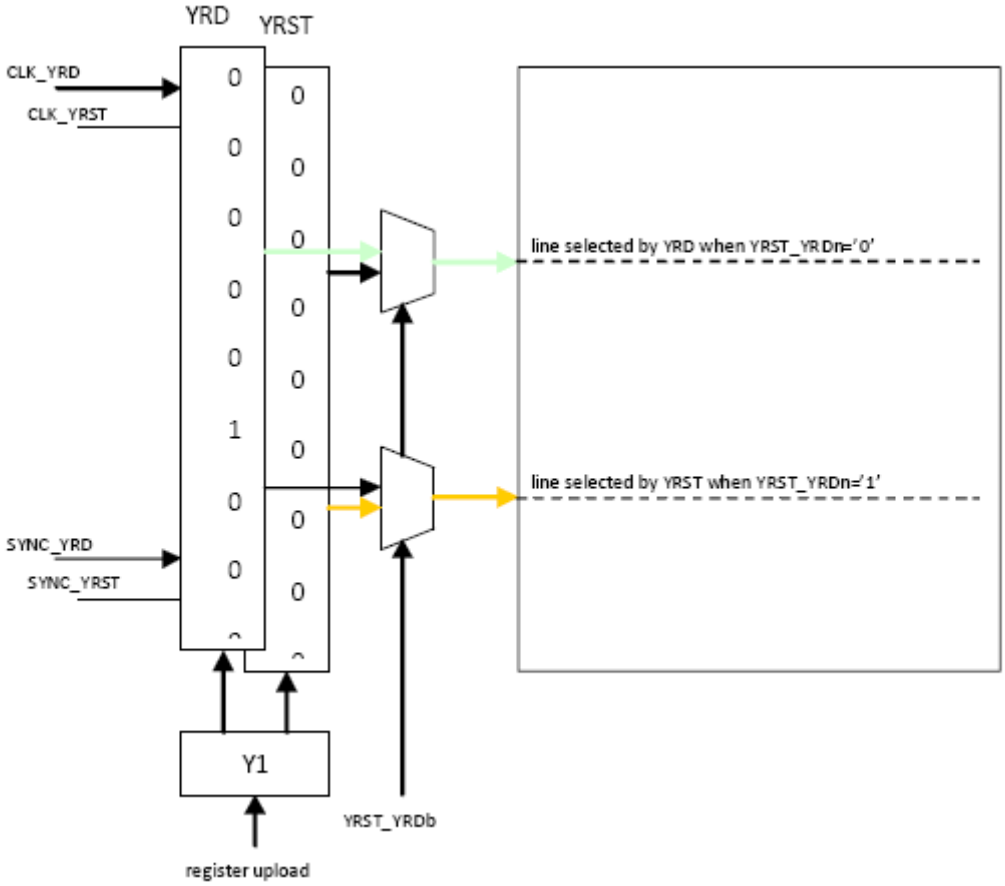

Figure 6-2 : Line Addressing Structures: YRD and YRST shift register pointers

Addressing per line means that the address of each line is uploaded in the Y1 programmable start-of-scan register.

Addressing per frame means that only the address of the 1st line of the frame is uploaded in Y1. The next lines are scanned by clocking the Y-address shift registers (incremental addressing). Previous testing has shown that image corruption can occur under heavy ions flux in this operating mode. A change in the density of particle induced events has been observed related to variation of integration time within a single frame. This behaviour is likely due to Y address pointers errors (whether Reset or Video pointer) inducing modification of the integration time on portion(s) of the image.

The camera system consists in 4 main components (Figure 6-3). The boards implemented in the system are detailed hereafter:

- A digital controller runs the image sensor controller, the frame grabber and the communication to a PC.
- A cable interface board contains the controllable power supplies, cable line drivers to drive the control signals to the DUT and receivers that receive the video signal from the DUT.
- A cable receiver board receives the driving signals from the controller and also contains buffers to drive the video signal to the 5 meter long cable.
- A radiation/burn-in board contains the DUT. The DUT returns a video signal to the controller.

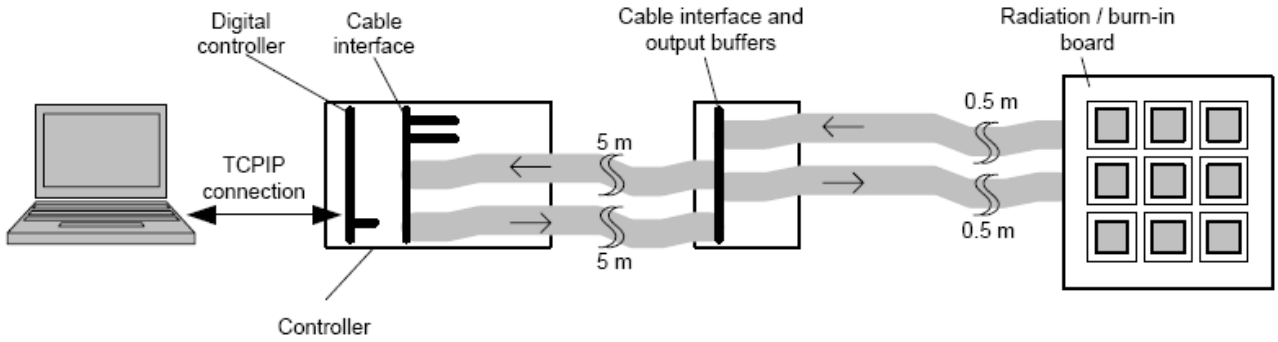

Figure 6-3 : Overview of the HAS2 test setup

The system operates one sample at nominal frequency. Read-back of the images is provided at nominal operating frequency. If a sustained transfer of images is not possible provisions are made to record a sequence of at least 256 images at nominal image sensor speed. A cable of at least 2 m is required between the driving system and the radiation board. The harnessing is compatible with the available space in the irradiation chamber. A TCIP connection is used between the irradiation chamber and the control room.

During irradiation the device supply currents are monitored separately. In case of latch-up or device failure, the following parameters can be logged: power supply where the latch-up condition occurred, time when the condition occurred, and latch-up current. In case of latch-up the current supplied to the device is limited to a safe value in order to prevent damage.

7.EXPERIMENTAL RESULTS

7.1.Testing protocol

The purpose of the proton test is to collect particle-induced upset events occurring in the HAS2 pixel array and in its registers. Movies of several images are stored. Each movie contains several images under beam and a few images in darkness (beam OFF) at the beginning of the movies. The few images acquired in darkness can be used to correct from FPN the images taken under proton beam. Incident proton flux is less than 1.0e+06 protons/cm²/s in order to collect isolated transient signals in the pixel array for integration time of 2.0 milliseconds (DR mode). This short integration time is possible in DR mode but not in NDR mode (200 ms is the minimum). Image acquired in NDR are only used to detect potential upset in HAS internal registers and multiplexer or mean signal increase. In DR mode, signal sizes of the pixel array are measured during irradiation under normal and tilted angle (60°) along X and Y axis.

7.2.Detailed run list and proton induced SET computation

The runs presented in Table 7-1 were performed. 2120 images were stored in DR mode (final images) and 630 images were stored in NDR mode (including reference, video, and final images). The images are available in TIFF format as full frame image of 2 Mbytes size.

The data obtained after image correction are illustrated in Figure 7-1. The cartography on the left side is a zoom on a few events. The related histogram is on the right side. Distribution is dominated by sensor noise with a few pixels emerging outside the Gaussian part (proton induced signal). Pixel intensity is 20 electrons/LSB.

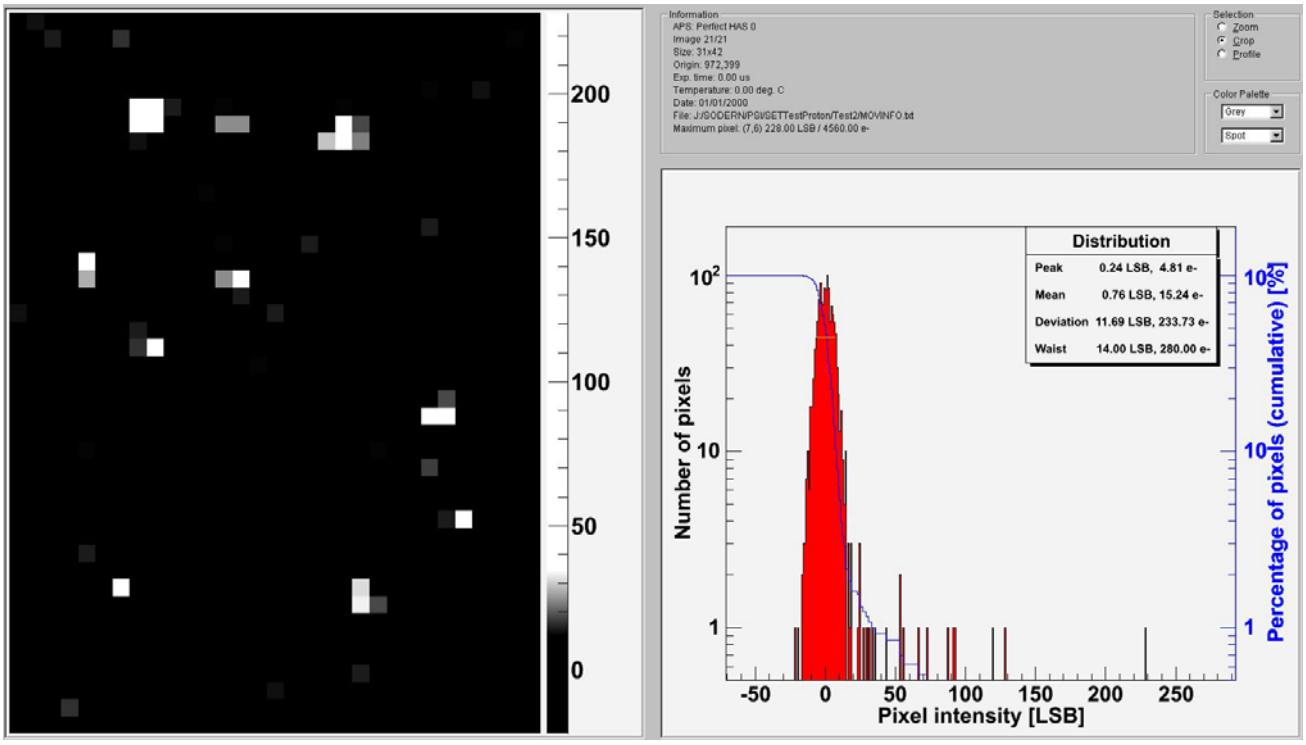

Figure 7-1 : 100 MeV proton induced events in DR mode with 2 ms integration time

In order to select relevant events, the pixels of the corrected images are scanned using a detection threshold at 6 times the noise floor of the detector. When a pixel above threshold is detected, the proton induced signal size is calculated according to two different methods. First method is a clustering method which makes the summation of adjacent pixels until pixel value is below 1.5 times the noise floor of the detector. Second method makes the summation of pixel signal in a 3x3 pixel pattern. This latter method is assumed to remove some merged events. When using a 5x5 pattern, the difference in the measured signal is negligible *wrt* 3x3 pattern.

The distributions of the spot signal obtained through the two methods are detailed in § 9 ANNEX. The raw histograms are extracted from one image per run. The SET computation histograms take into account the whole events obtained on several images. The average number of events per image is indicated. The distribution of the spot size obtained through the first method (i.e. quantity of pixels clustered to form the total proton induced signal) is plotted as well. The spot signal and spot size are obtained by taking the value at maximum population of the histograms.

The computed spot sizes and spot signals are summarized in Table 7-1. Proton induced transient signals are generated in the pixel array by direct ionization. Effective LET (LET_{eff}) is derived from the proton energy together with beam angle enhancement effect (i.e. LET_{eff} is the result of LET divided by the beam angle cosine). The interaction thickness ($l_{th.}$) is obtained from the ratio between measured signal and LET_{eff}.

Table 7-1: Run list for proton induced Single Event Effects characterization

Test Run n°	Sample	Proton energy [MeV]	Beam flux [p+/cm²/s]	Beam Angle	Irradiation duration [seconds]	Readout Mode	Integration Time [ms]	Stored Image	Effective LET [e-/µm]	Events expected count [SET/frame]	Selected images	Events mean count [SET/frame]	Clustering method Determination			3x3 method Determination		Histogram peak shift method		COMMENT
													Signal [e-]	Size [pixel]	Ith [µm]	Signal [e-]	Ith [µm]	Signal [e-]	Ith [µm]	
1	A	100	5.00E+05	0°	20	DR	2	20	378											beam off
2	A	100	5.00E+05	0°	20	DR	2	100	378	3.40E+03	5 to 25	2842	1995	4.4	5.3	2013	5.3			
3	A	100	5.00E+05	0°	20	DR	1.2	100	378	2.04E+03	25 to 44	1776	1822	4.2	4.8	1924	5.1			
4	A	100	5.00E+05	0°	20	DR	2	100	378	3.40E+03	25 to 44	2905	1935	4.4	5.1	1992	5.3			
5	A	175	5.00E+05	0°	20	DR	2	100	256	3.40E+03	26 to 45	2175	1302	2.9	5.1	1437	5.6			
6	A	230	5.00E+05	0°	20	DR	2	100	215	3.40E+03	25 to 43	2222	1072	2.2	5.0	1227	5.7			
7	A	230	5.00E+05	0°	40	NDR	200	30	215	3.40E+05										incorrect offset
8	A	230	5.00E+05	0°	40	NDR	200	30	215	3.40E+05	1 to 30							8.2E+02	11.8	
9	A	100	1.00E+06	60° Y axis	20	DR	2	100	756	3.40E+03	29 to 48	4212	4001	6.4	5.3	3831	5.1			double flux
10	A	100	5.00E+05	60° Y axis	20	DR	2	100	756	1.70E+03	20 to 39	1772	3601	5.6	4.8	3547	4.7			
11	A	175	5.00E+05	60° Y axis	20	DR	2	100	512	1.70E+03	25 to 44	1737	2275	4.7	4.4	2301	4.5			
12	A	230	5.00E+05	60° Y axis	20	DR	2	100	430	1.70E+03	25 to 44	1603	1914	4.2	4.5	1978	4.6			
13	A	230	5.00E+05	60° Y axis	40	NDR	200	30	430	1.70E+05	1 to 30							7.8E+02	11.2	
14	A	100	5.00E+05	60° X axis	20	DR	2	100	756	1.70E+03	25 to 44	1444	3982	5.8	5.3	3934	5.2			
15	A	175	5.00E+05	60° X axis	20	DR	2	100	512	1.70E+03	25 to 44	1608	2644	5.3	5.2	2608	5.1			
16	A	230	5.00E+05	60° X axis	20	DR	2	100	430	1.70E+03	25 to 44	1648	2184	4.6	5.1	2235	5.2			
17	A	230	5.00E+05	60° X axis	40	NDR	200	30	430	1.70E+05	1 to 30							7.8E+02	11.2	
18	B	100	5.00E+05	0°	20	DR	2	100	378	3.40E+03	25 to 44	2932	2098	4.4	5.6	2018	5.3			
19	B	175	5.00E+05	0°	20	DR	2	100	256	3.40E+03	25 to 44	1960	1330	2.8	5.2	1545	6.0			
20	B	230	5.00E+05	0°	20	DR	2	100	215	3.40E+03	25 to 44	1557	1287	-	6.0	1320	6.1			
21	B	230	5.00E+05	0°	40	NDR	200	30	215	3.40E+05	1 to 30							8.6E+02	12.3	
22	C	100	5.00E+05	0°	20	DR	2	100	378	3.40E+03										not computed
23	C	175	5.00E+05	0°	20	DR	2	100	256	3.40E+03										not computed
24	C	230	5.00E+05	0°	20	DR	2	100	215	3.40E+03										not computed
25	C	230	5.00E+05	0°	40	NDR	200	30	215	3.40E+05	1 to 30							8.8E+02	12.6	
26	D	100	5.00E+05	0°	20	DR	2	100	378	3.40E+03	25 to 44	2938				1767	4.7			
27	D	175	5.00E+05	0°	20	DR	2	100	256	3.40E+03	25 to 44	2227				1460	5.7			
28	D	230	5.00E+05	0°	20	DR	2	100	215	3.40E+03	25 to 44	2581				1253	5.8			
29	D	230	5.00E+05	0°	40	NDR	200	30	215	3.40E+05	1 to 30							9.4E+02	13.5	
													MEAN Ith		**5.1**		**5.3**			

7.3.Observations

7.3.1.Pixel array SET

The measured spot size presented in Table 7-1 is consistent with sensor pixel crosstalk [RD 1] characterized under visible illumination. Various patterns are obtained depending on the position of the proton hit. The SET spot size at 0° beam angle is illustrated in Figure 7-1 (DR mode 2 ms integration time). SET cartography for 60° beam incidence is shown in Figure 7-2. Though proton beam is tilted wrt normal incidence, extension in spot size is not evidenced. Indeed, the size of the spot is driven by the carrier diffusion effect in the epitaxial layer of the sensor. Local interaction of proton inside the pixel volume (18×18×6 µm³) is negligible compared to the diffusion length.

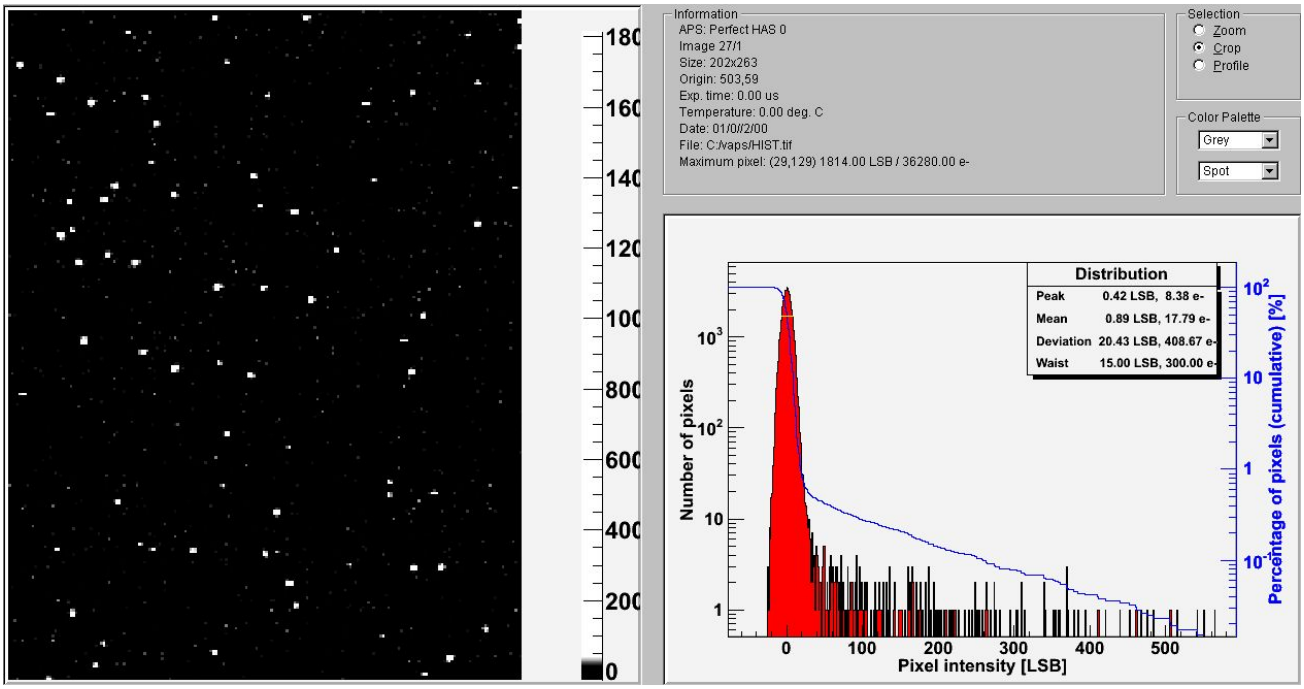

Figure 7-2 : Pixel array SET captured under angle100 MeV proton at 60° in DR mode

The signal size under normal incidence is within expectations with a mean silicon interaction thickness of 5.2 µm, close to the technology epitaxial layer of 5 µm. This value follows the trend observed in [RD 4] where the active layer thickness is found to be 5.5 µm at 55 MeV and 6.4 µm at 29 MeV proton energy.

Spot signal distributions exhibit a large width and a systematic skewed shape. These energetic events can be modelled by taking into account particle-to-particle energy deposition variation (straggling process [RD 5]).

On the raw histograms, a small quantity of pixels (5 to 10) is going below the normal offset (see § 9.1). These “negative” events can be explained by a proton hit occurring in the photodiode right after the reset pulse and just before the end of the reference sampling (temporal window of 2.0 µs).

No difference has been observed between neutron or total dose irradiated device and unirradiated devices.

7.3.2. NDR addressing per frame operating mode

The full frame images acquired in NDR mode have been reviewed including reference, video and final (video levels corrected from reference levels) images. The beam flux is the same as the one applied for DR mode testing. Integration time is 100 times higher compared to DR testing condition. As a consequence, much more SET spots are generated in the video images. A typical image is presented in Figure 7-3 (final image). A few secondary particles are captured at grazing angles with respect to the pixel array plane. A reference image is shown in Figure 7-4. Because of the very short time between reset and reference sampling, no pixel array SET spots are captured.

The scanned images did not reveal any corruption or sensitivity of the sensor control registers even at the highest energy level. Although the upset of the address registers has a heavy ion LET threshold in the range of 10-20 MeV.cm²/mg [RD 7], no events have been observed under highly energetic protons.

A rough estimation of the interaction thickness is included in Table 7-1. This estimation is made by measuring the shift of the raw histogram peak between beam OFF and beam ON. The shift is considered to represent the mean signal per pixel (*Moy_pixel*) generated by the impinging protons. The interaction thickness ($I_{th.}$) is obtained from the ratio between the total measured signal (*Moy_pixel* × *1024* × *1024*) and the proton induced signal (*Events_count* × LET_{eff}). The purpose of this calculation is to compare irradiated and non irradiated devices. The interaction thickness based on DR mode experimental results is considered to be far more accurate.

No difference has been observed between neutron or total dose irradiated devices and unirradiated device.

Figure 7-3 : Typical full frame final image acquired under 230 MeV proton flux with 200 ms integration time in addressing per frame NDR mode

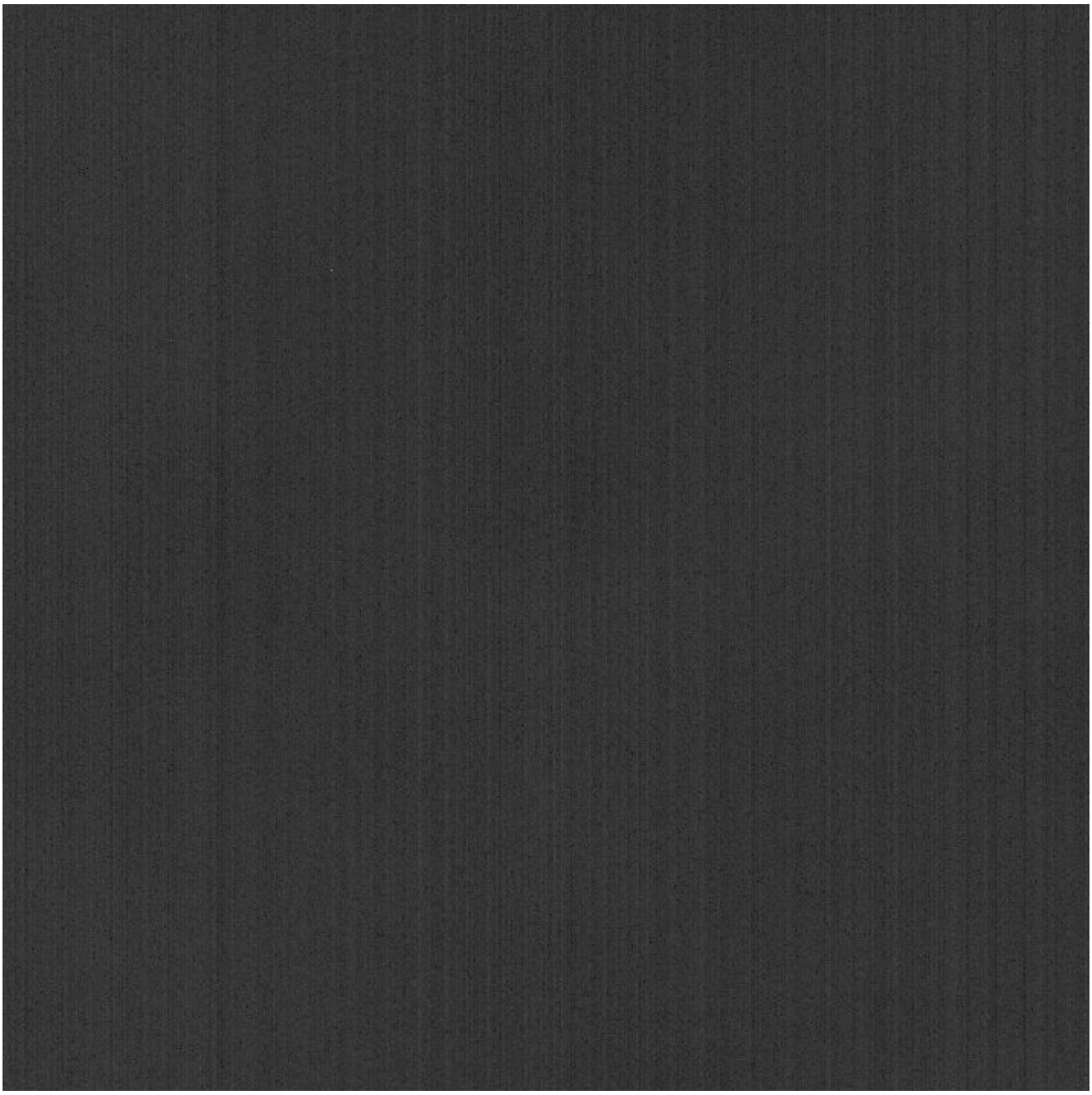

Figure 7-4 : Reference image acquired under 230 MeV proton flux at 200 ms integration time in addressing per frame NDR mode

8.CONCLUSIONS

The HAS2 image sensor has been tested at room temperature under high energy proton flux in both Destructive and Non Destructive Readout mode.

The proton induced spot size measured in the HAS2 pixel array is consistent with cross-talk figure of this sensor.

The proton induced SET signal is within expectation with mean signals corresponding to an active layer thickness of 5.2 µm.

Similar images and signal levels are found between irradiated and non irradiated devices.

Experimental results have confirmed that the HAS2 control registers are not sensitive up to 230 MeV proton energy.

9.ANNEX

9.1.Raw Histograms

9.1.1.All runs – beam OFF – DR mode

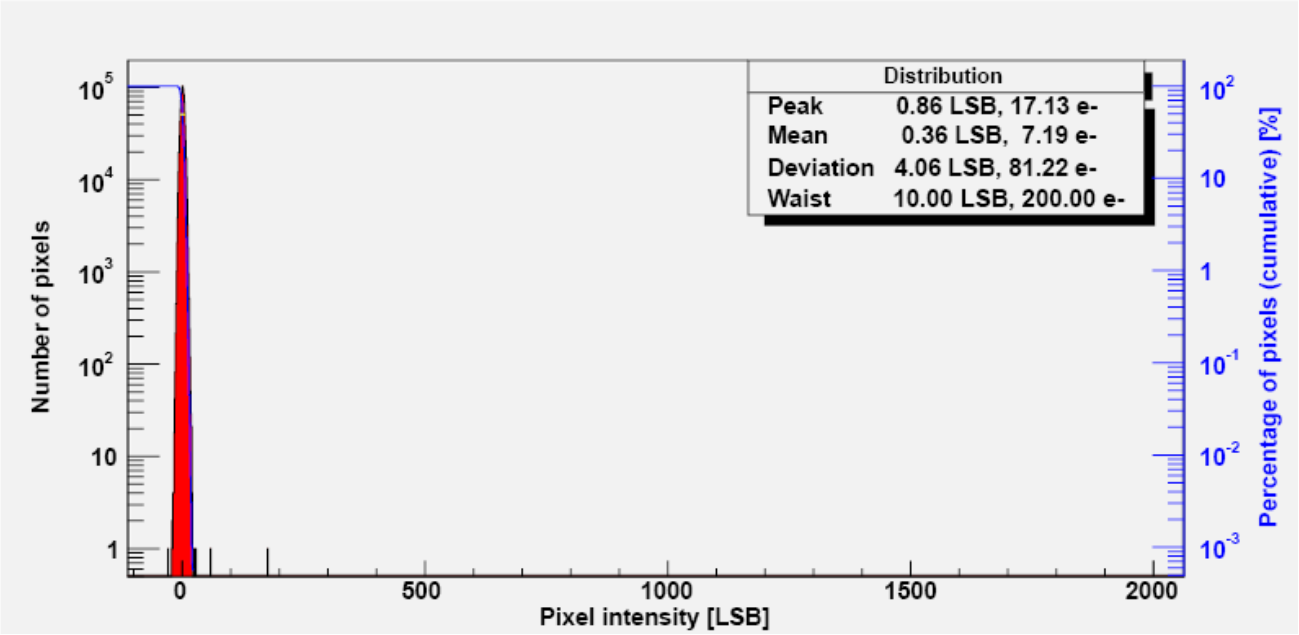

Figure 9-1: All runs – beam OFF – DR mode (average of 9 images)

9.1.2.Run 2 – 100 MeV – no tilt – DR mode

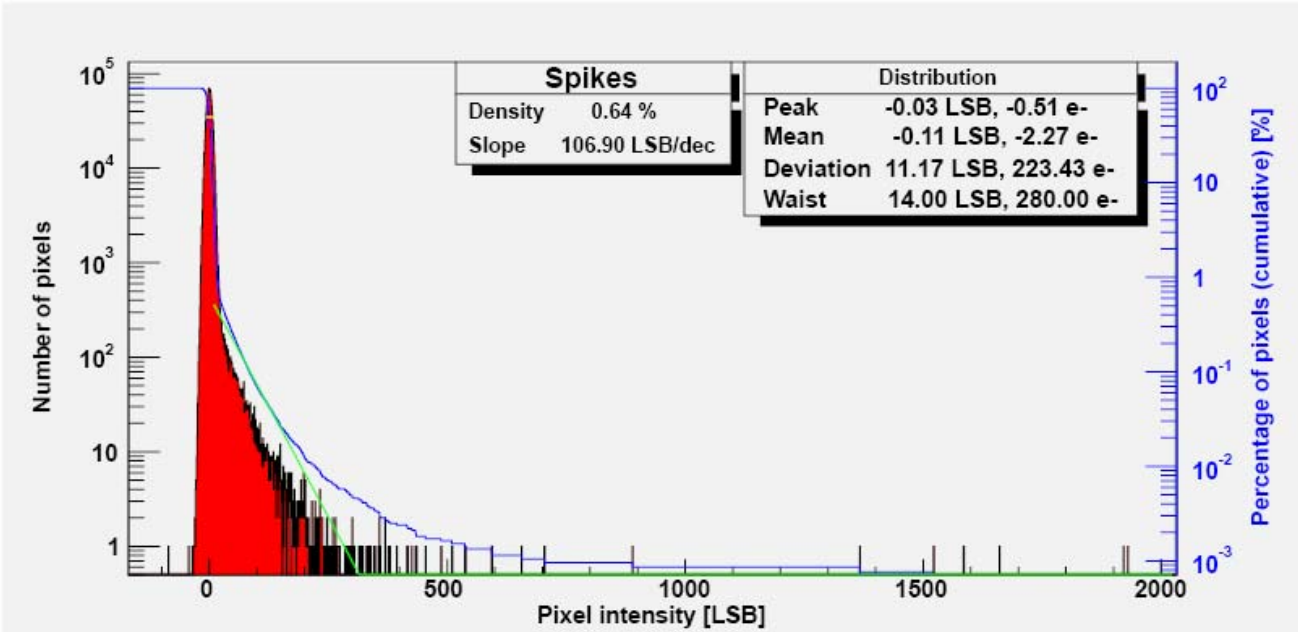

Figure 9-2: Run 2 – 100 MeV– no tilt – DR mode – 2 ms

9.1.3.Run 3 – 100 MeV – no tilt – DR mode

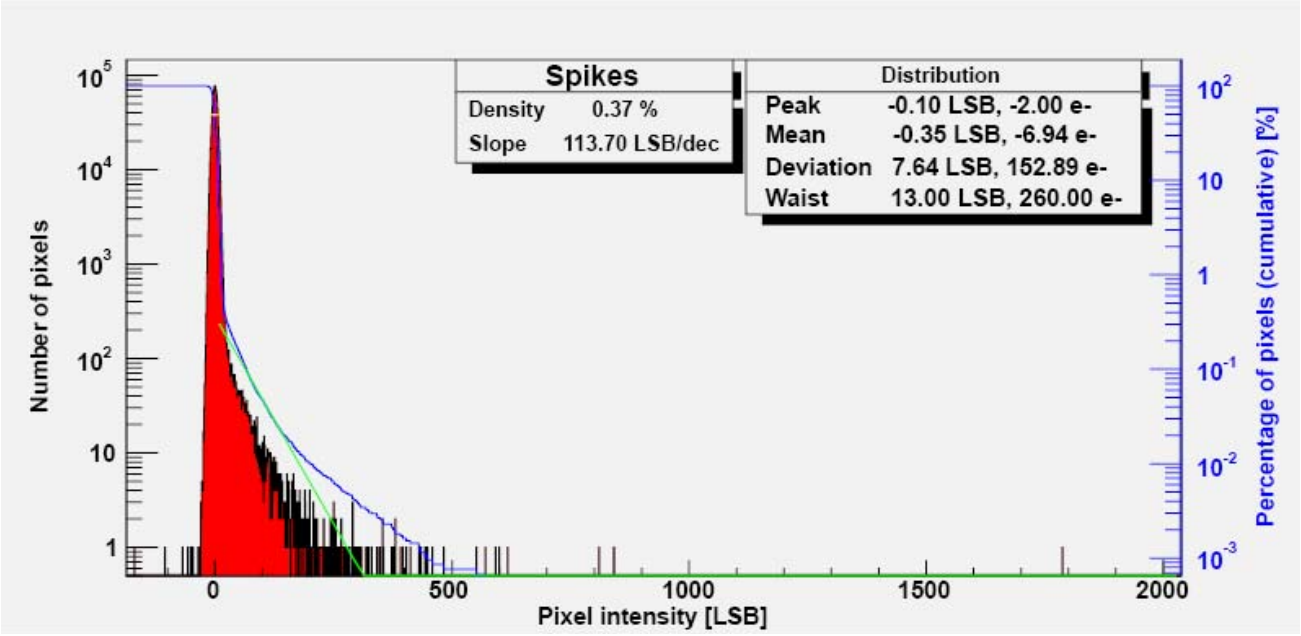

Figure 9-3: Run 3 – 100 MeV– no tilt – DR mode – 1.2 ms

9.1.4.Run 4 – 100 MeV – no tilt – DR mode

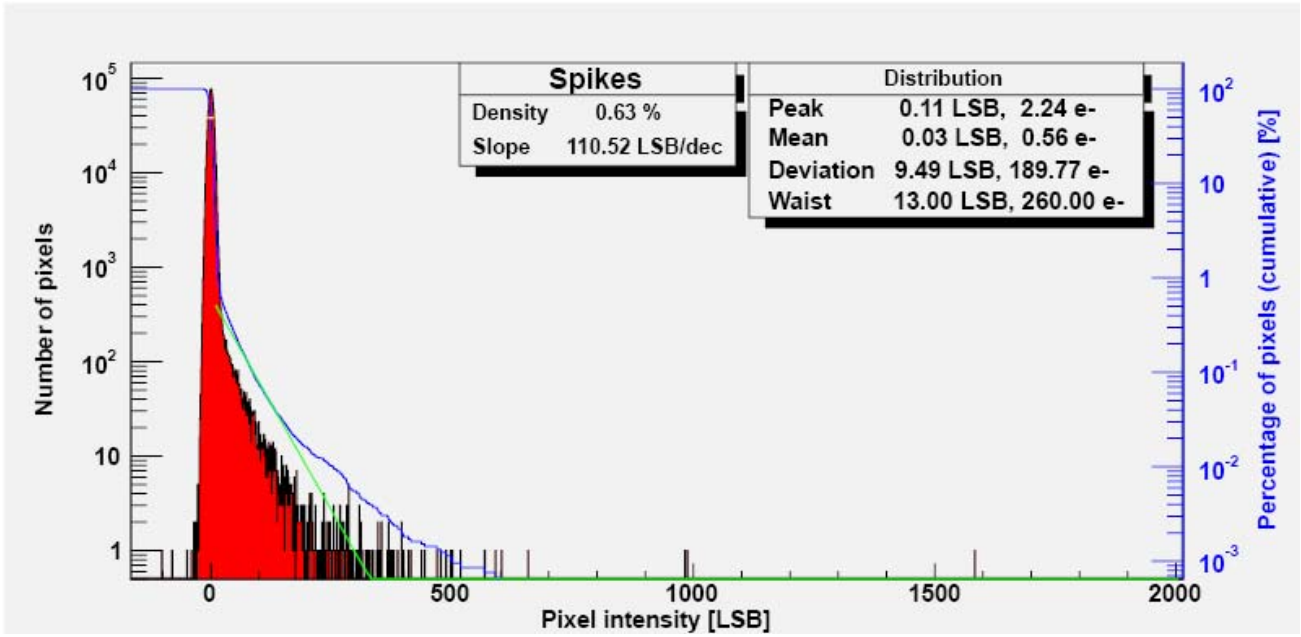

Figure 9-4: Run 4 – 100 MeV– no tilt – DR mode – 2 ms

9.1.5.Run 5 – 175 MeV – no tilt – DR mode

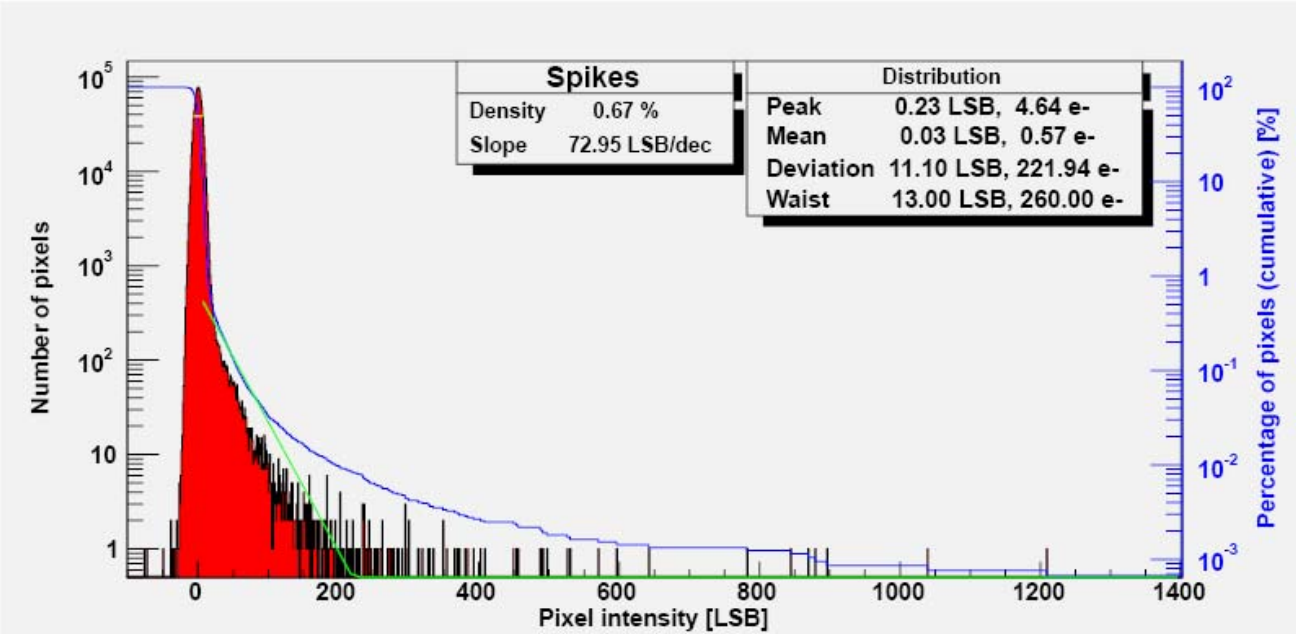

Figure 9-5: Run 5 – 175 MeV– no tilt – DR mode – 2 ms

9.1.6.Run 6 – 230 MeV – no tilt – DR mode

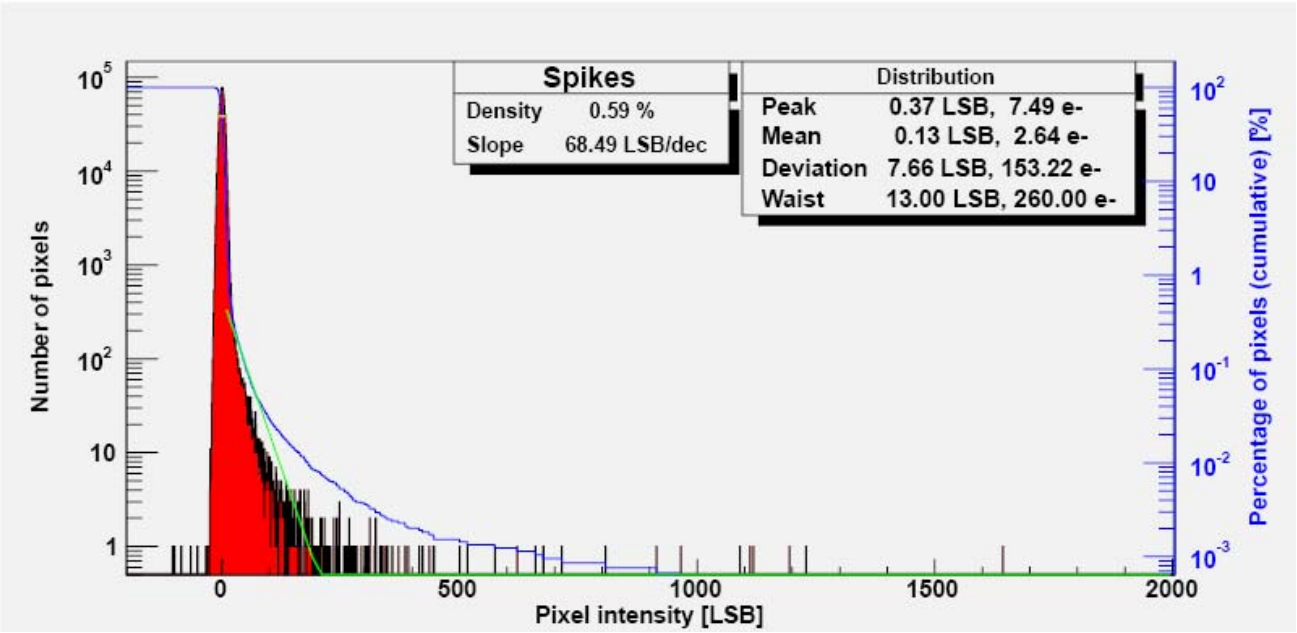

Figure 9-6: Run 6 – 230 MeV– no tilt – DR mode – 2 ms

9.1.7.Run 8 – 230 MeV – no tilt – NDR mode

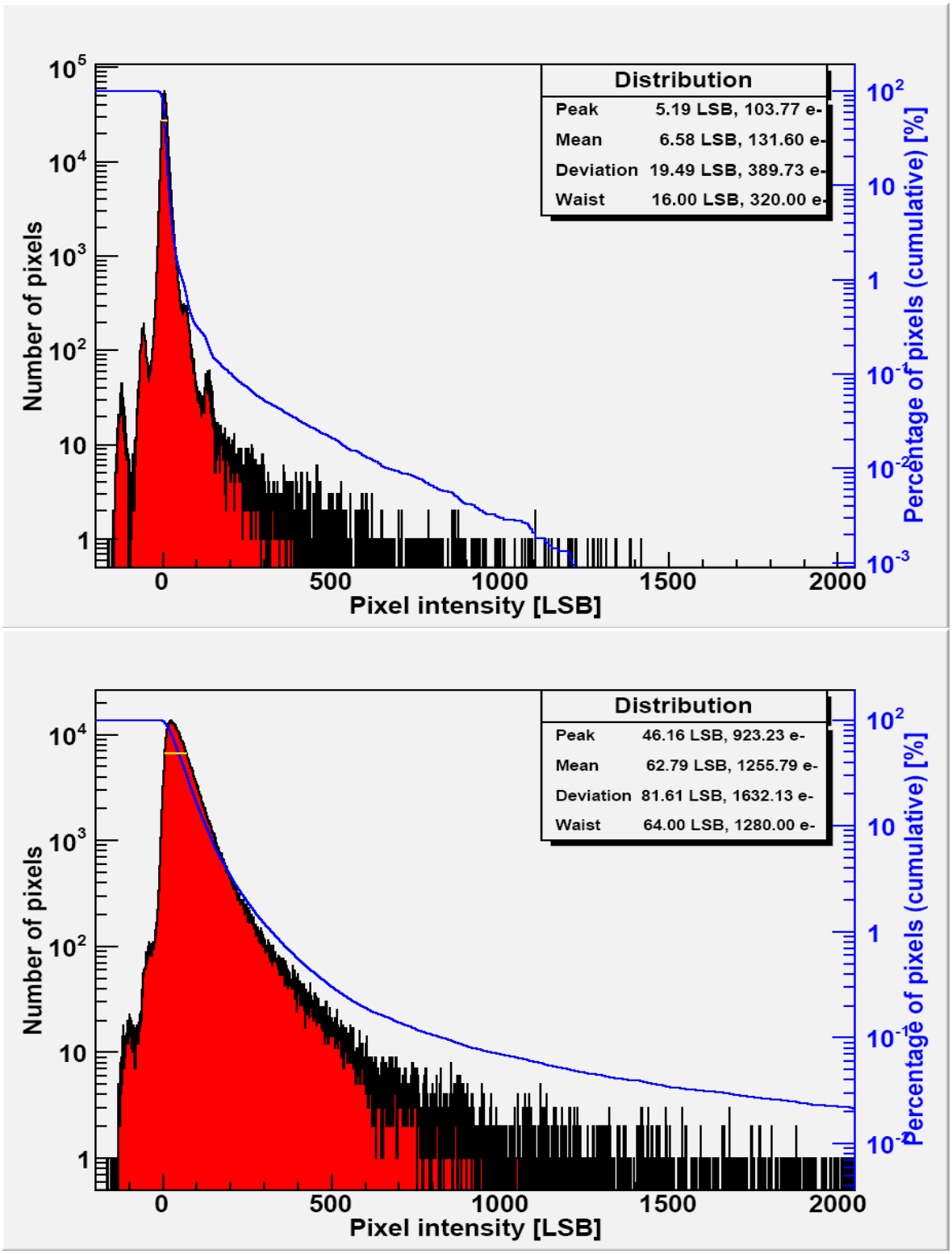

Figure 9-7: Run 8 – beam OFF (top side) and under 230 MeV proton beam (bottom side) not tilted – 200 ms integration time in NDR mode

9.1.8.Run 9 – 100 MeV – tilt 60° along Y axis – DR mode

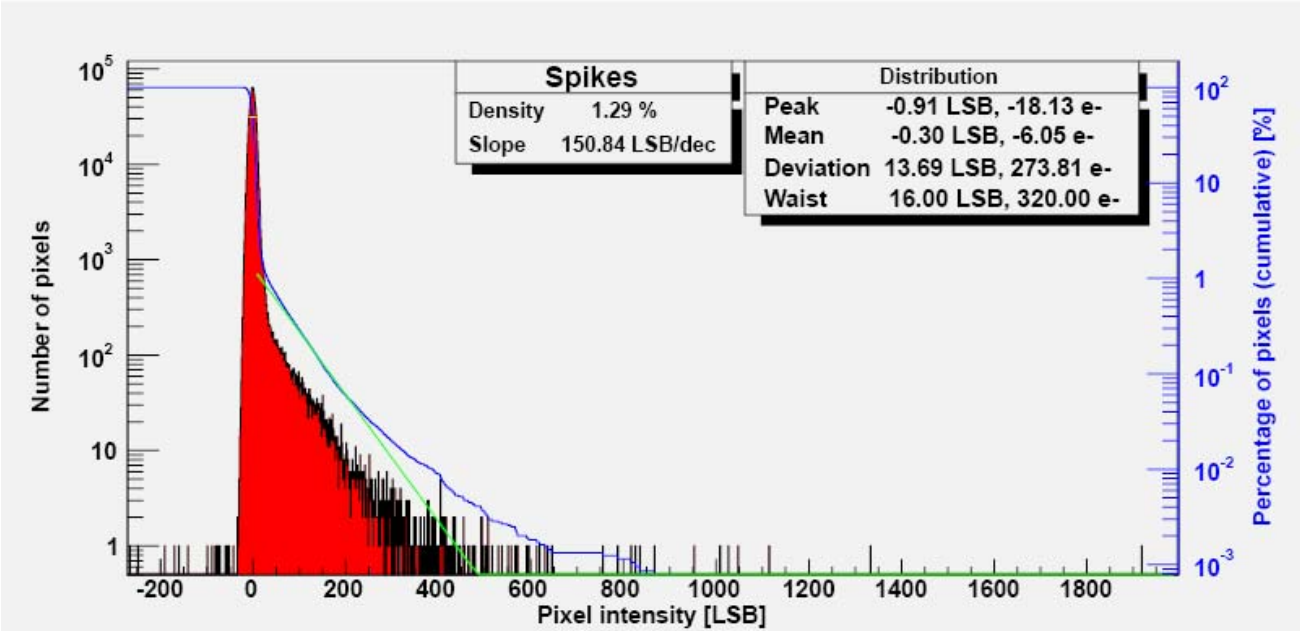

Figure 9-8: Run 9 – 100 MeV– tilt 60° along Y axis – DR mode – 2 ms

9.1.9.Run 10 – 100 MeV – tilt 60° along Y axis – DR mode

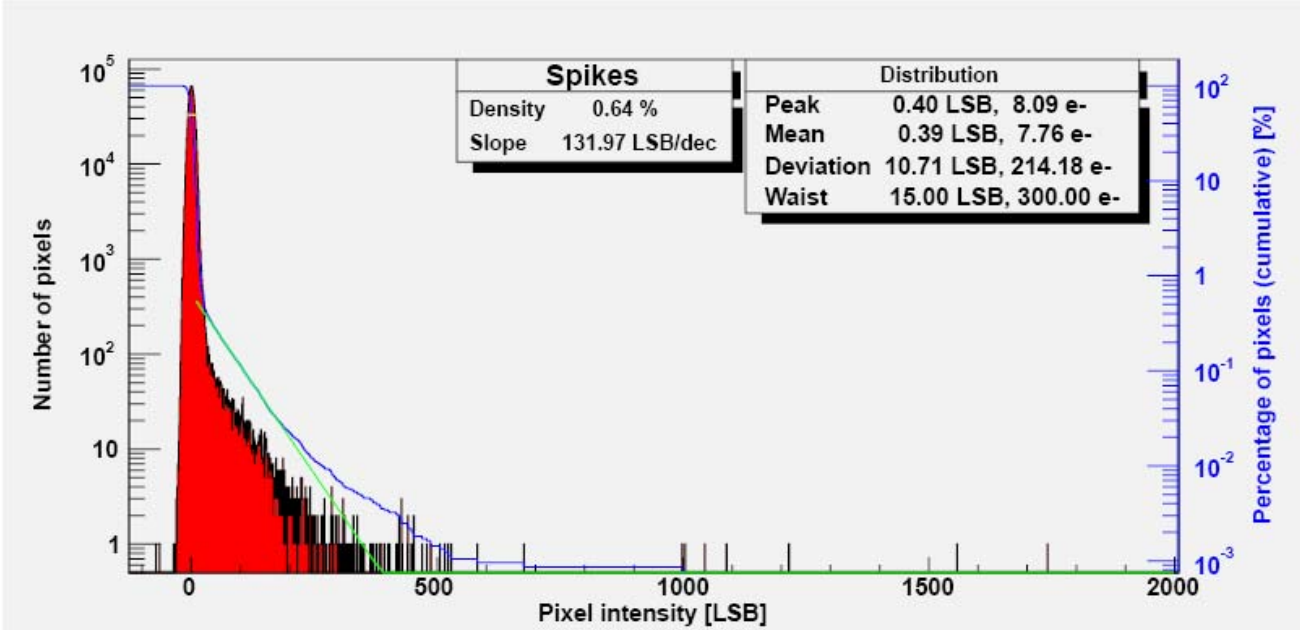

Figure 9-9: Run 10 – 100 MeV– tilt 60° along Y axis – DR mode – 2 ms

9.1.10. Run 11 – 175 MeV – tilt 60° along Y axis – DR mode

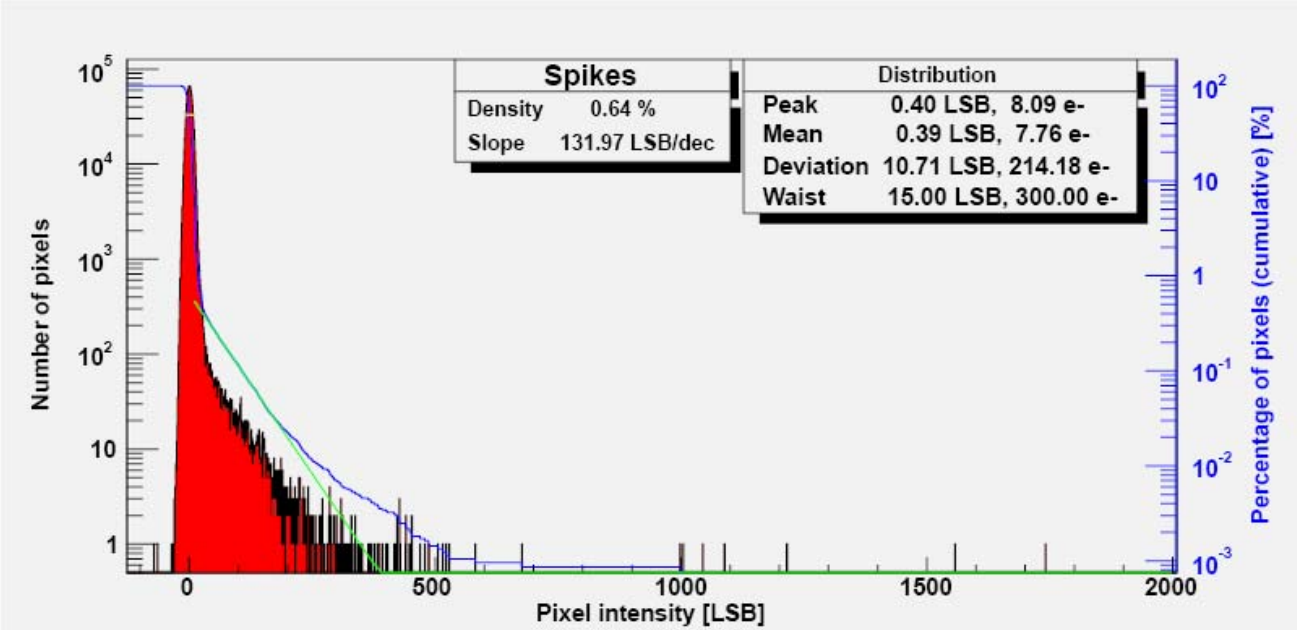

Figure 9-10: Run 11 – 175 MeV– tilt 60° along Y axis – DR mode – 2 ms

9.1.11. Run 12 – 230 MeV – tilt 60° along Y axis – DR mode

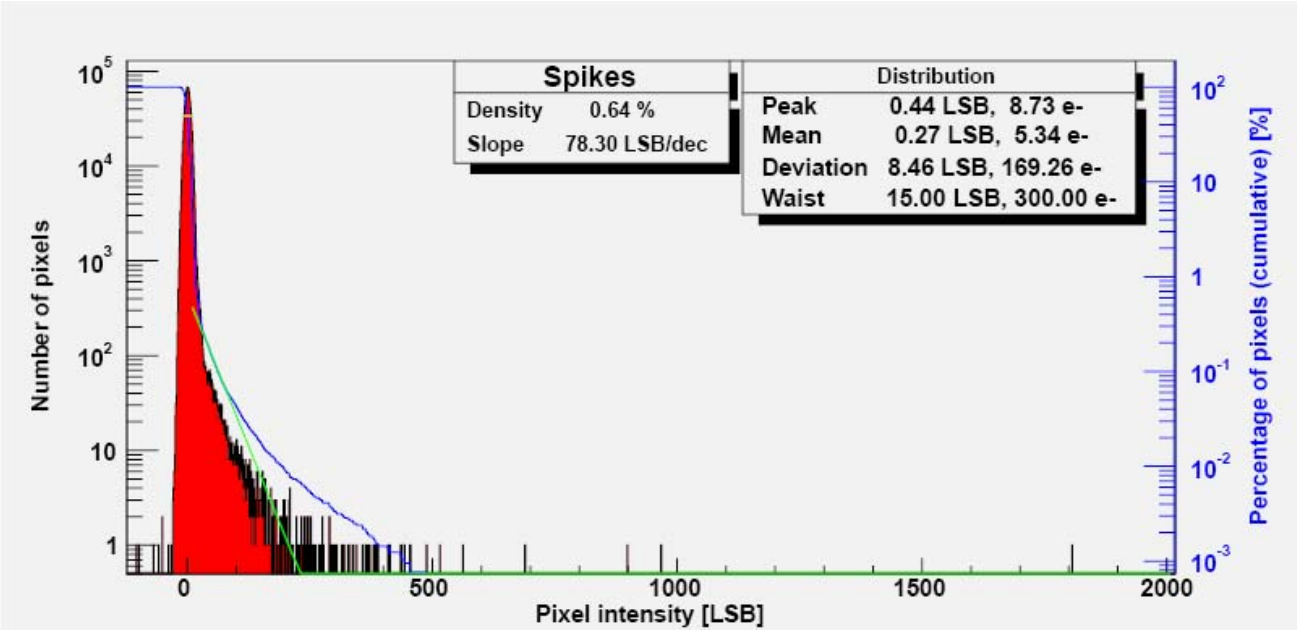

Figure 9-11: Run 12 – 230 MeV– tilt 60° along Y axis – DR mode – 2 ms

9.1.12.Run 13 – 230 MeV – tilt 60° along Y axis – NDR mode

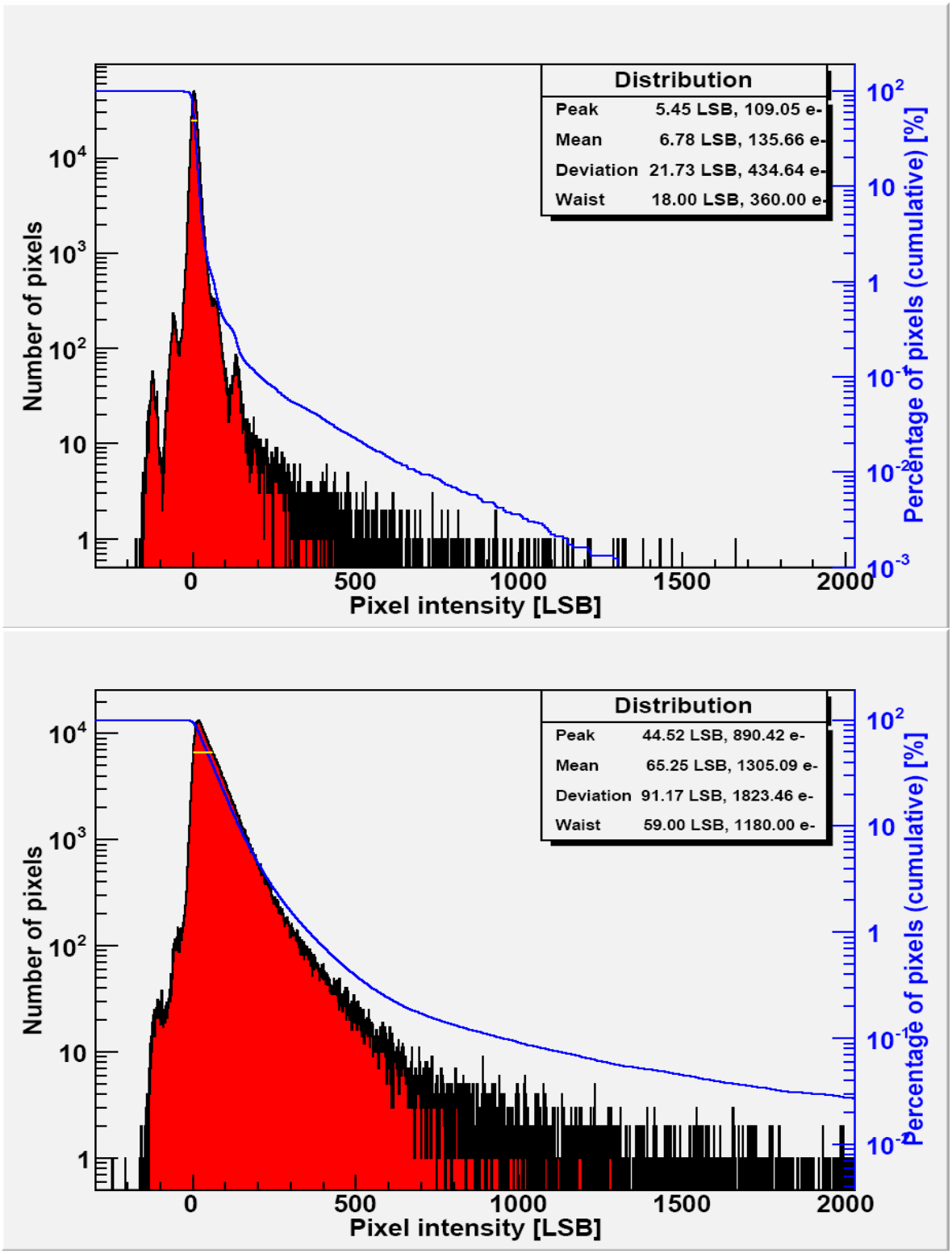

Figure 9-12: Run 13 – beam OFF (top side) & under 230 MeV proton beam (bottom side) tilt 60° along Y axis – NDR mode – 200 ms integration time

9.1.13. Run 14 – 100 MeV – tilt 60° along X axis – DR mode

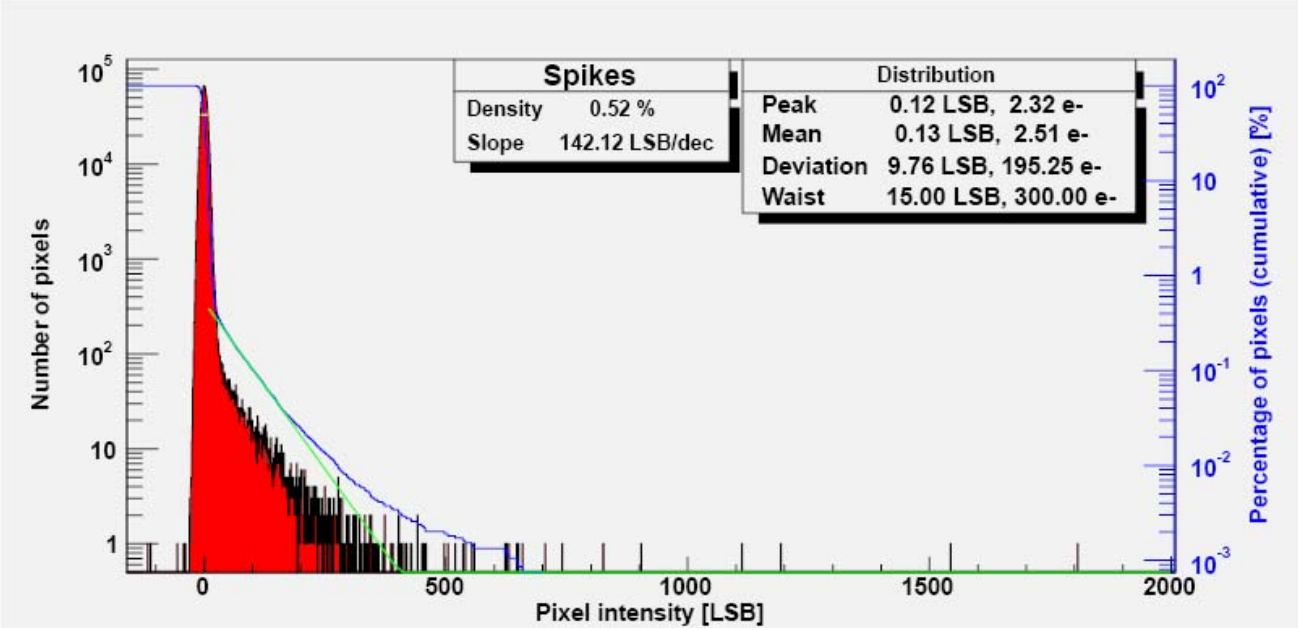

Figure 9-13: Run 14 – 100 MeV– tilt 60° along X axis – DR mode – 2 ms

9.1.14. Run 15 – 175 MeV – tilt 60° along X axis – DR mode

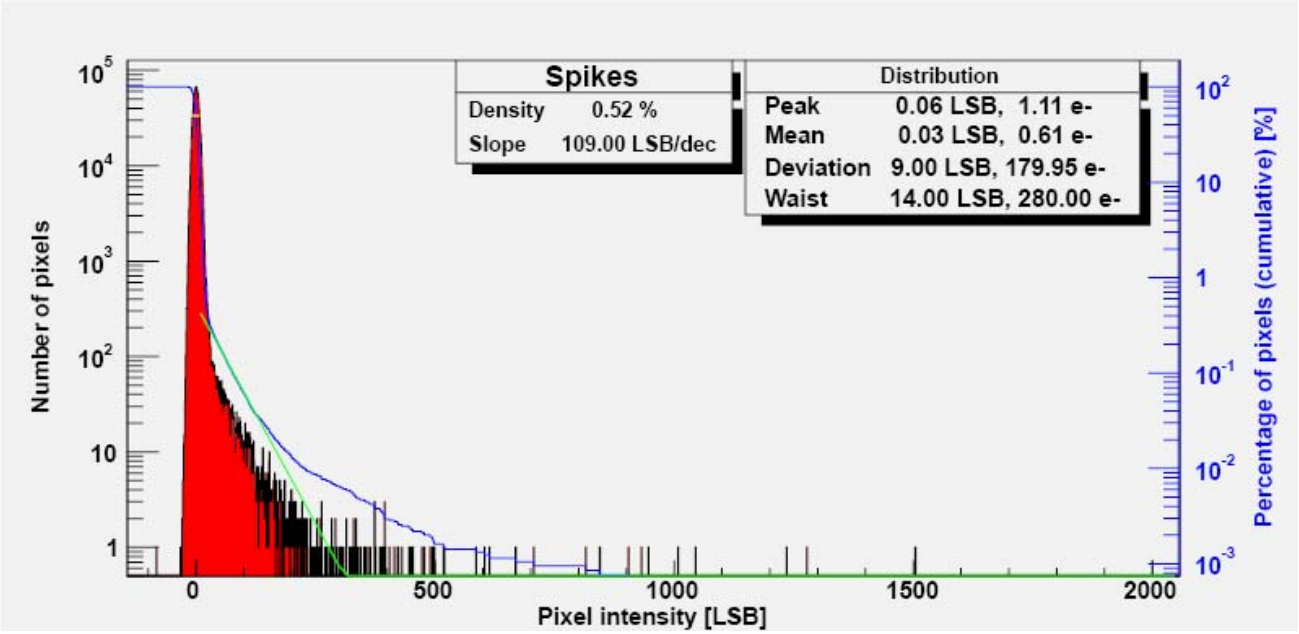

Figure 9-14: Run 15 – 175 MeV– tilt 60° along X axis – DR mode – 2 ms

9.1.15.Run 16 – 230 MeV – tilt 60° along X axis – DR mode

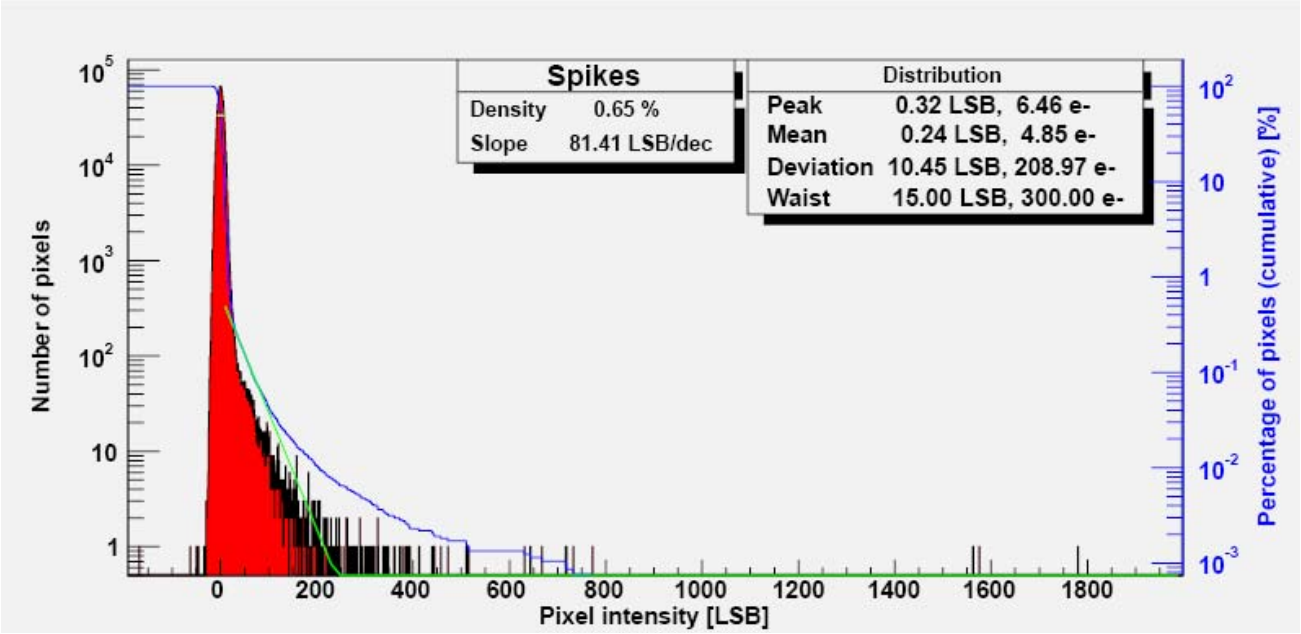

Figure 9-15: Run 16 – 230 MeV– tilt 60° along X axis – DR mode – 2 ms

9.1.16. Run 17 – 230 MeV – tilt 60° along X axis – NDR mode

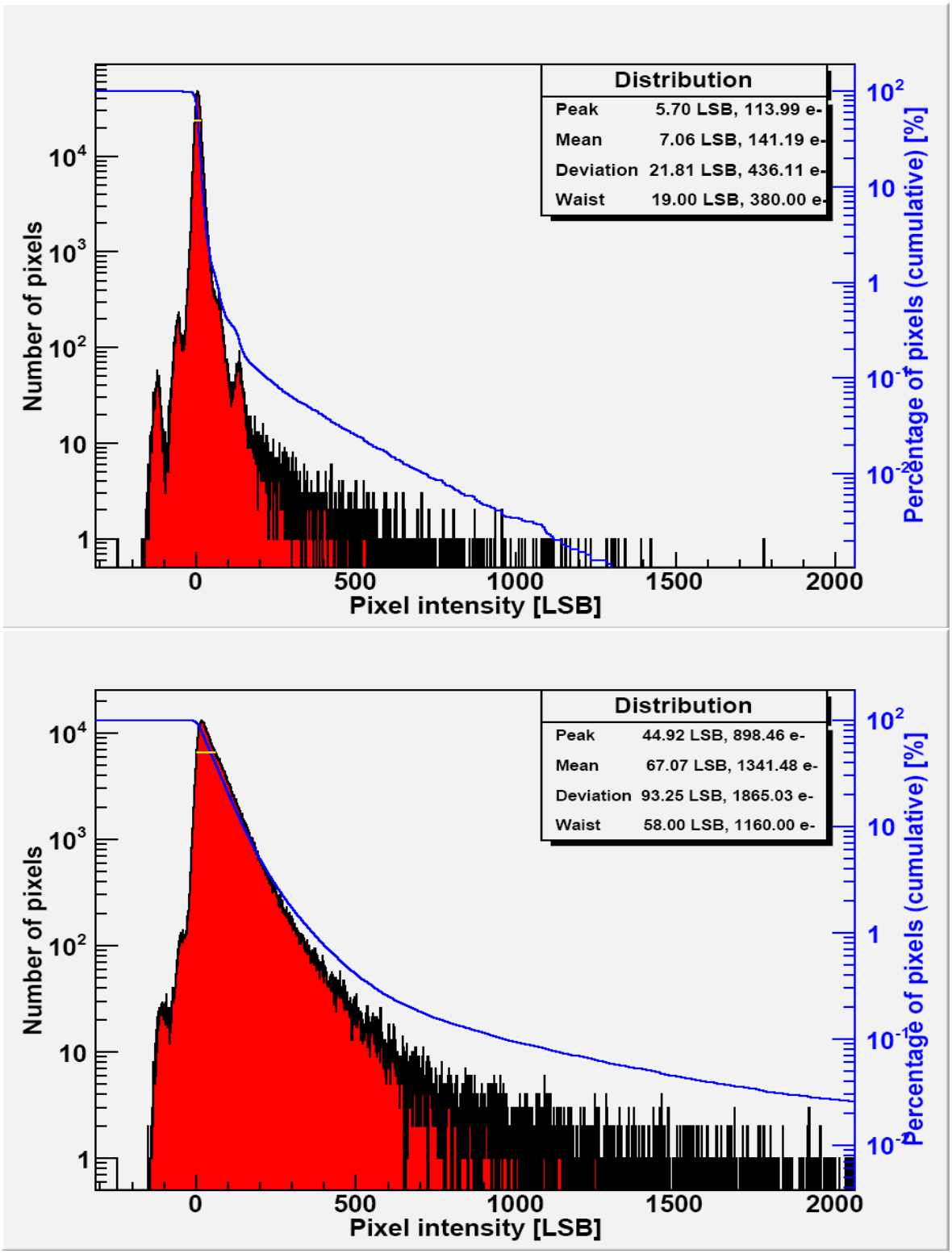

Figure 9-16: Run 17 – beam OFF (top side) & under 230 MeV proton beam (bottom side) tilt 60° along X axis – NDR mode – 200 ms integration time

9.1.17.Run 18 – 100 MeV– no tilt – DR mode

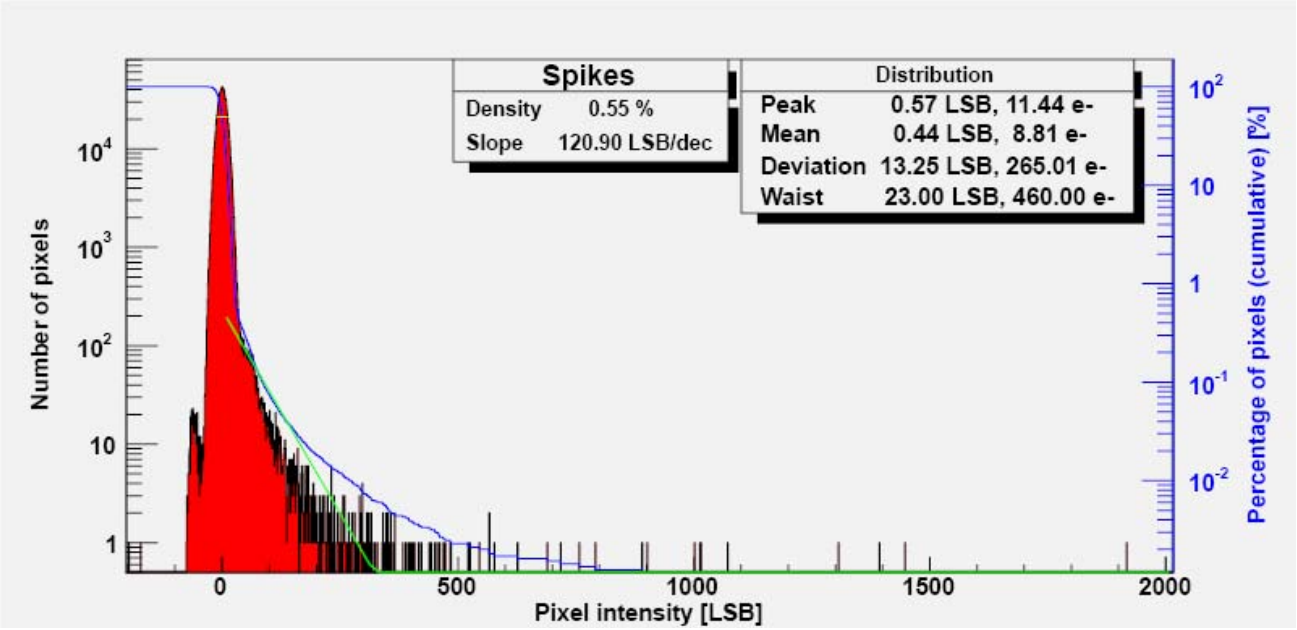

Figure 9-17: Run 18 – 100 MeV– no tilt – DR mode – 2 ms

9.1.18.Run 19 – 175 MeV– no tilt – DR mode

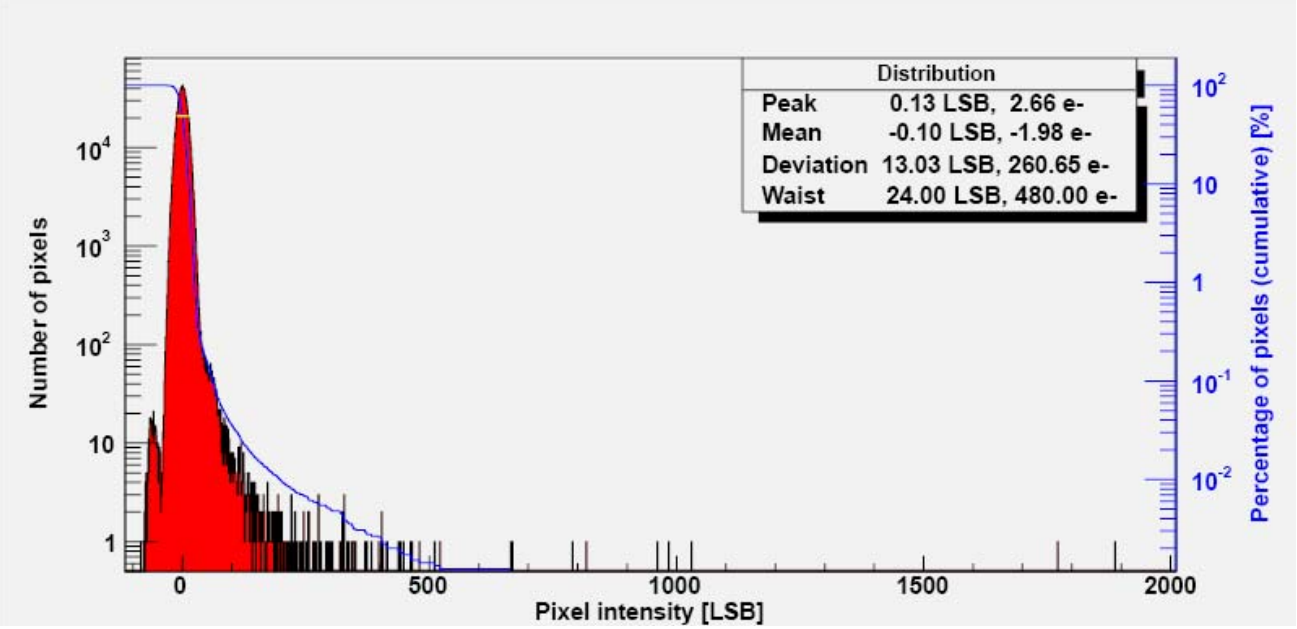

Figure 9-18: Run 19 – 175 MeV– no tilt – DR mode – 2 ms

9.1.19.Run 20 – 230 MeV– no tilt – DR mode

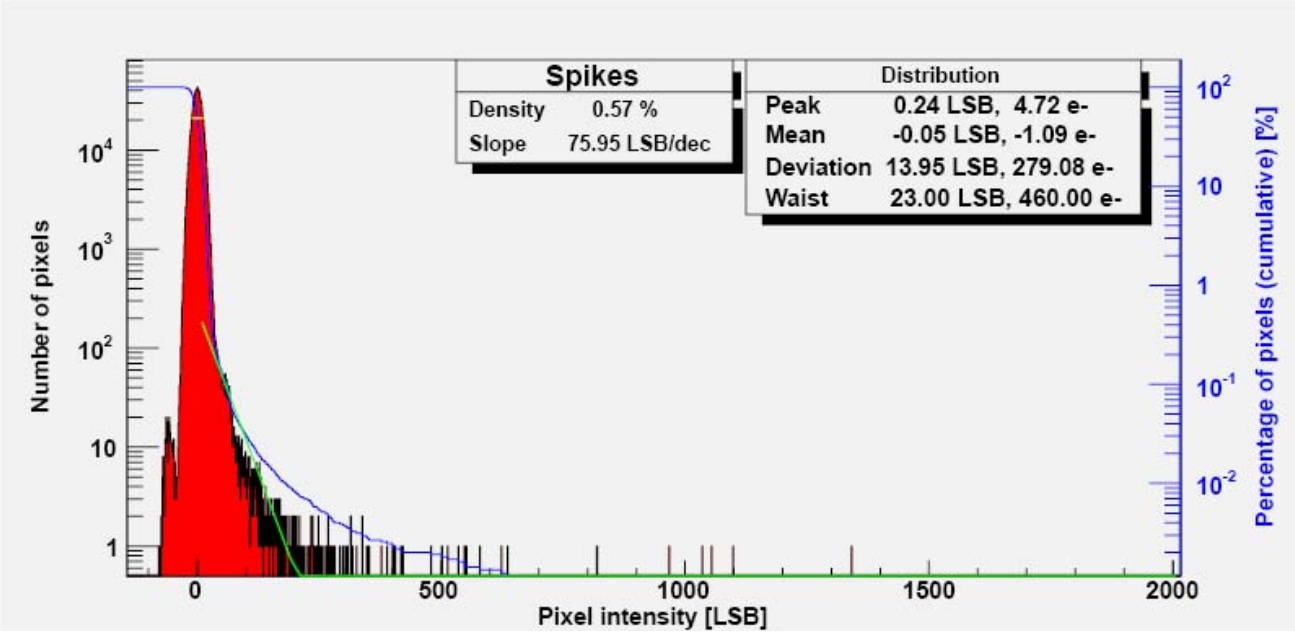

Figure 9-19: Run 20 – 230 MeV– no tilt – DR mode – 2 ms

9.1.20. Run 21 – 230 MeV – no tilt – NDR mode

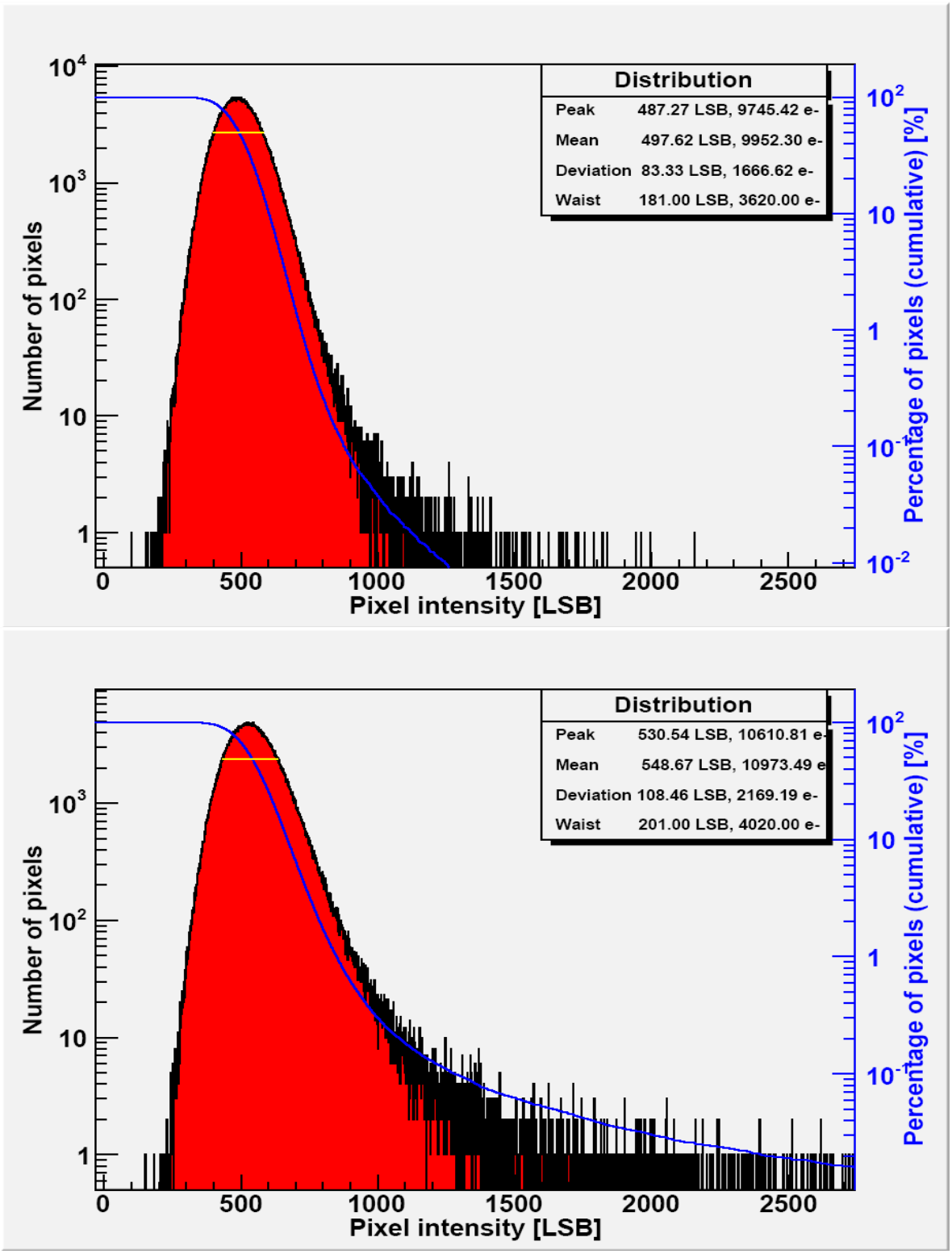

Figure 9-20: Run 21 – beam OFF (top side) & under 230 MeV proton beam (bottom side) no tilt – NDR mode – 200 ms integration time

9.1.21. Run 25 – 230 MeV – no tilt – NDR mode

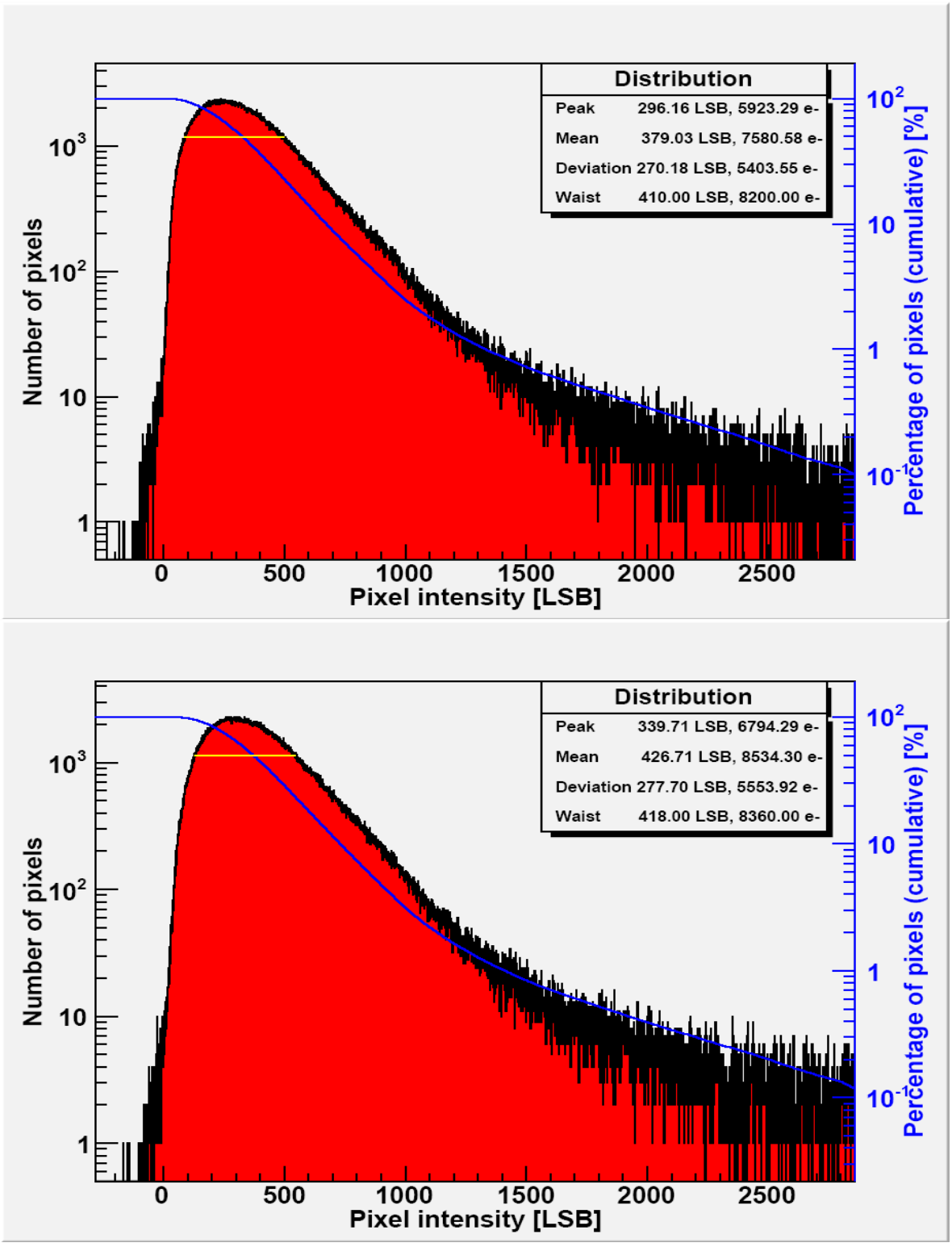

Figure 9-21: Run 25 – beam OFF (top side) & under 230 MeV proton beam (bottom side) no tilt – NDR mode – 200 ms integration time

9.1.22. Run 29 – 230 MeV – no tilt – NDR mode

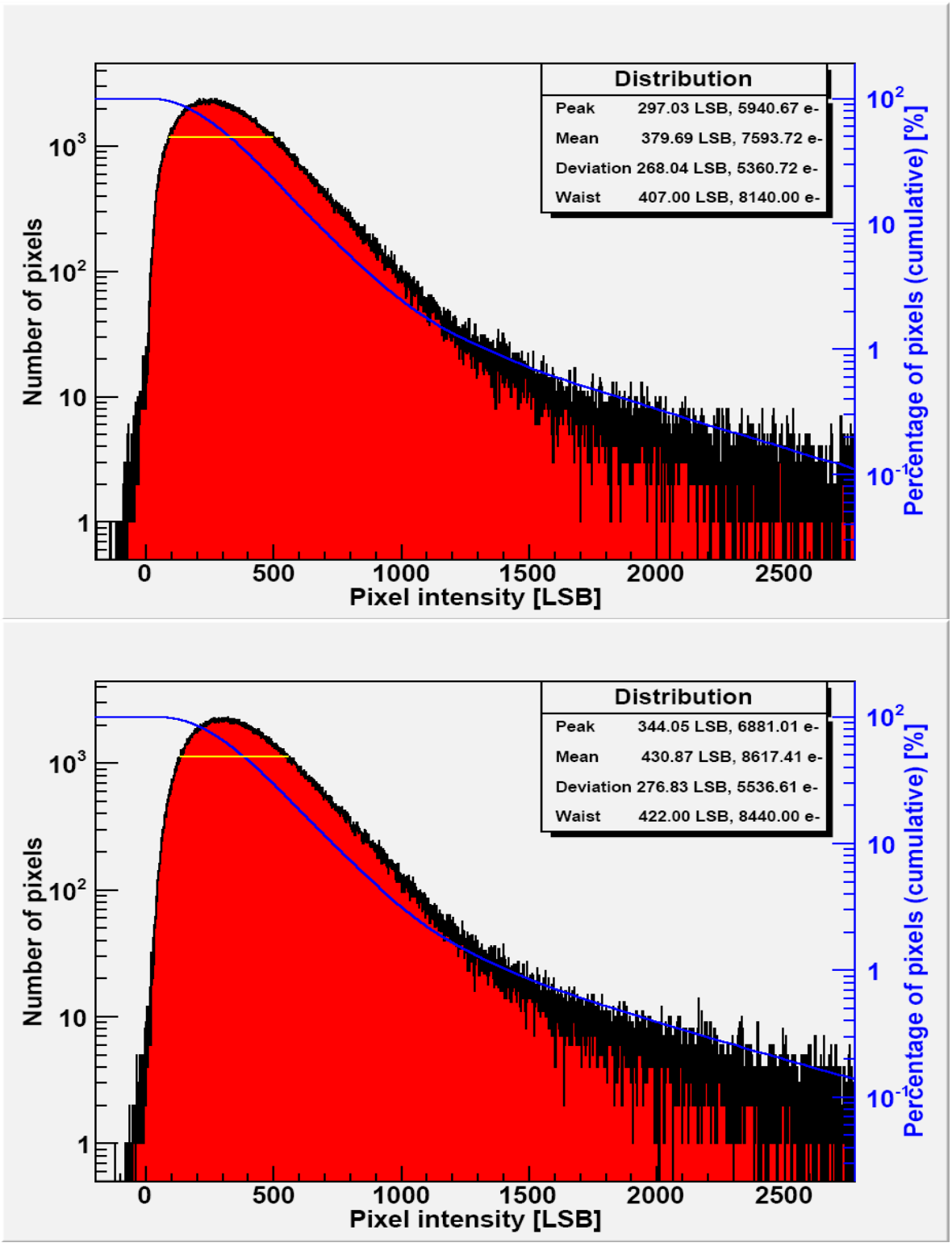

Figure 9-22: Run 29 – beam OFF (top side) & under 230 MeV proton beam (bottom side) no tilt – NDR mode – 200 ms integration time

9.2.Proton-induced SET computation

Several images in each runs have been computed in order to extract:

- the mean signal of the proton induced spots according to the clustering method,
- the mean size of proton induced spots,
- the mean signal of the proton induced spots according to the 3x3 pixels summation method.

9.2.1. Run 2 – 100 MeV – no tilt – DR mode – 2 ms

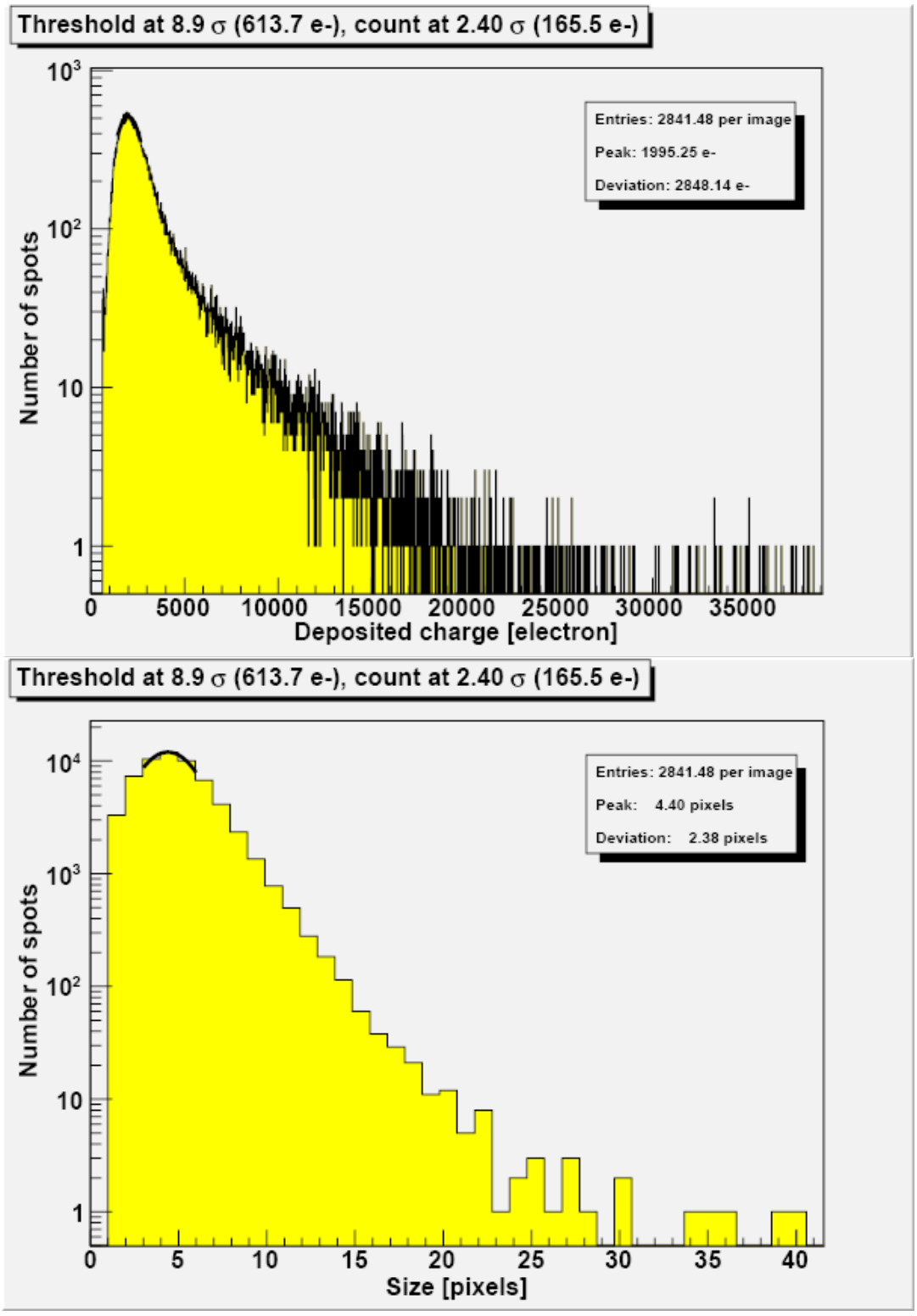

Figure 9-23: Clustering analysis - Run 2 – 100 MeV – no tilt – DR mode – 2 ms

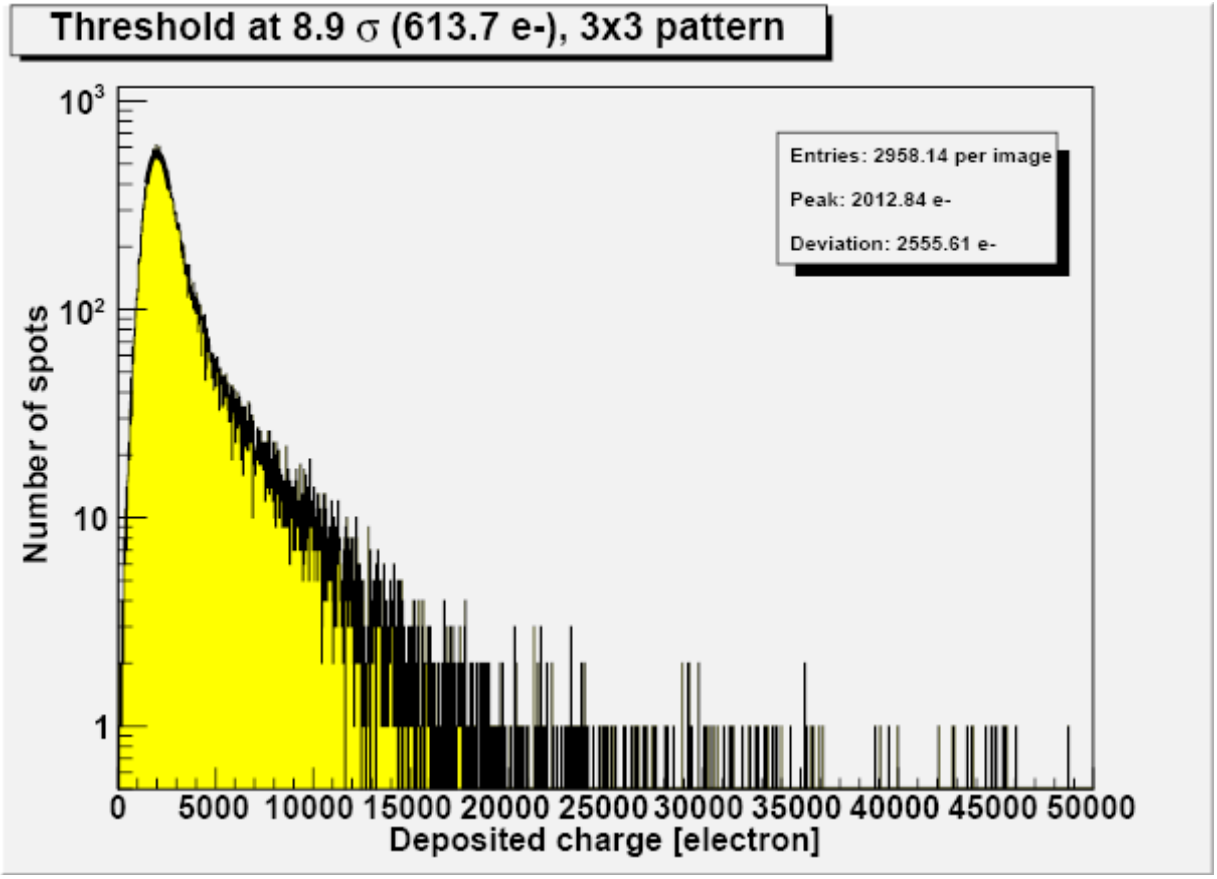

Figure 9-24: 3x3 pattern analysis - Run 2 – 100 MeV – no tilt – DR mode – 2 ms

9.2.2.Run 3 – 100 MeV – no tilt – DR mode – 1.2 ms

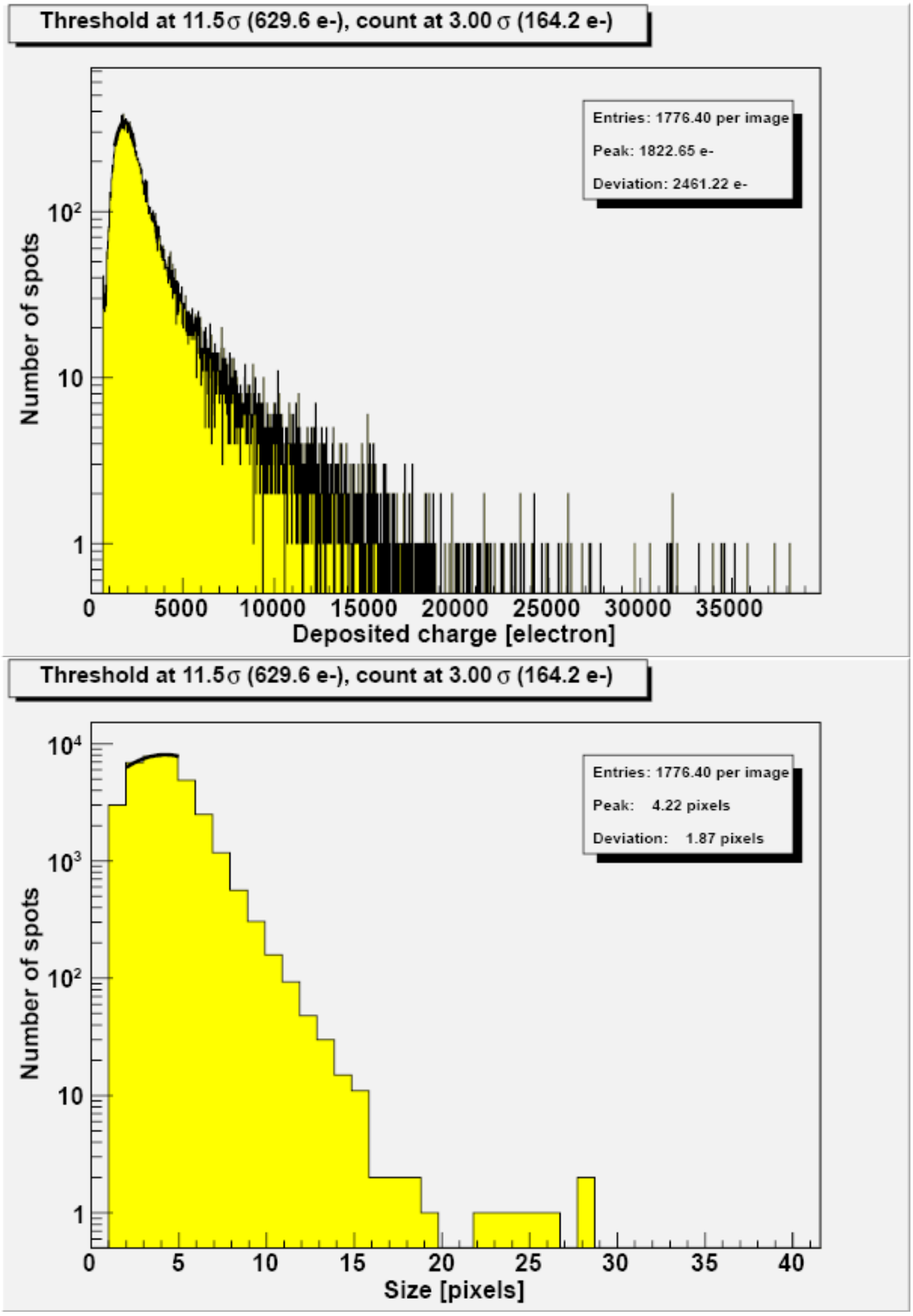

Figure 9-25: Clustering analysis - Run 3 – 100 MeV – no tilt – DR mode – 1.2 ms

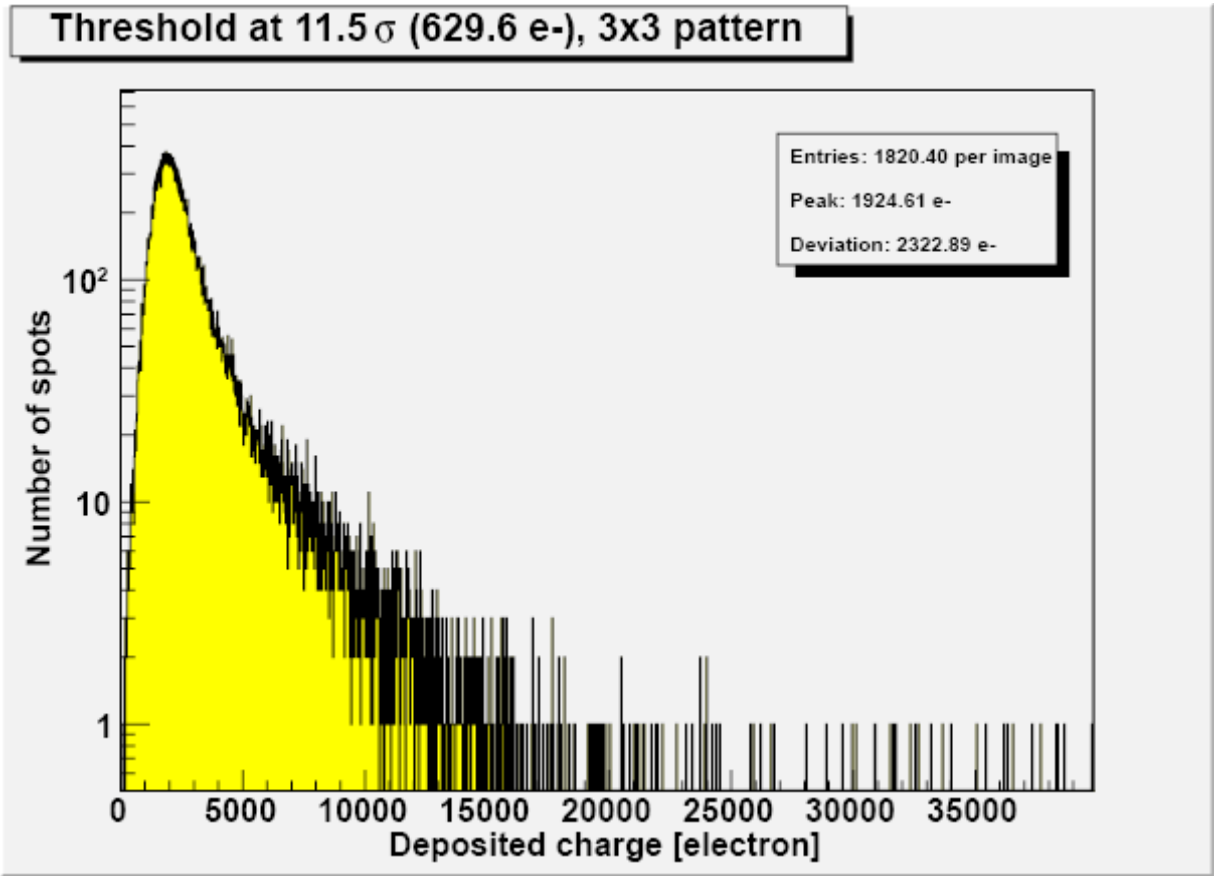

Figure 9-26: 3x3 pattern analysis - Run 3 – 100 MeV – no tilt – DR mode – 1.2 ms

9.2.3. Run 4 – 100 MeV – no tilt – DR mode – 2 ms

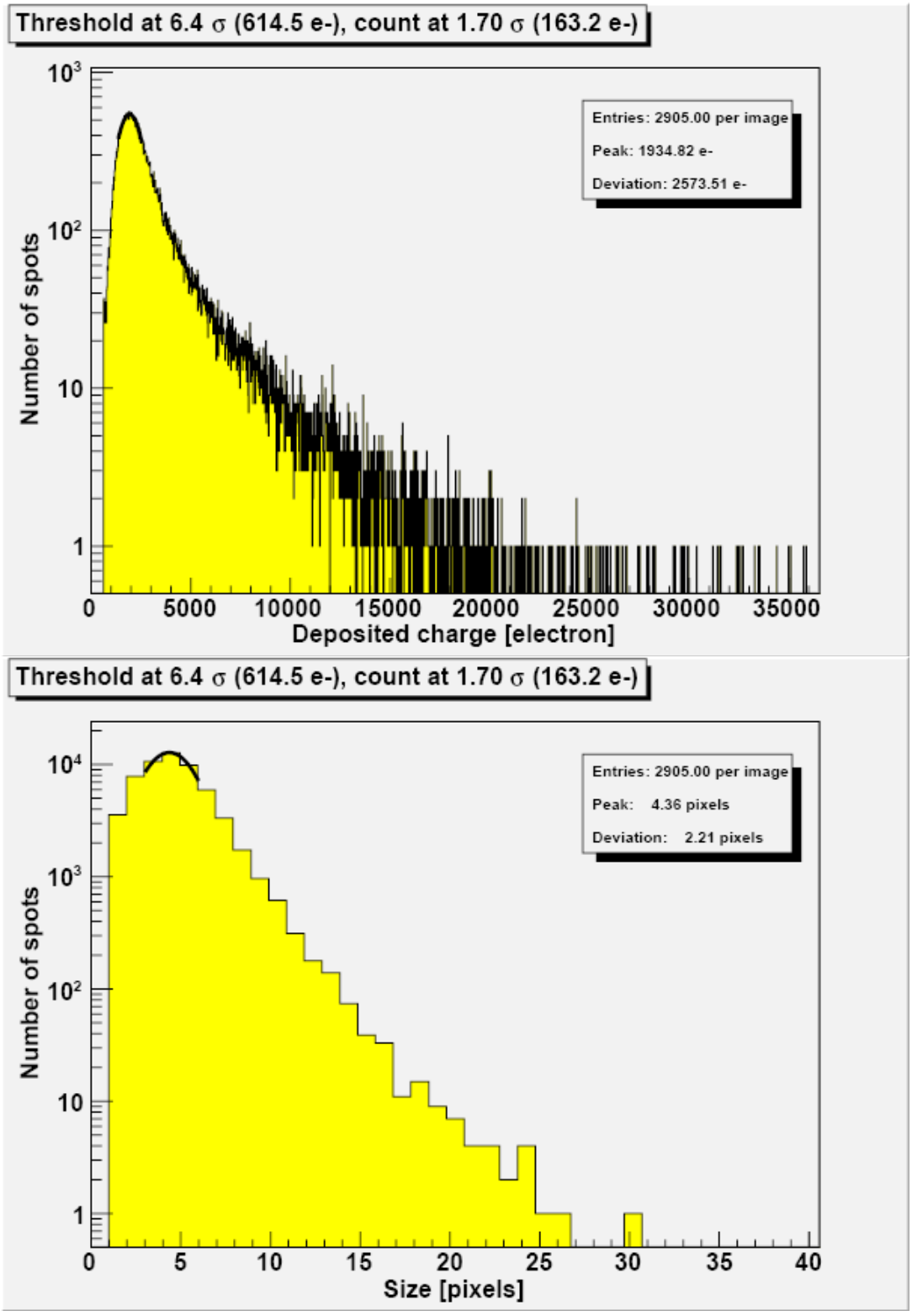

Figure 9-27: Clustering analysis - Run 4 – 100 MeV – no tilt – DR mode – 2 ms

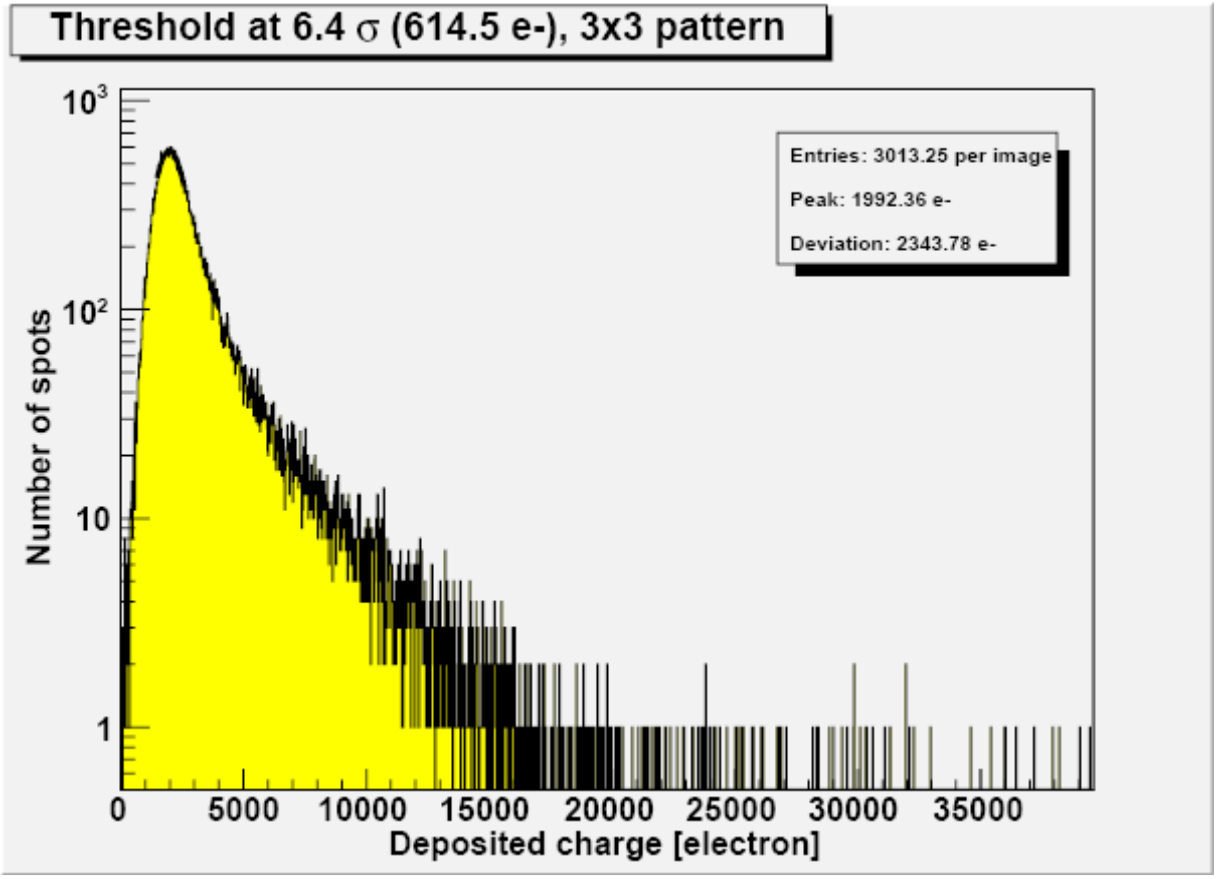

Figure 9-28: 3x3 pattern analysis - Run 4 – 100 MeV – no tilt – DR mode – 2 ms

9.2.4. Run 5 – 175 MeV – no tilt – DR mode – 2 ms

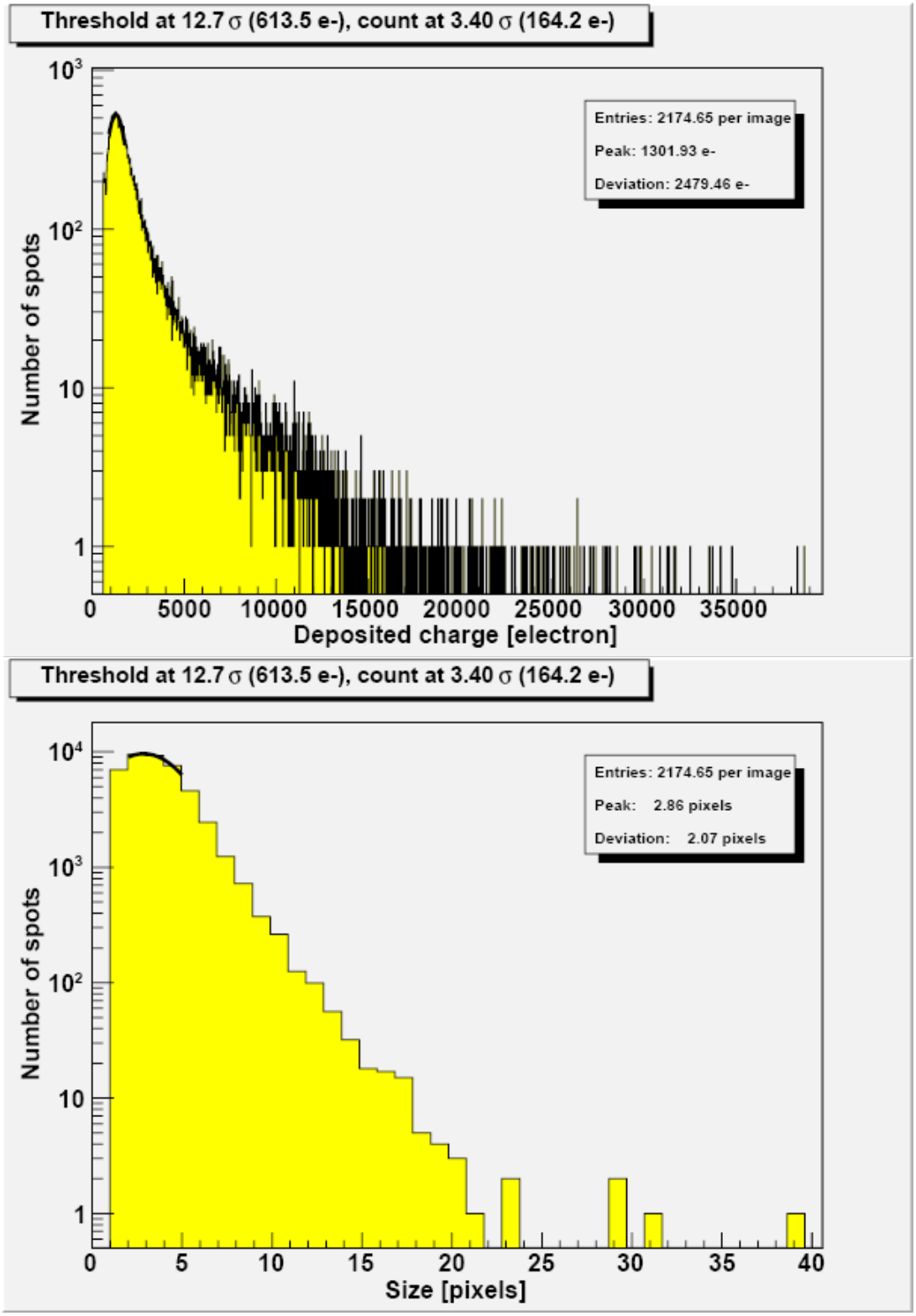

Figure 9-29: Clustering analysis - Run 5 – 175 MeV – no tilt – DR mode – 2 ms

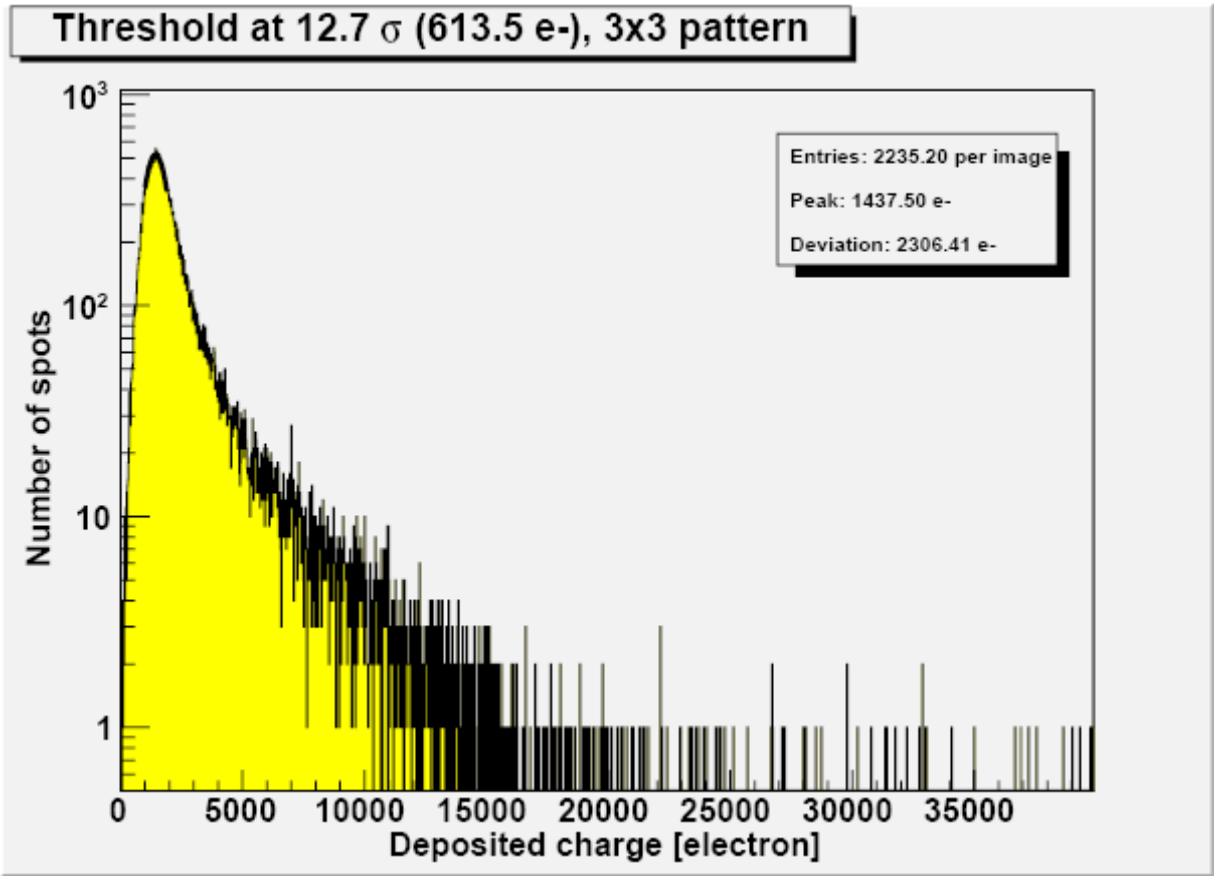

Figure 9-30: 3x3 pattern analysis - Run 5 – 175 MeV – no tilt – DR mode – 2 ms

9.2.5. Run 6 – 230 MeV – no tilt – DR mode – 2 ms

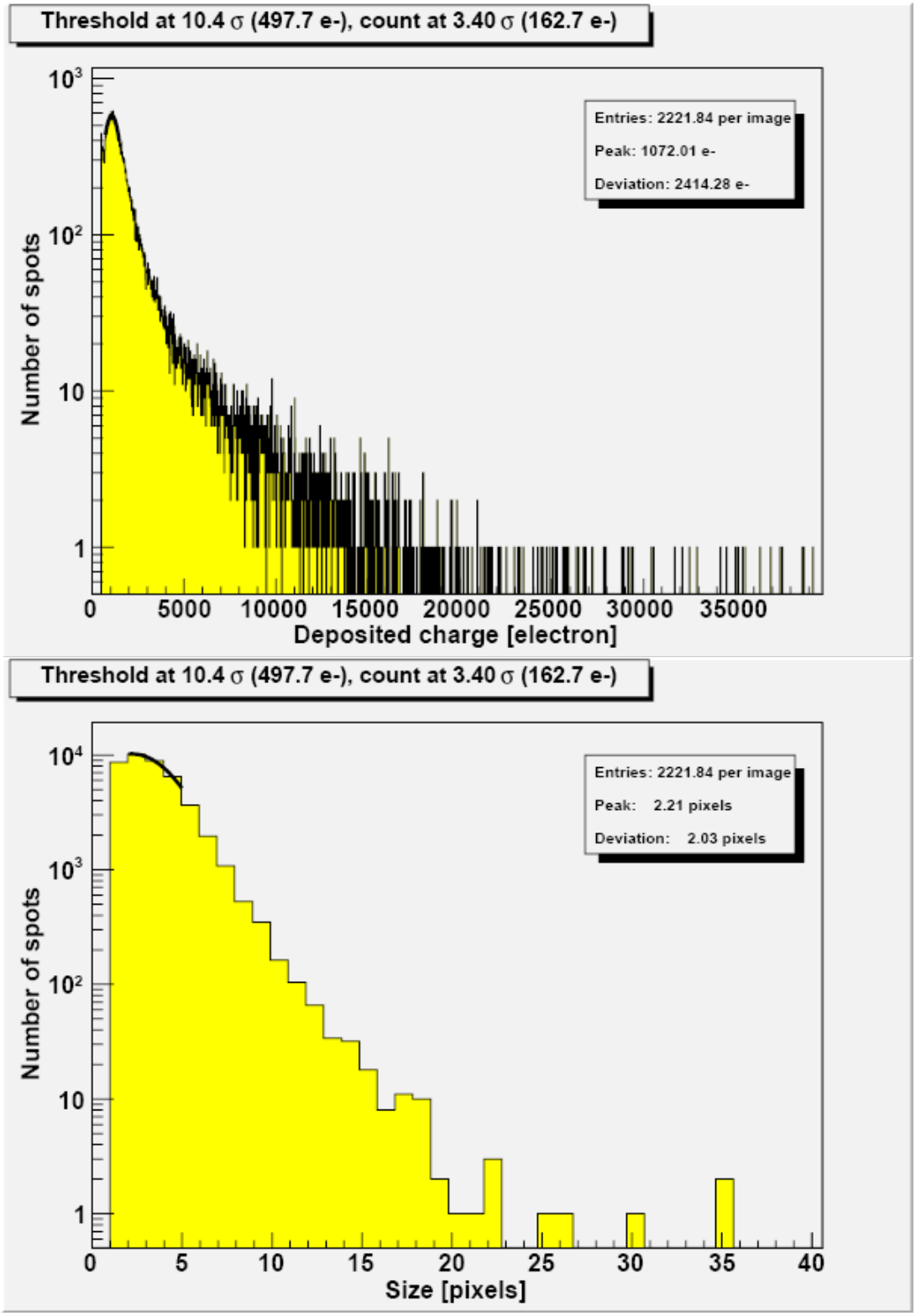

Figure 9-31: Clustering analysis - Run 6 – 230 MeV – no tilt – DR mode – 2 ms

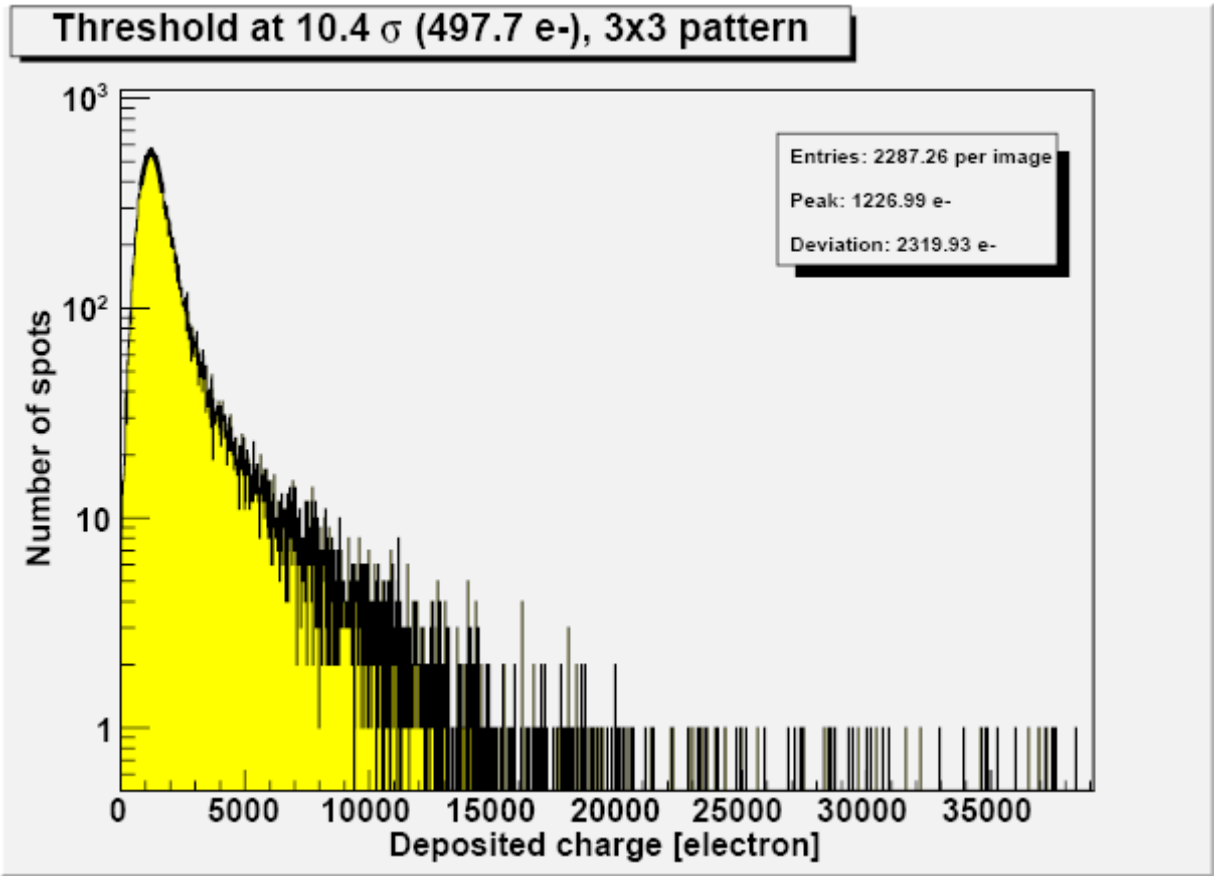

Figure 9-32: 3x3 pattern analysis - Run 6 – 230 MeV – no tilt – DR mode – 2 ms

9.2.6. Run 9 – 100 MeV – tilt 60° along Y axis – DR mode – 2 ms

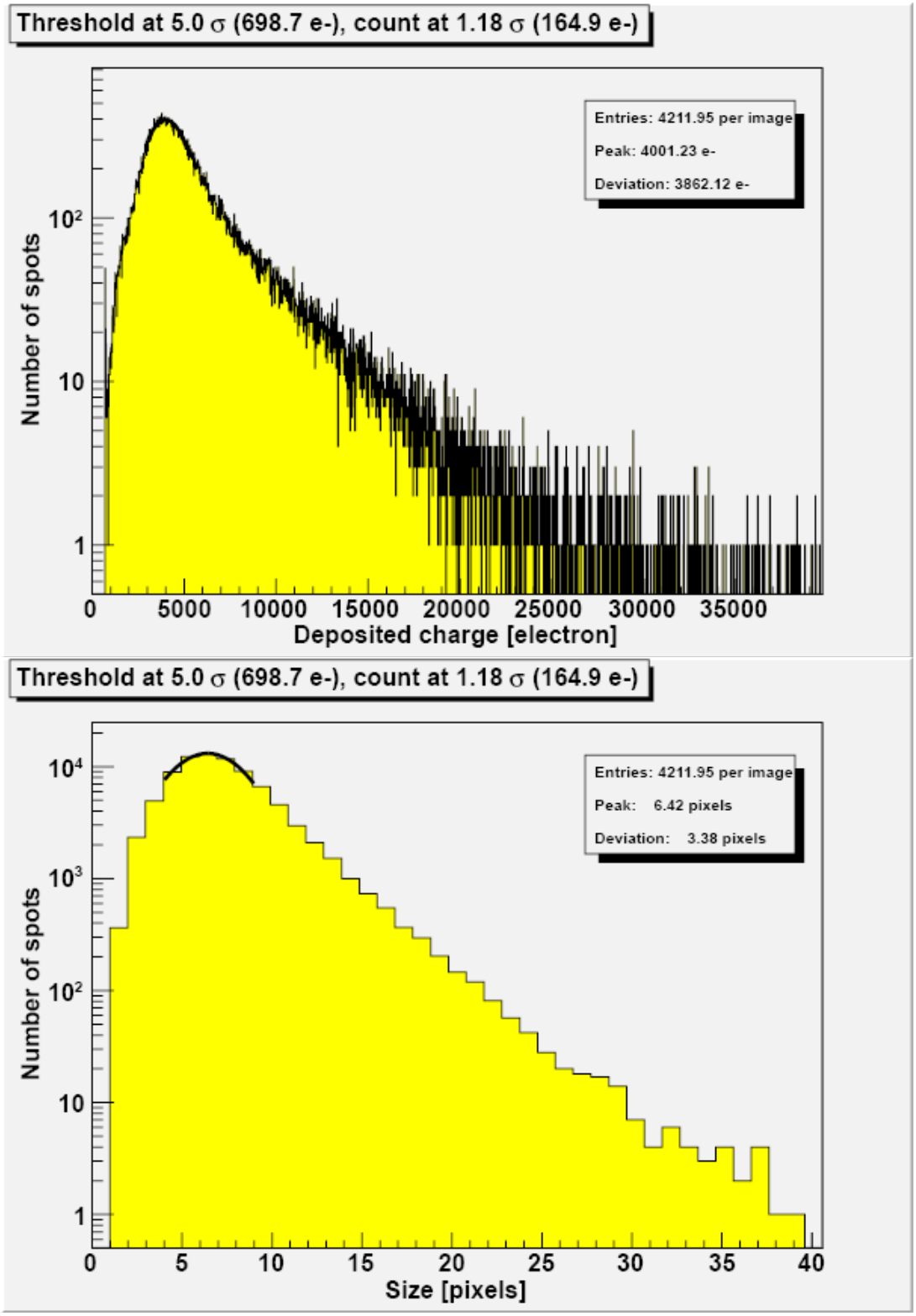

Figure 9-33: Clustering analysis - Run 9 – 100 MeV – tilt 60° along Y axis – DR mode

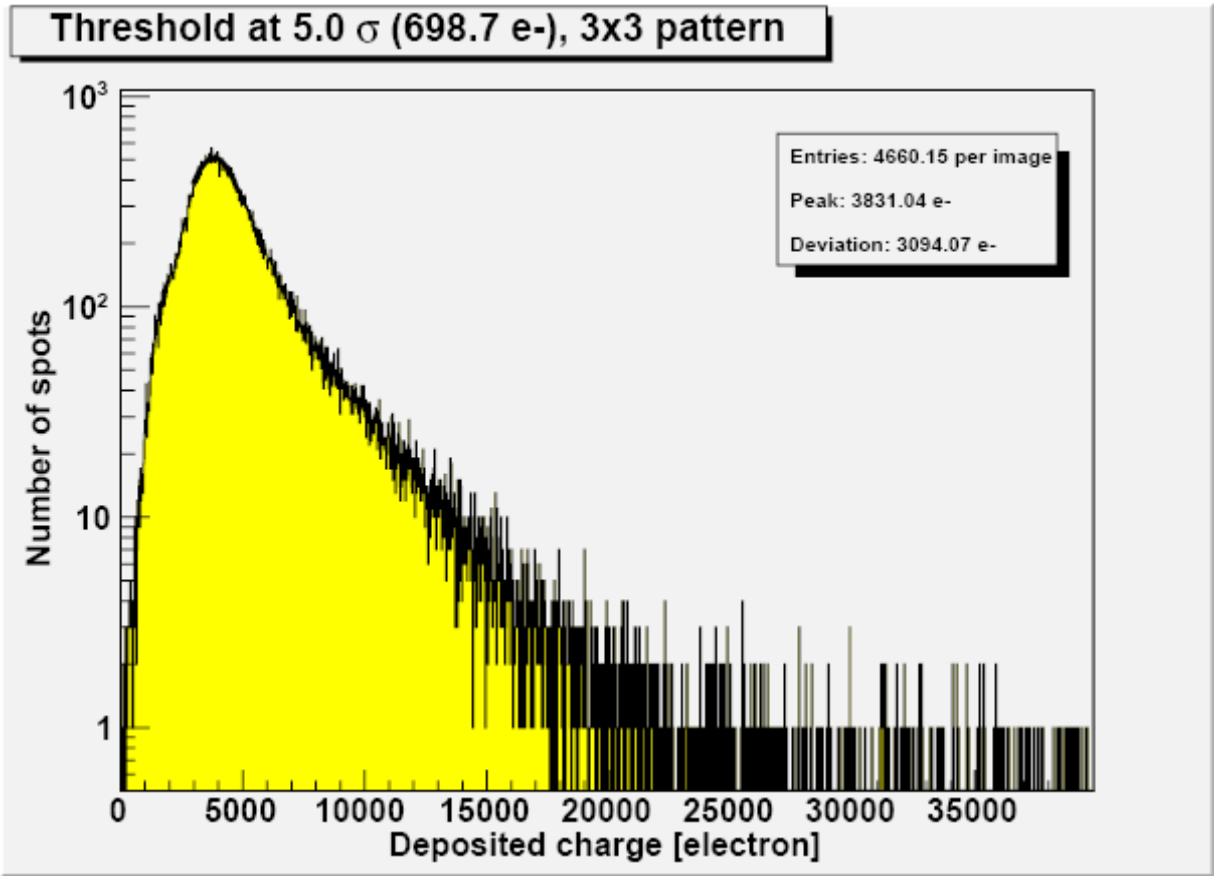

Figure 9-34: 3x3 pattern analysis - Run 9 – 100 MeV – tilt 60° along Y axis – DR mode

9.2.7. Run 10 – 100 MeV – tilt 60° along Y axis – DR mode – 2 ms

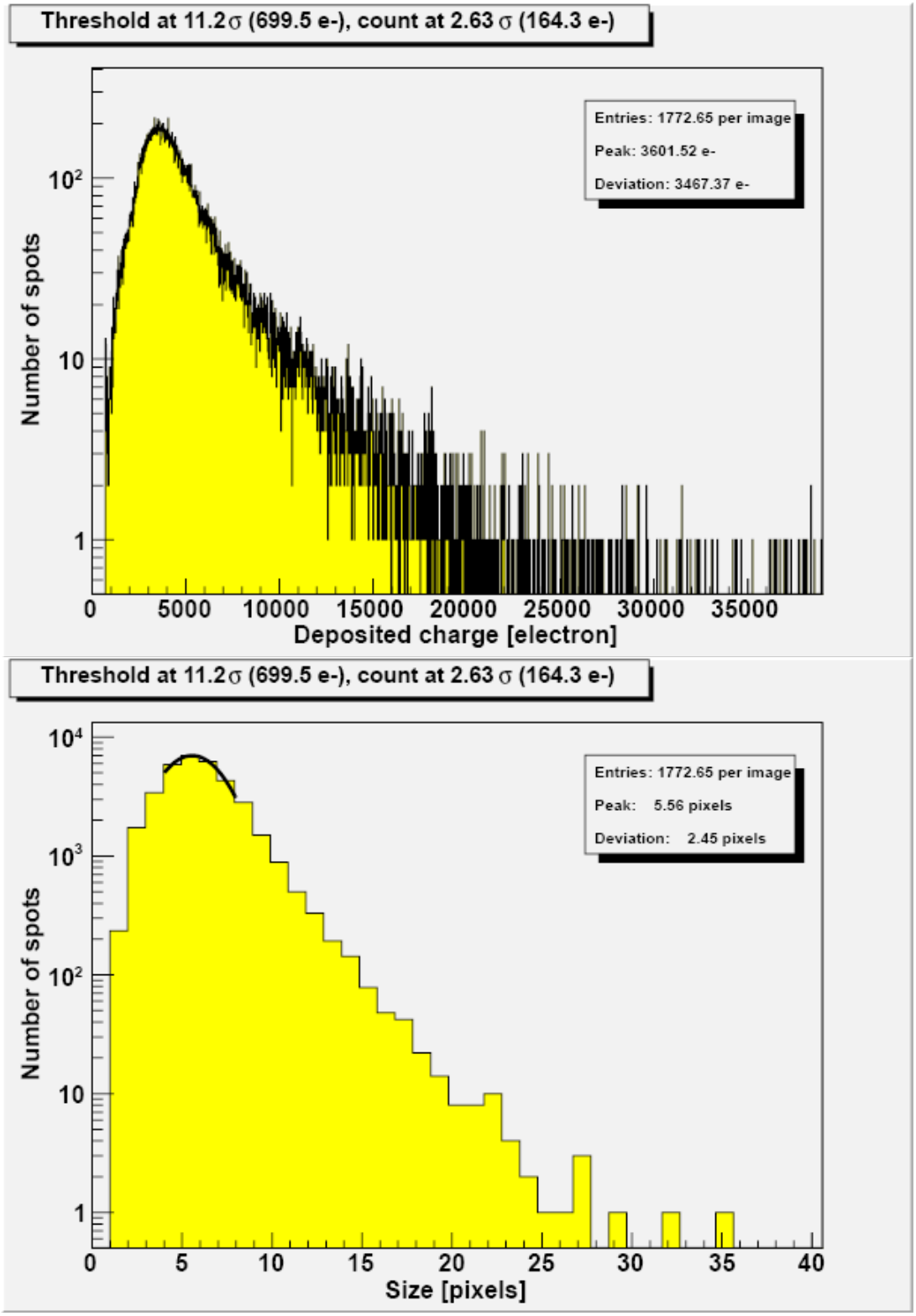

Figure 9-35: Clustering analysis - Run 10 – 100 MeV – tilt 60° along Y axis – DR mode

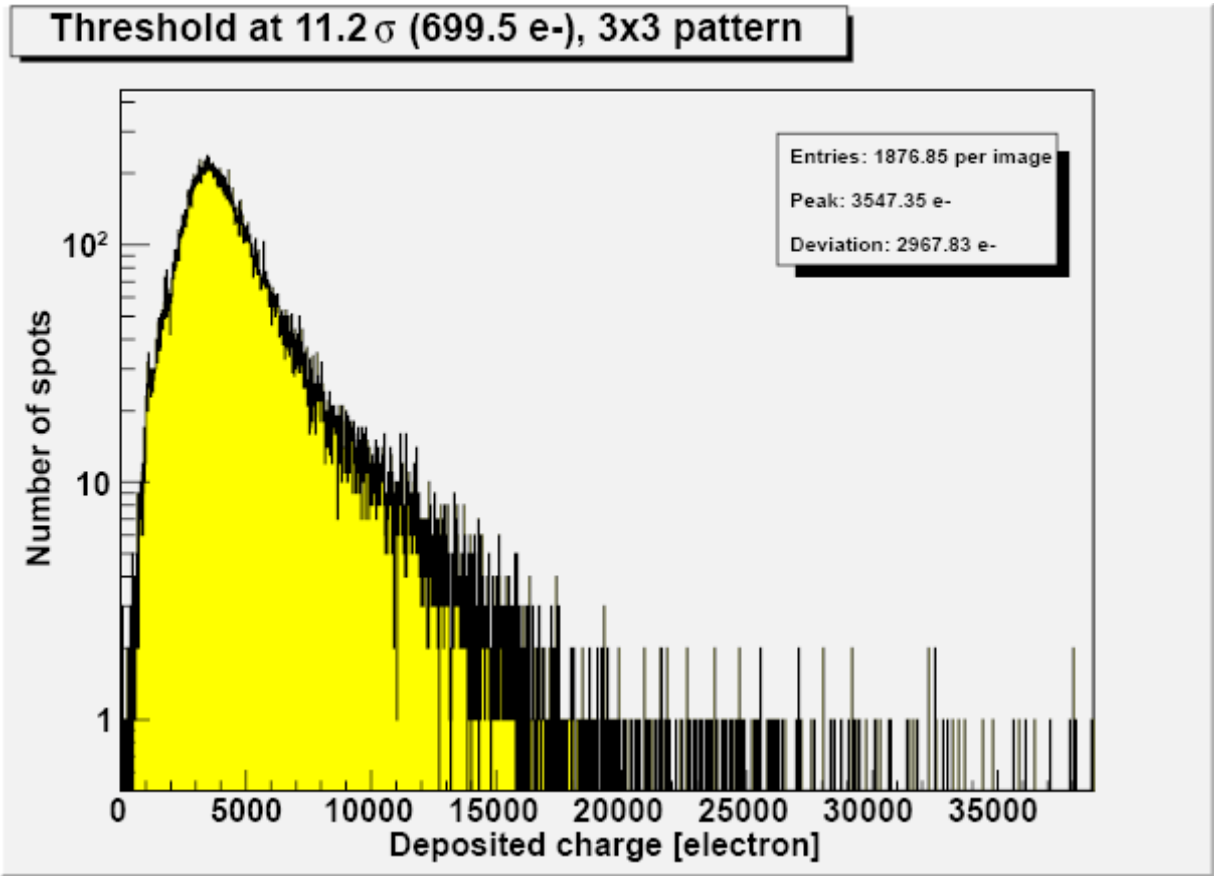

Figure 9-36: 3x3 pattern analysis - Run 10 – 100 MeV – tilt 60° along Y axis – DR mode

9.2.8. Run 11 – 175 MeV – tilt 60° along Y axis – DR mode – 2 ms

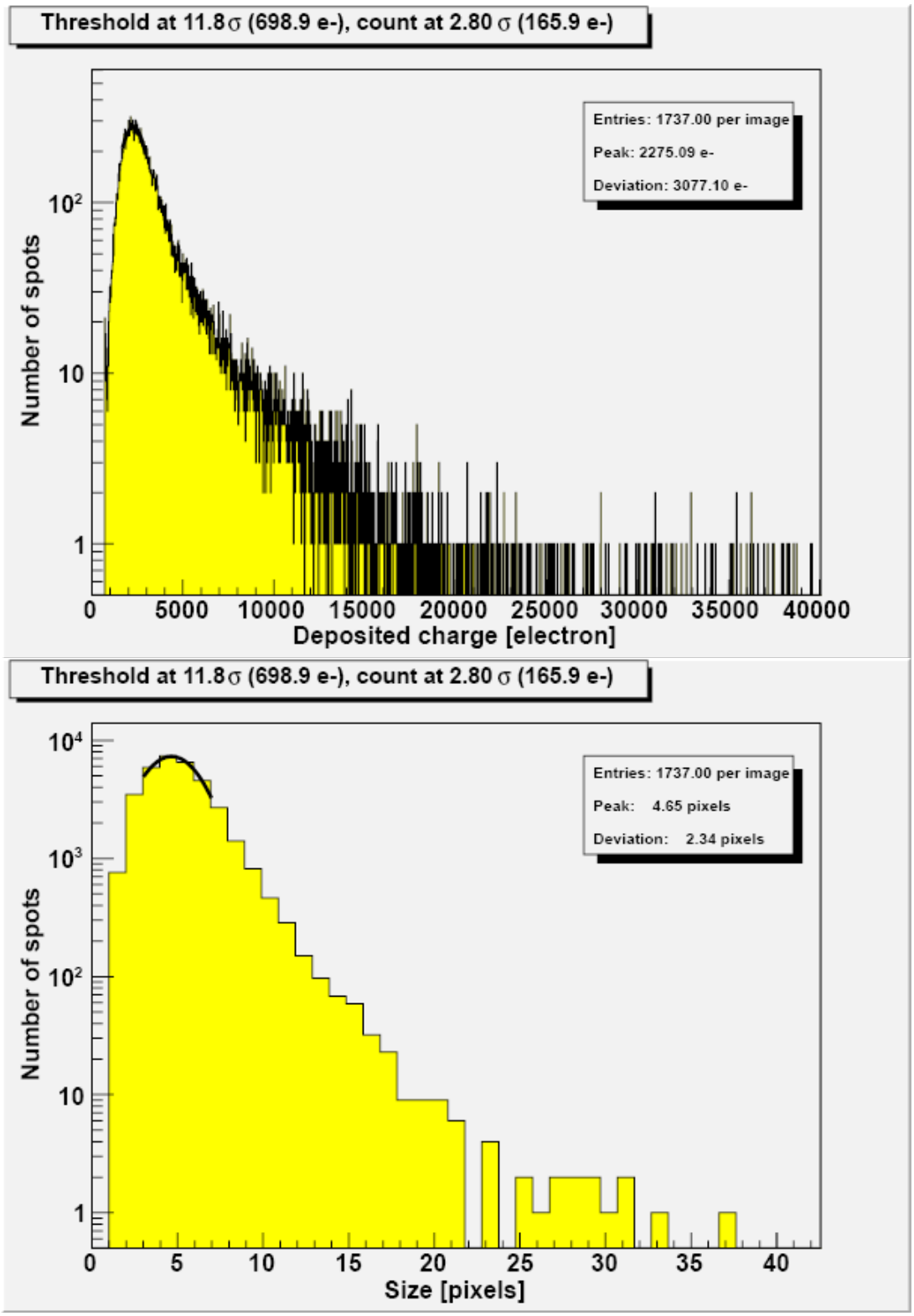

Figure 9-37: Clustering analysis - Run 11 – 175 MeV – tilt 60° along Y axis – DR mode

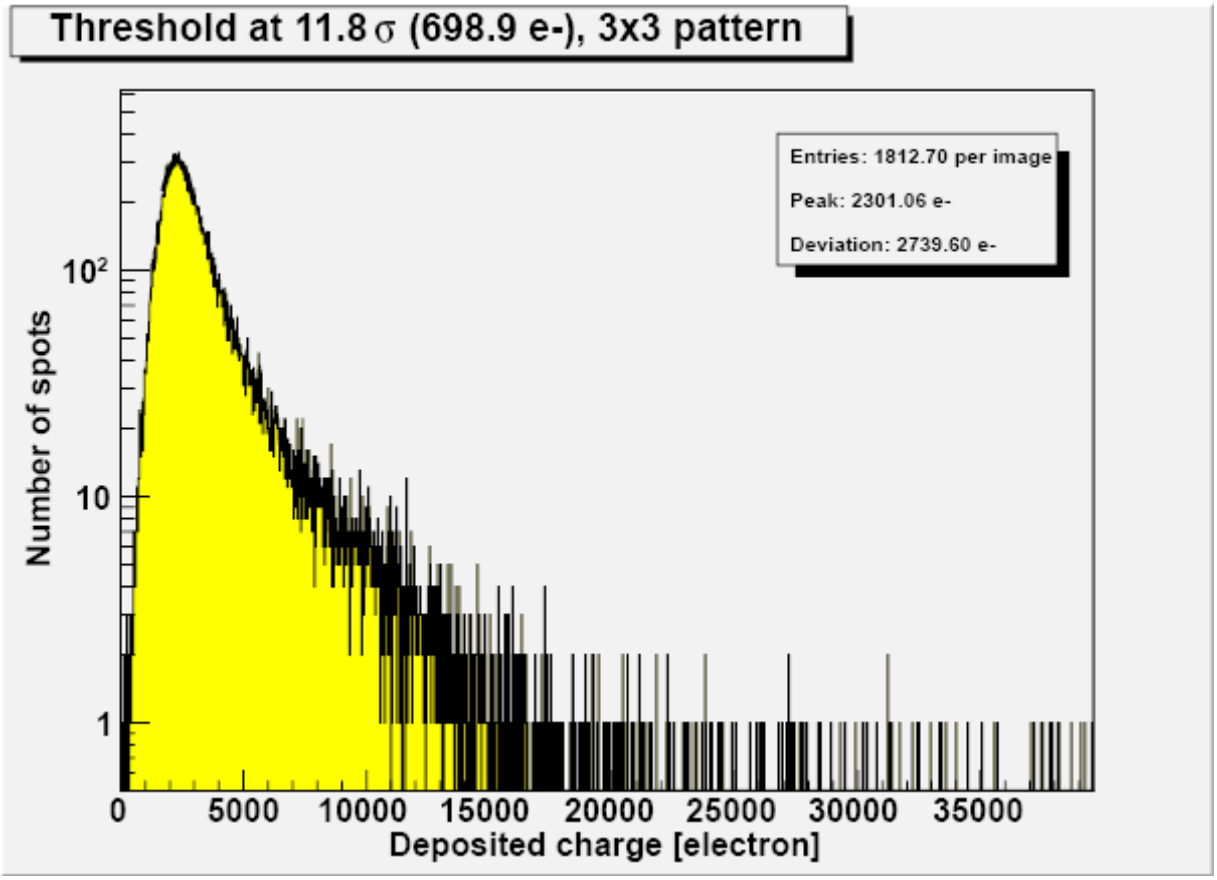

Figure 9-38: 3x3 pattern analysis - Run 11 – 175 MeV – tilt 60° along Y axis – DR mode

9.2.9. Run 12 – 230 MeV – tilt 60° along Y axis – DR mode – 2 ms

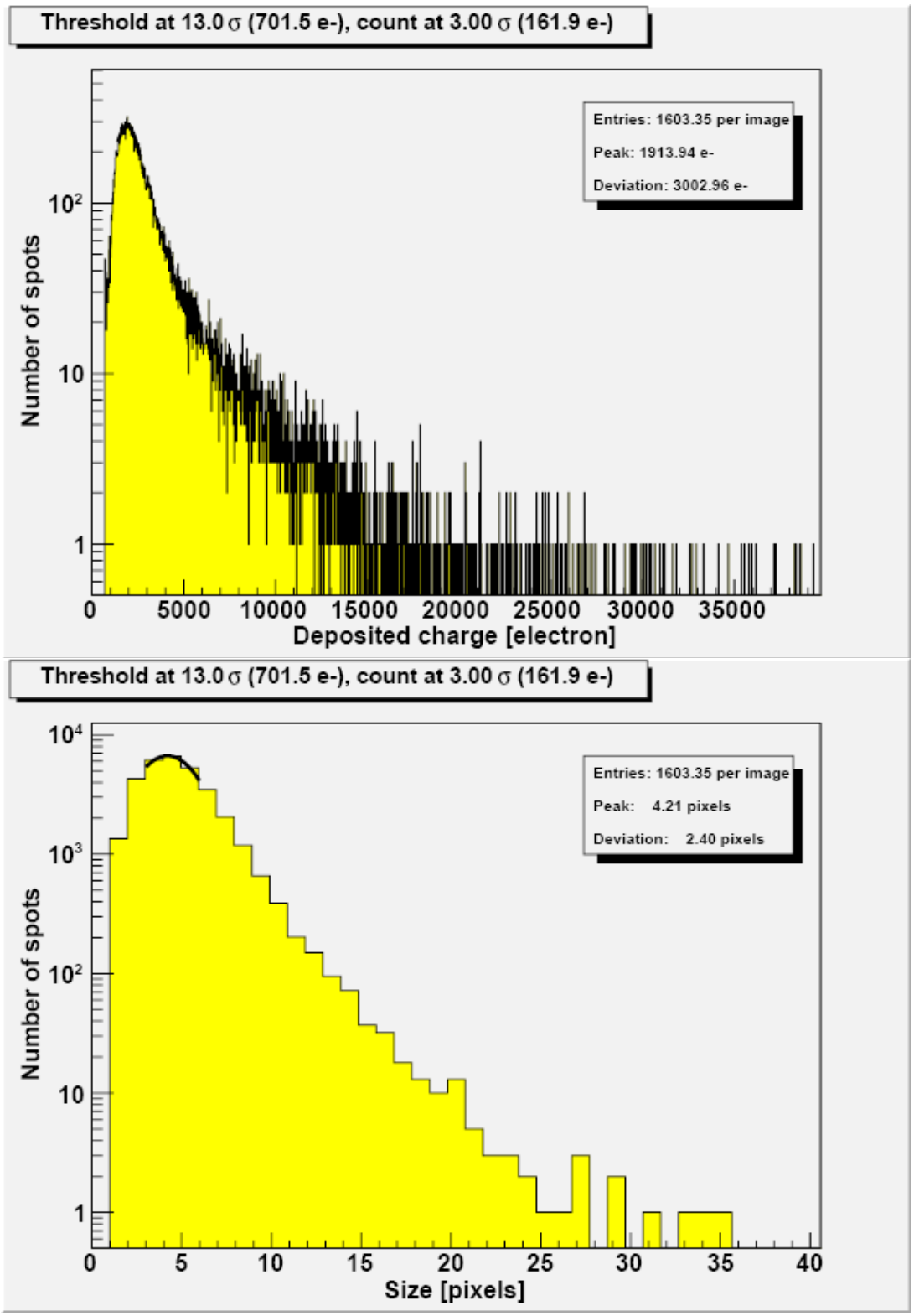

Figure 9-39: Clustering analysis - Run 12 – 230 MeV – tilt 60° along Y axis – DR mode

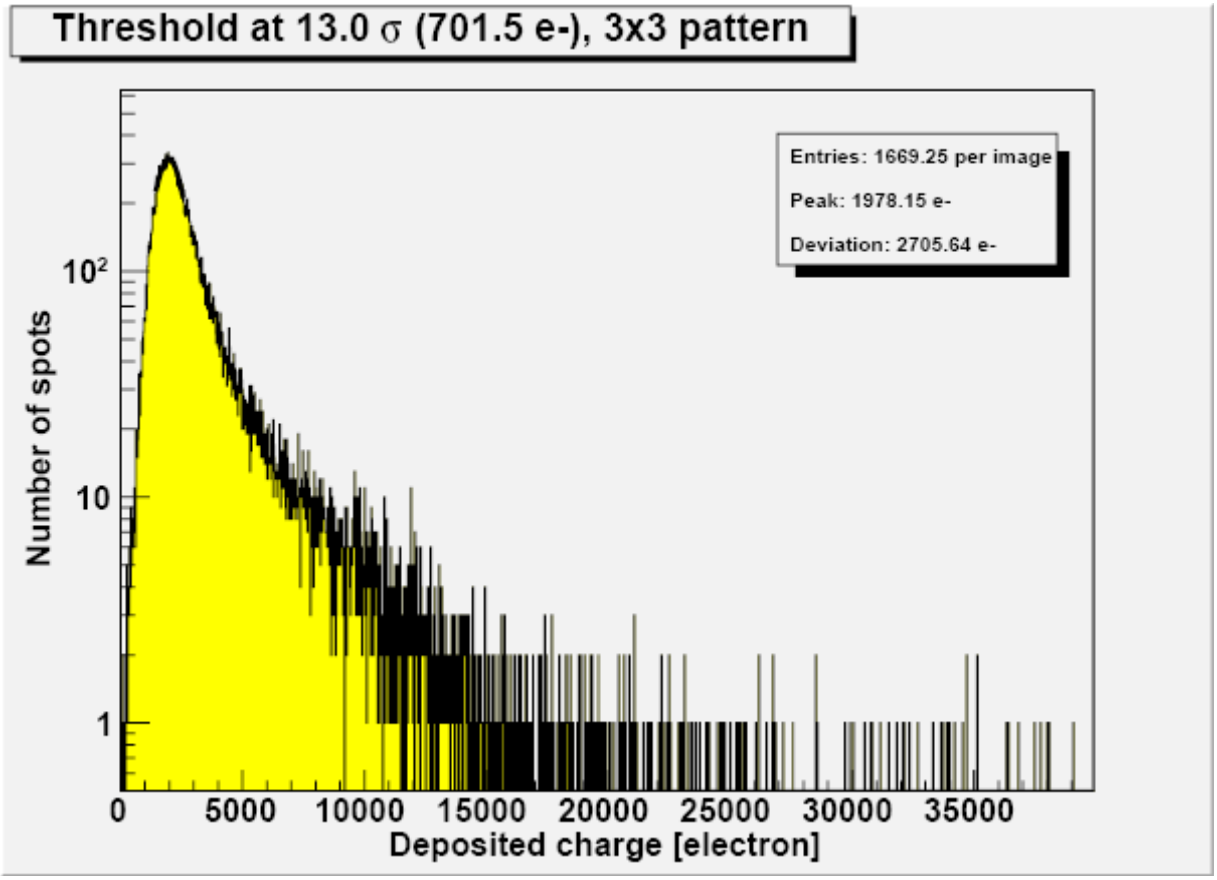

Figure 9-40: 3x3 pattern analysis - Run 12 – 230 MeV – tilt 60° along Y axis – DR mode

9.2.10. Run 14 – 100 MeV – tilt 60° along X axis – DR mode – 2 ms

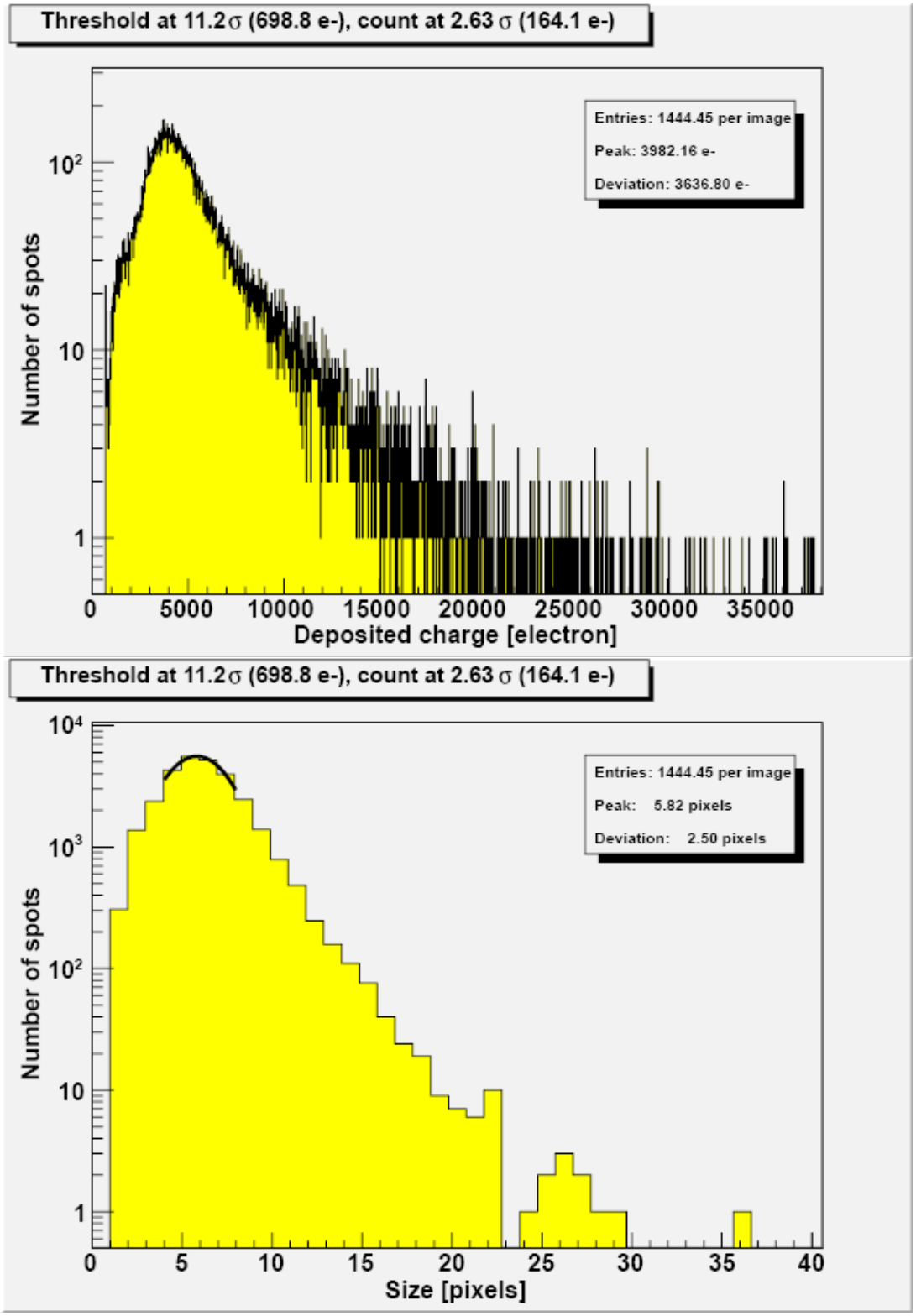

Figure 9-41: Clustering analysis - Run 14 – 100 MeV – tilt 60° along X axis – DR mode

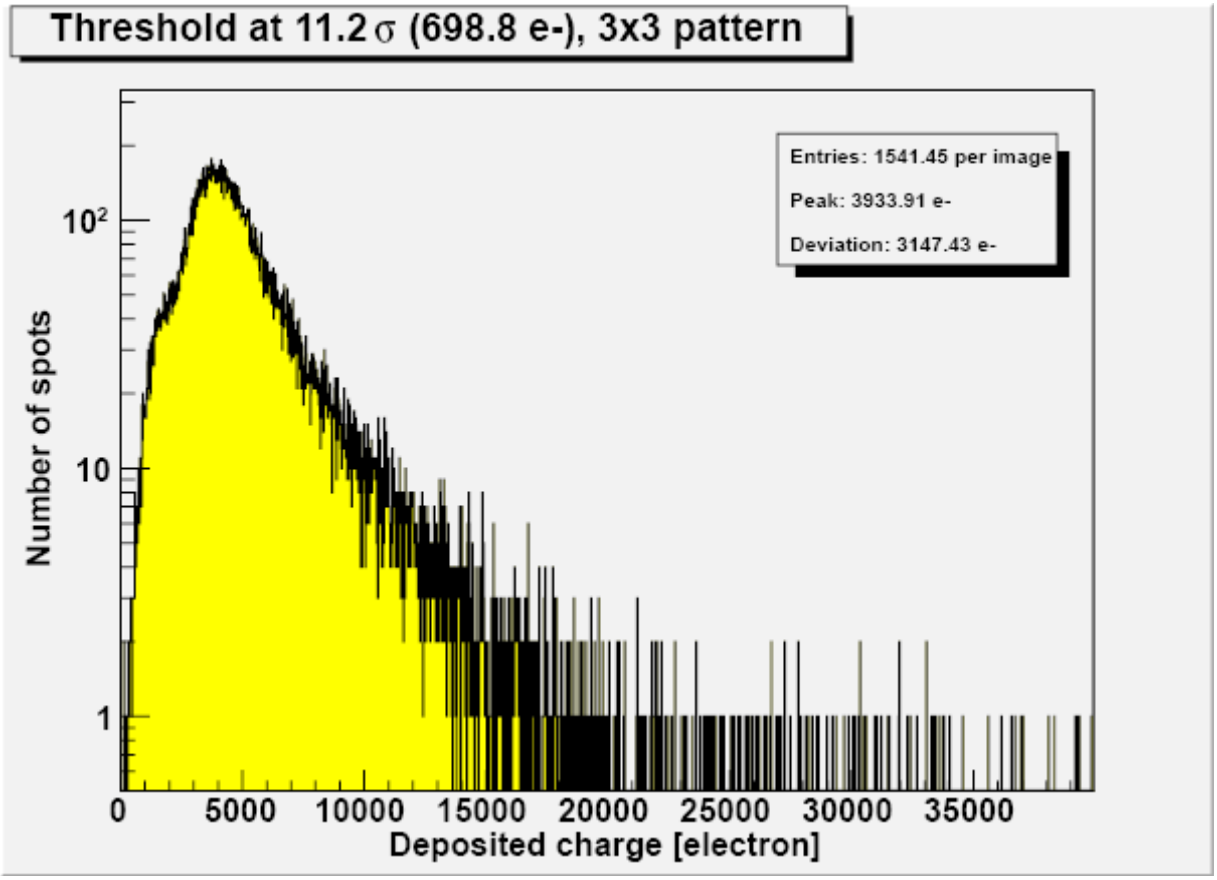

Figure 9-42: 3x3 pattern analysis - Run 14 – 100 MeV – tilt 60° along X axis – DR mode

9.2.11. Run 15 – 175 MeV – tilt 60° along X axis – DR mode – 2 ms

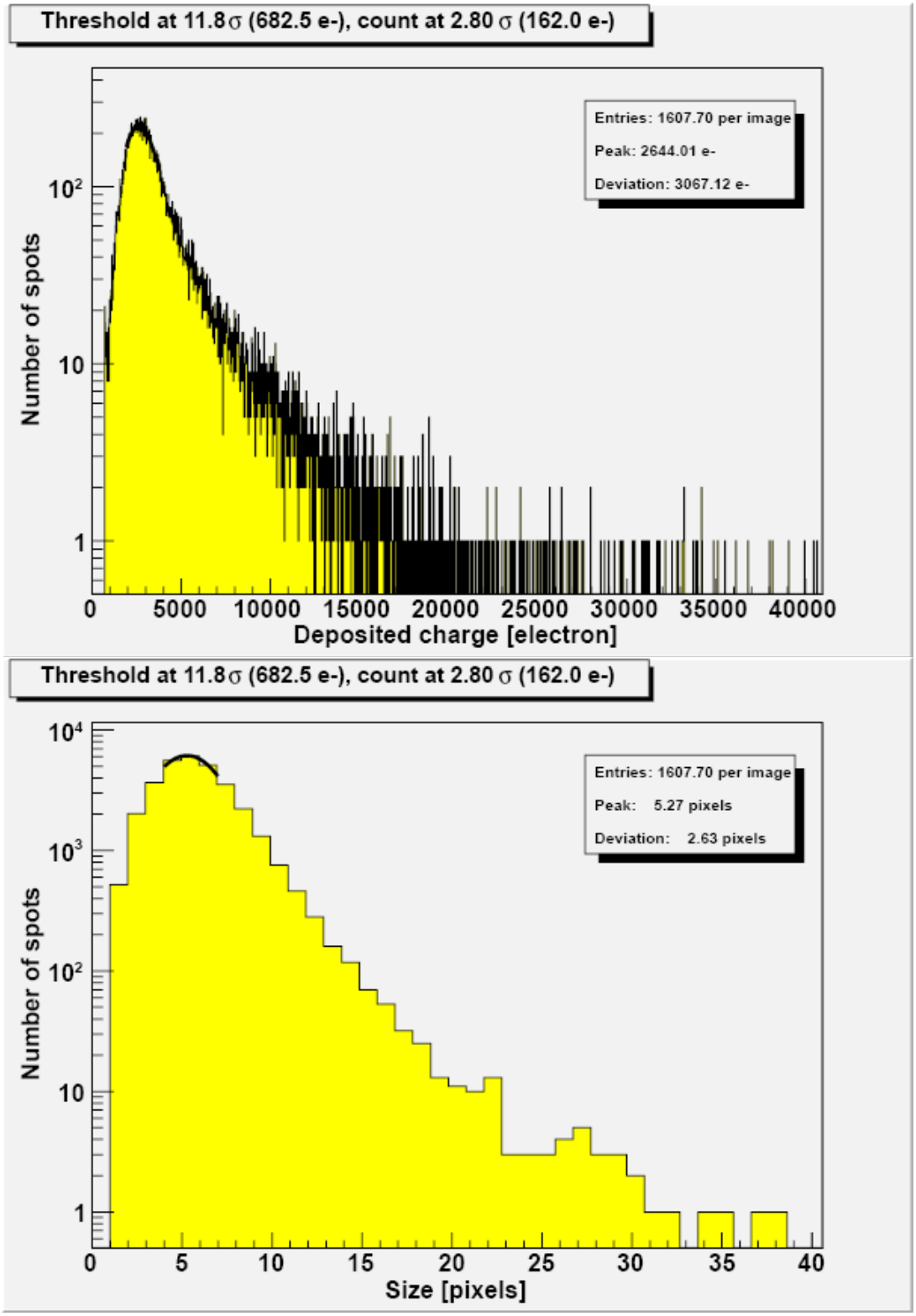

Figure 9-43: Clustering analysis - Run 15 – 175 MeV – tilt 60° along X axis – DR mode

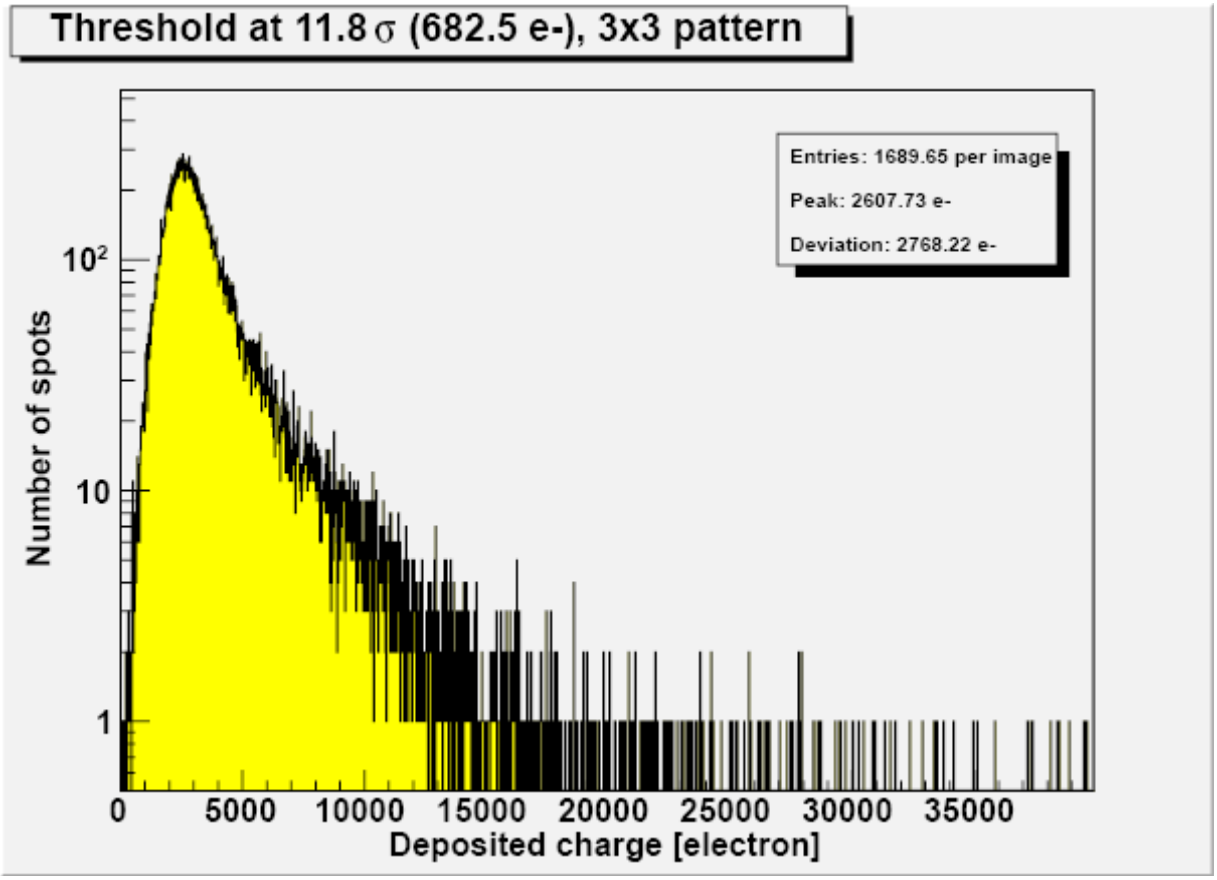

Figure 9-44: 3x3 pattern analysis - Run 15 – 175 MeV – tilt 60° along X axis – DR mode

9.2.12. Run 16 – 230 MeV – tilt 60° along X axis – DR mode – 2 ms

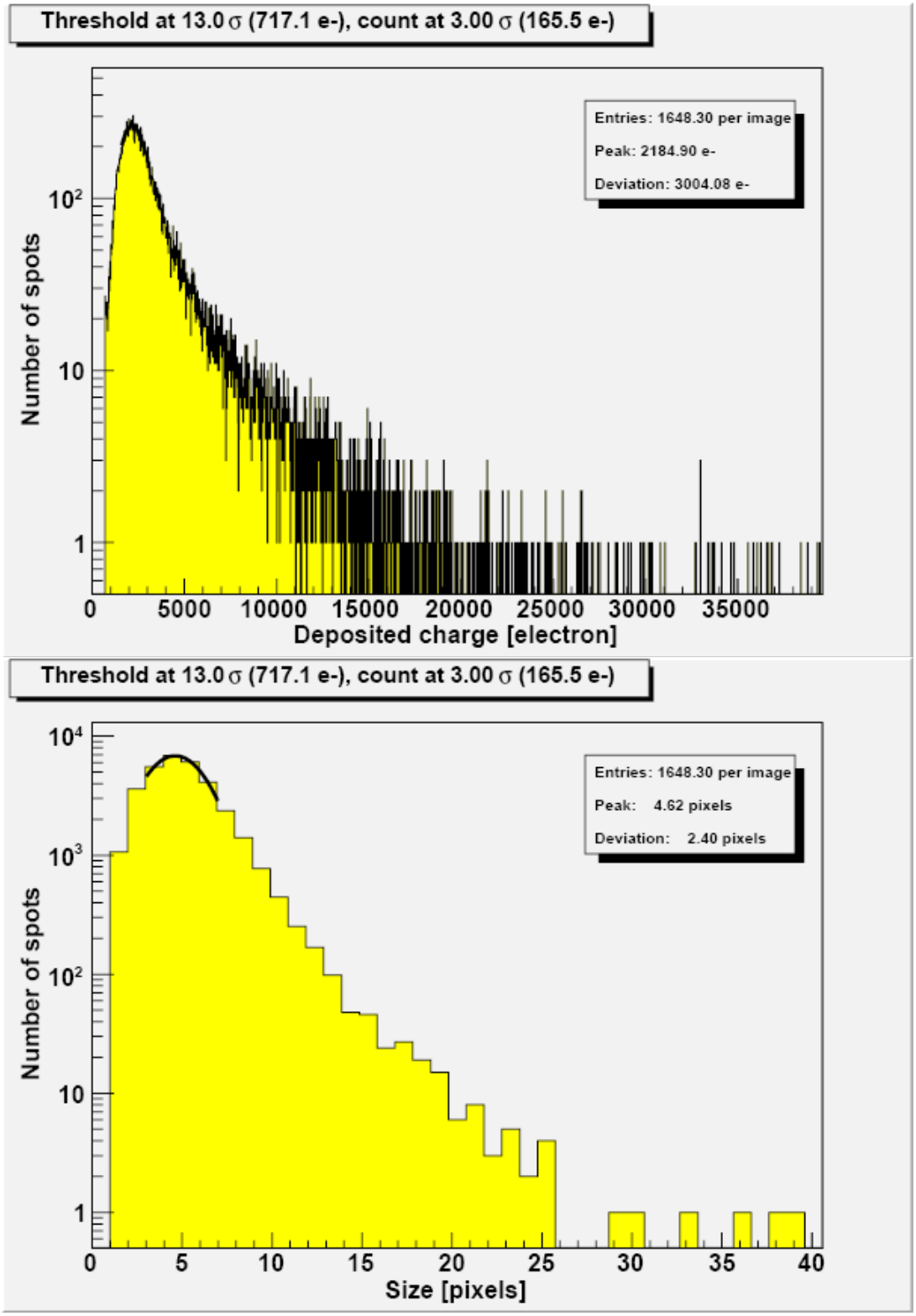

Figure 9-45: Clustering analysis - Run 16 – 230 MeV – tilt 60° along X axis – DR mode

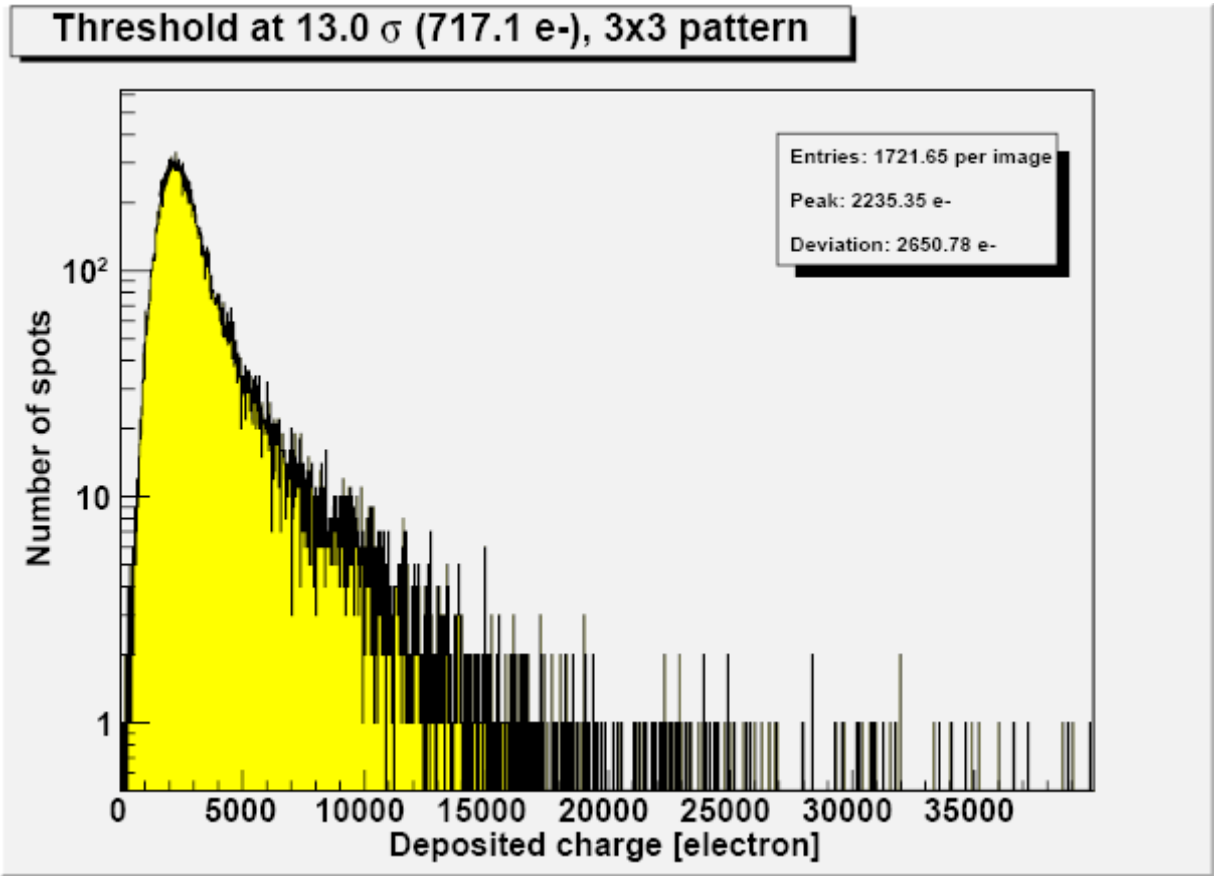

Figure 9-46: 3x3 pattern analysis - Run 16 – 230 MeV – tilt 60° along X axis – DR mode

9.2.13. Run 18 – 100 MeV – no tilt – DR mode – 2 ms

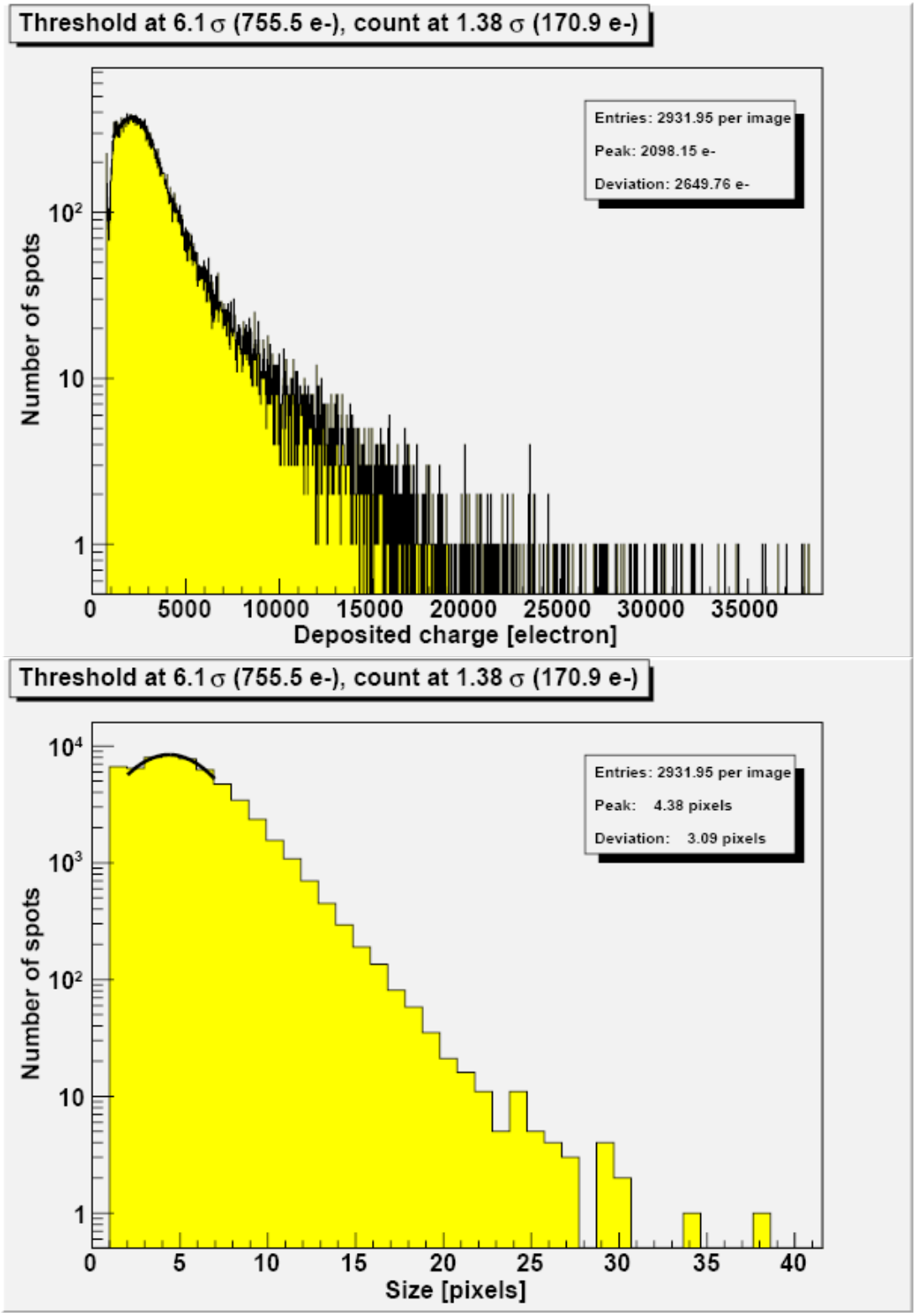

Figure 9-47: Clustering analysis - Run 18 – 100 MeV – no tilt – DR mode – 2 ms

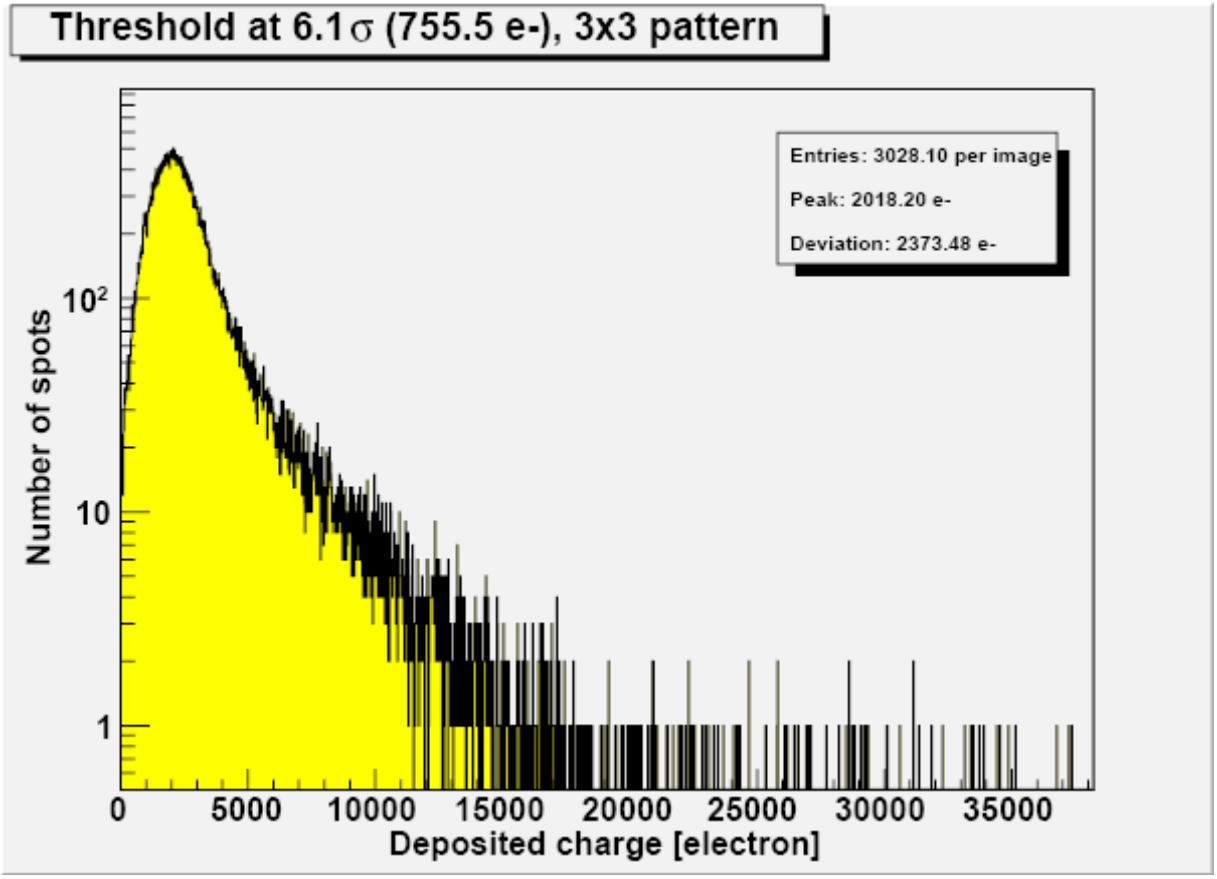

Figure 9-48: 3x3 pattern analysis - Run 18 – 100 MeV – no tilt – DR mode – 2 ms

9.2.14. Run 19 – 175 MeV – no tilt – DR mode – 2 ms

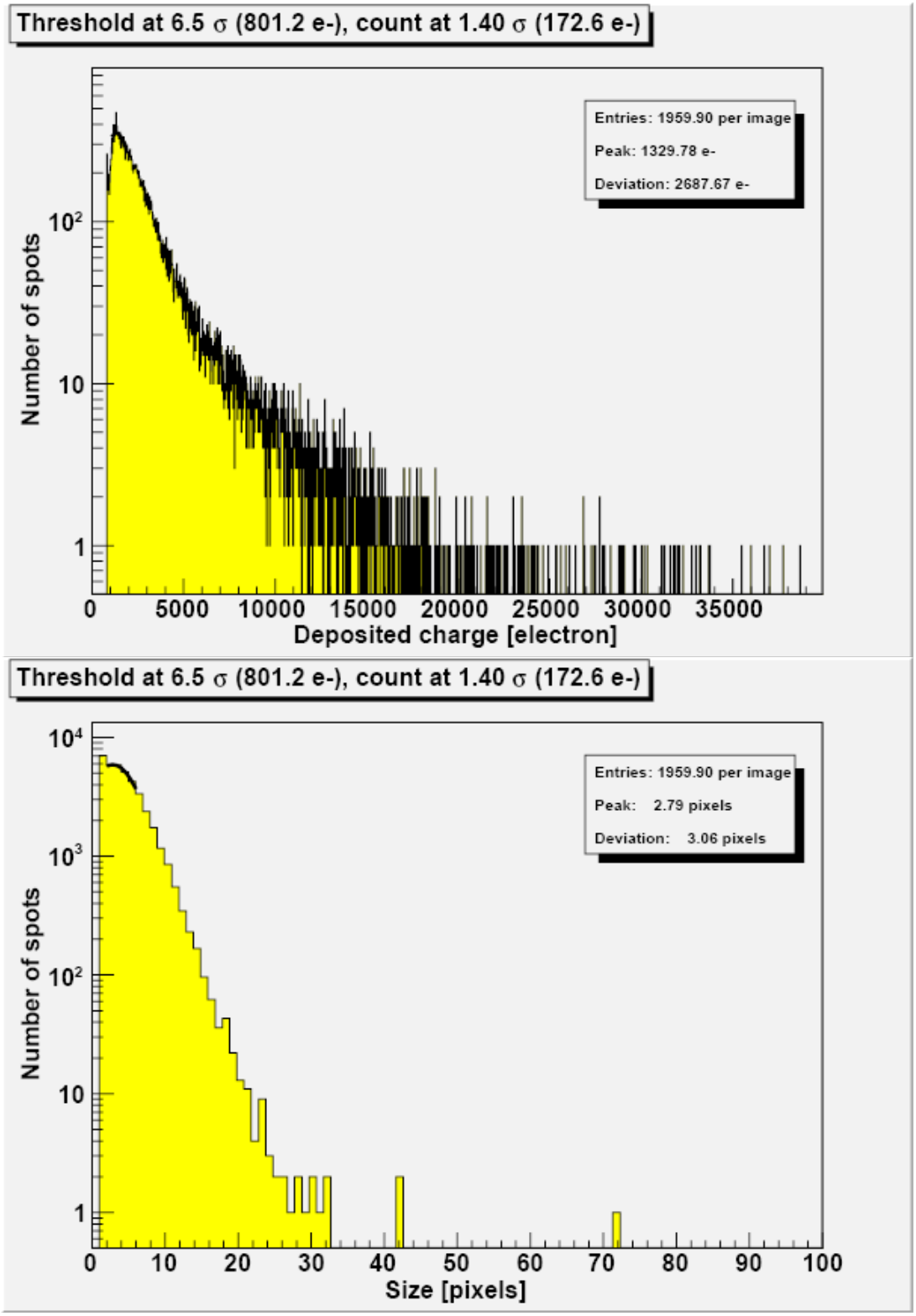

Figure 9-49: Clustering analysis - Run 19 – 175 MeV – no tilt – DR mode – 2 ms

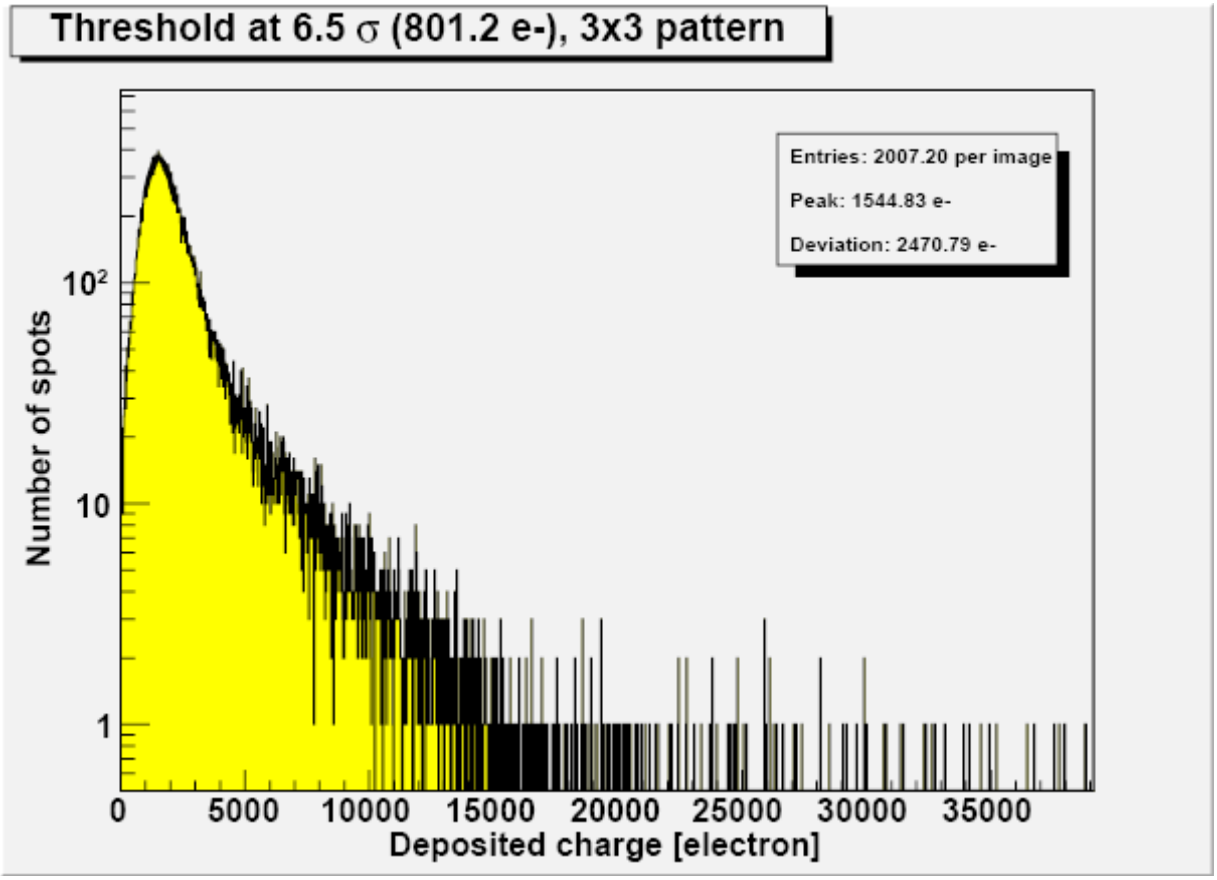

Figure 9-50: 3x3 pattern analysis - Run 19 – 175 MeV – no tilt – DR mode – 2 ms

9.2.15. Run 20 – 230 MeV – no tilt – DR mode – 2 ms

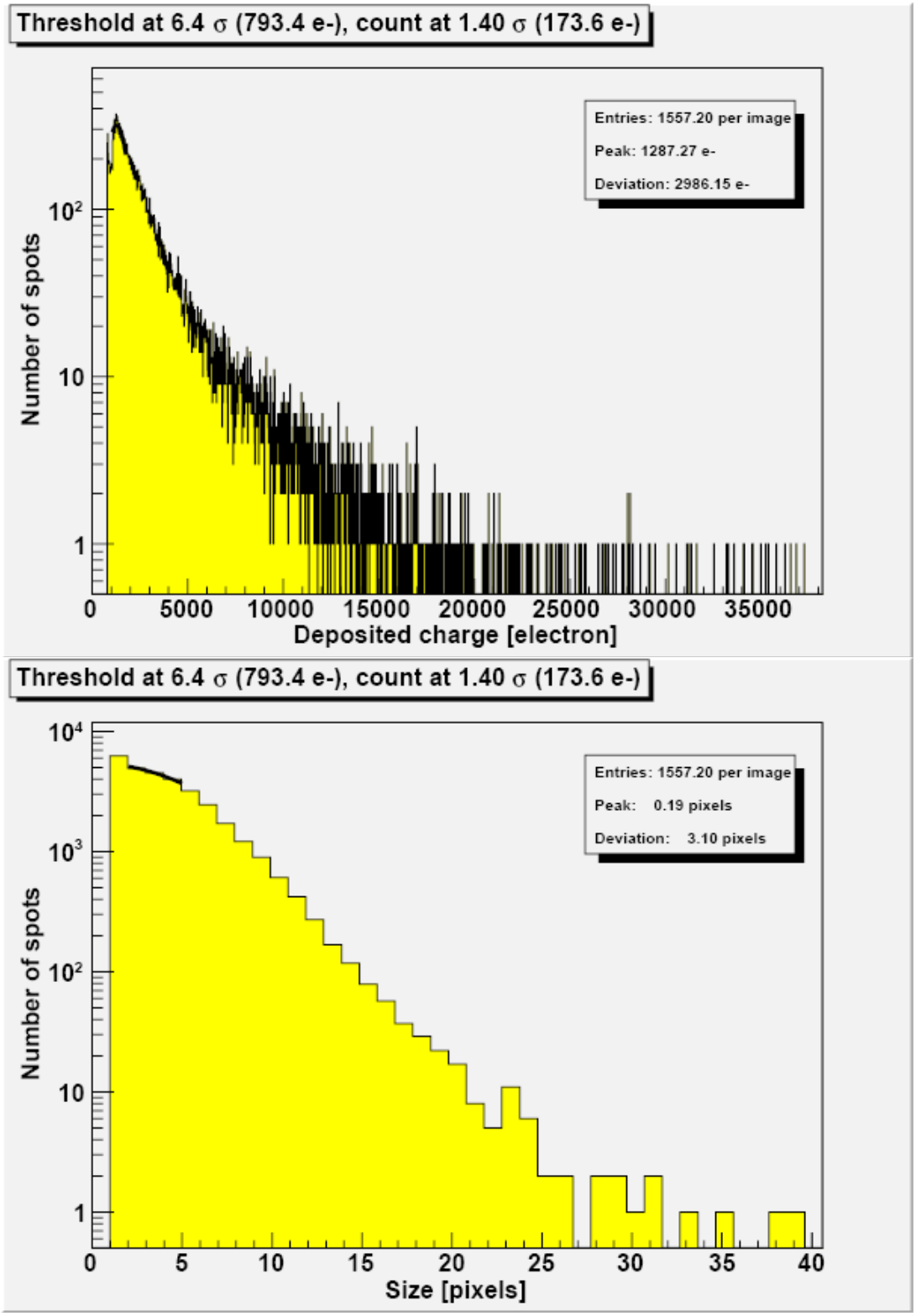

Figure 9-51: Clustering analysis - Run 20 – 230 MeV – no tilt – DR mode – 2 ms

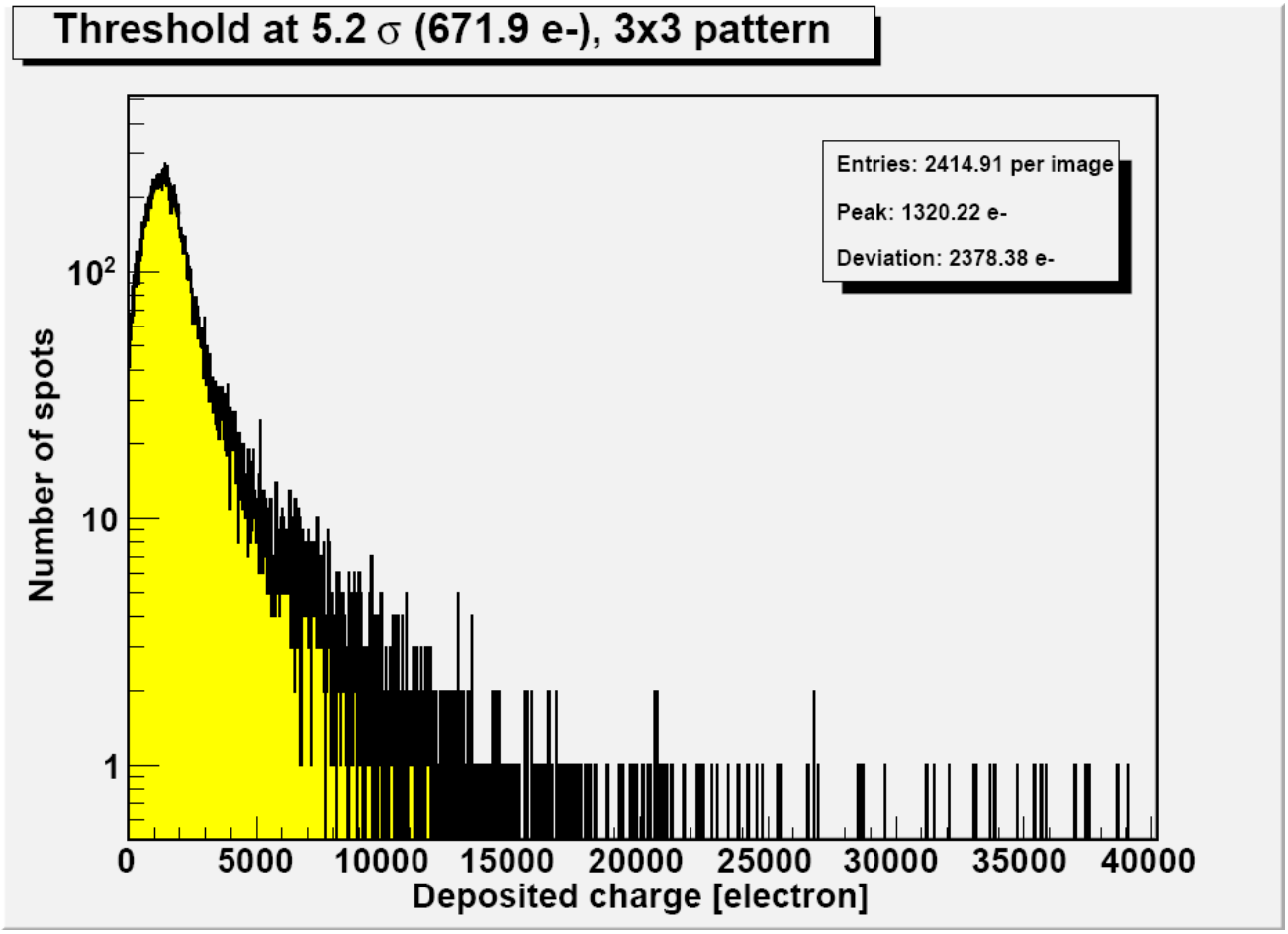

Figure 9-52: 3x3 pattern analysis - Run 20 – 230 MeV – no tilt – DR mode – 2 ms

9.2.16. Run 26 – 100 MeV – no tilt – DR mode – 2 ms

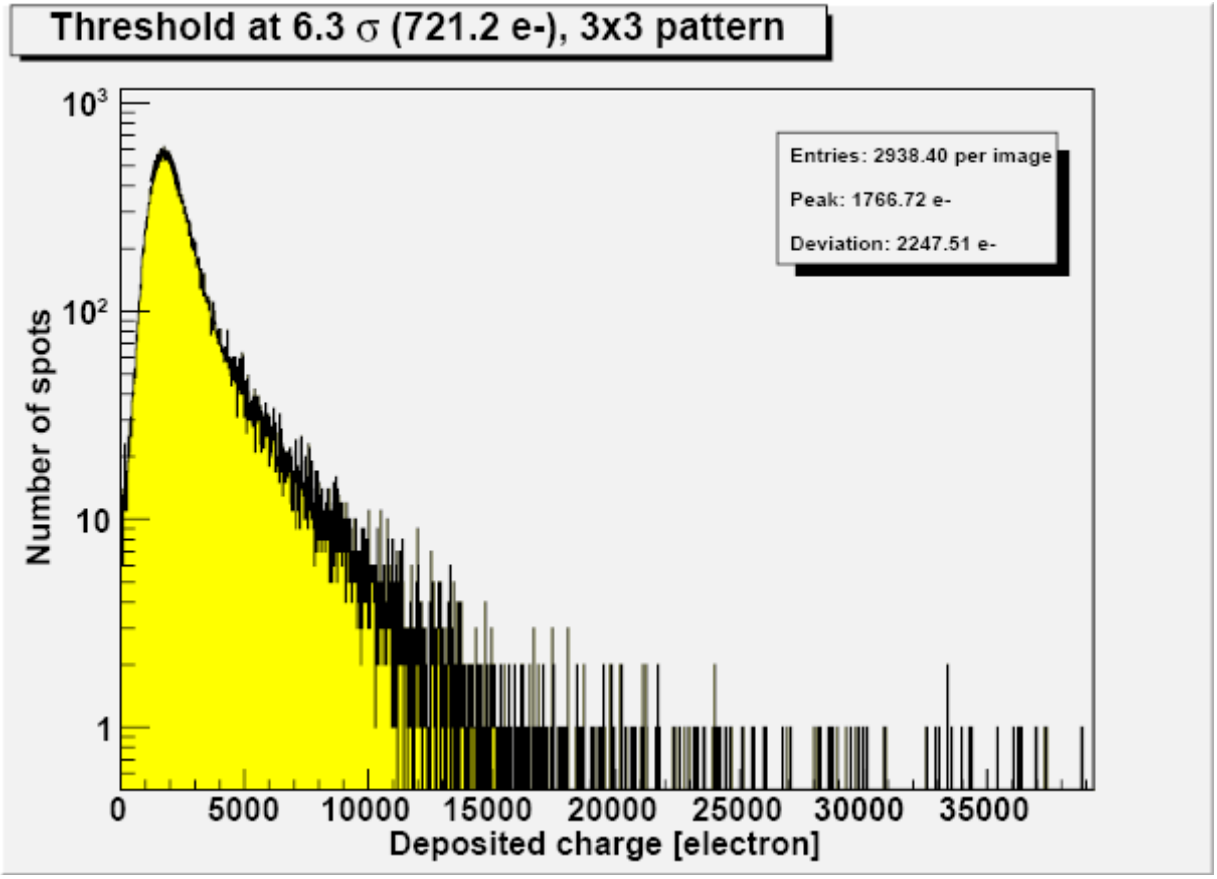

Figure 9-53: 3x3 pattern analysis - Run 26 – 100 MeV – no tilt – DR mode – 2 ms

9.2.17. Run 27 – 175 MeV – no tilt – DR mode – 2 ms

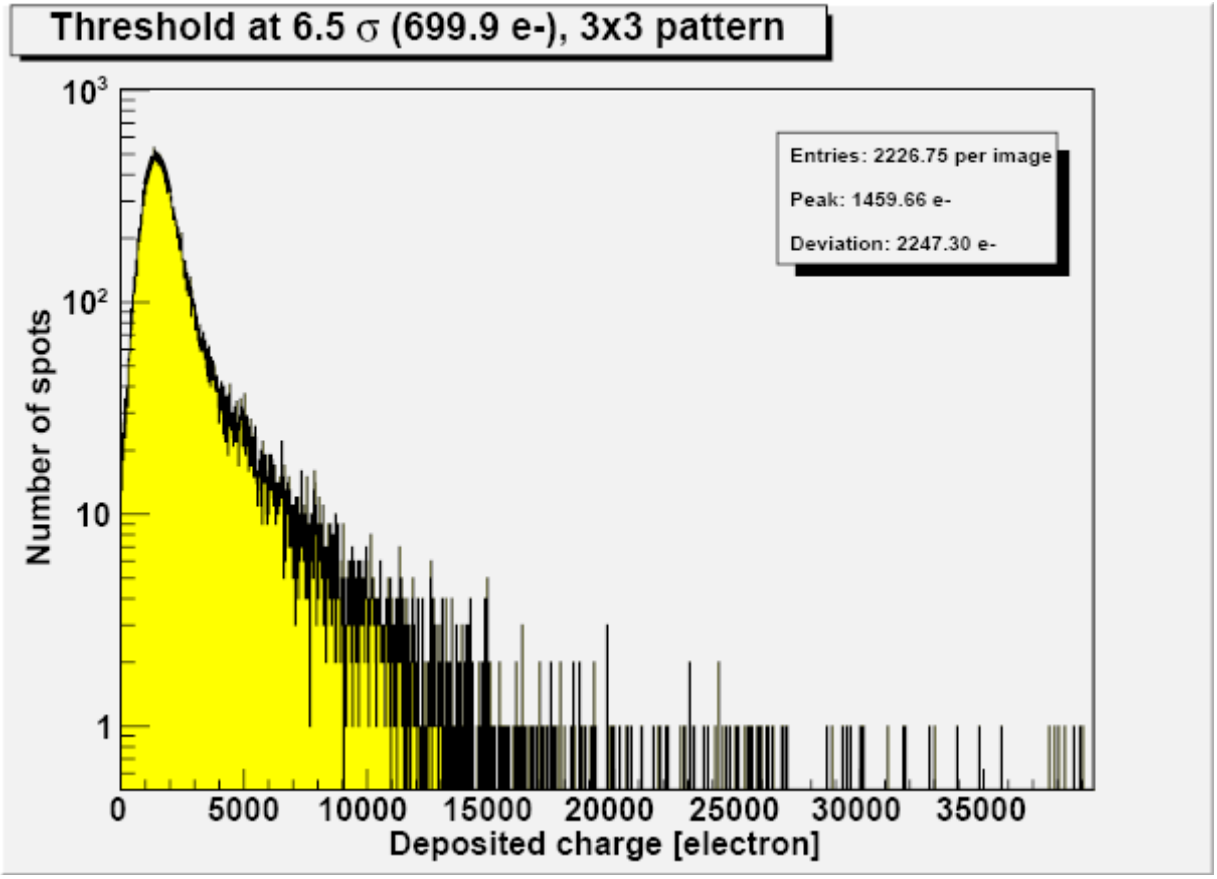

Figure 9-54: 3x3 pattern analysis - Run 27 – 175 MeV – no tilt – DR mode – 2 ms

9.2.18.Run 28 – 230 MeV – no tilt – DR mode – 2 ms

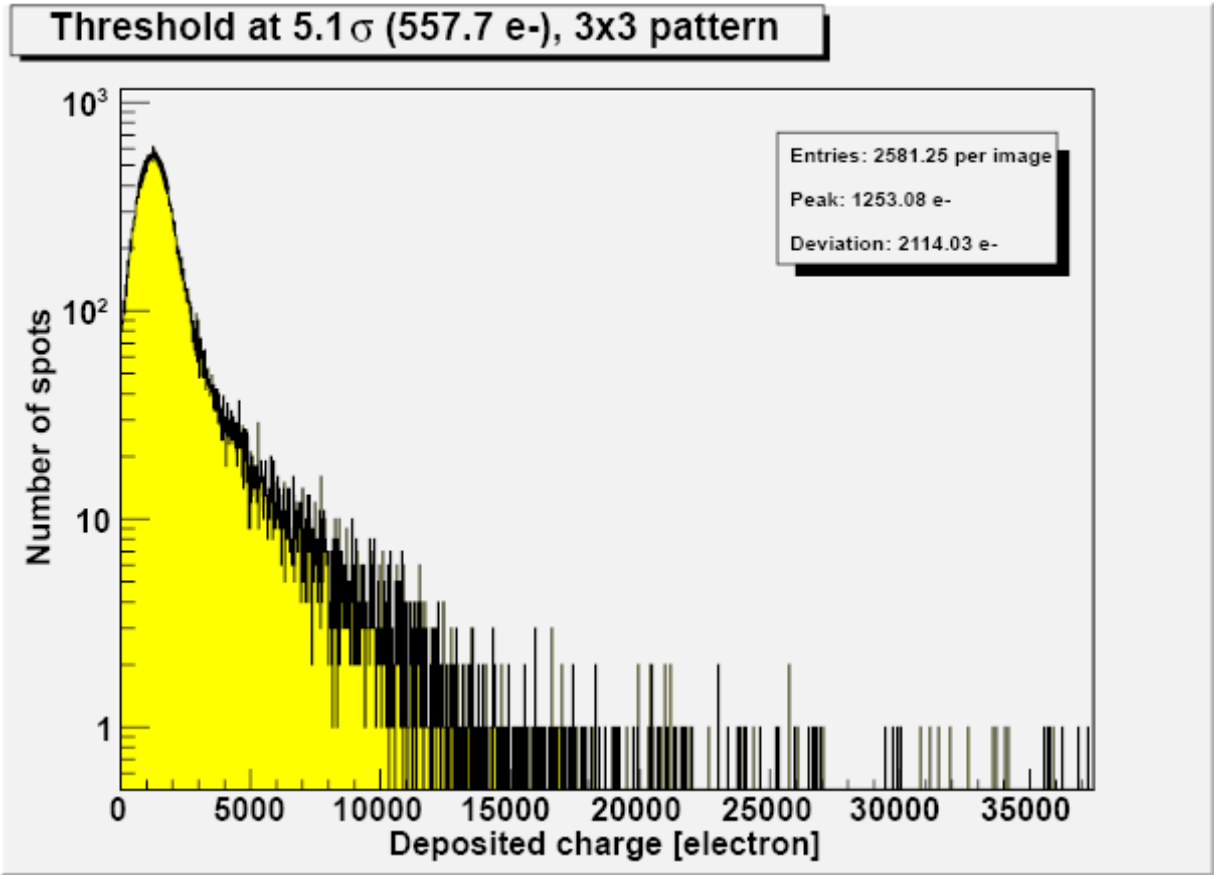

Figure 9-55: 3x3 pattern analysis - Run 28 – 230 MeV – no tilt – DR mode – 2 ms